IN THE UNITED STATES DISTRICT COURT

FOR THE DISTRICT OF DELAWARE

ZYMOGENETICS, INC., a Washington Corporation, Plaintiff, v. BRISTOL-MYERS SQUIBB CO., a Delaware Corporation, and DOES 1 through 100, Defendants.	)	C.A. No. 06-500-SLR **PUBLIC VERSION**

DECLARATION OF LISA KOBIALKA IN SUPPORT OF ZYMOGENETICS, INC.'S OPPOSITION TO BRISTOL-MYERS SQUIBB CO.'S MOTION FOR SUMMARY JUDGMENT OF NONINFRINGEMENT

OF COUNSEL:

Paul J. André
Lisa Kobialka
KING & SPALDING LLP
1000 Bridge Parkway
Suite 1000
Redwood City, CA 94065
(650) 590-0700

Philip A. Rovner (#3215)
POTTER ANDERSON & CORROON LLP
Hercules Plaza
P. O. Box 951
Wilmington, DE 19899
(302) 984-6000
provner@potteranderson.com

Attorneys for Plaintiff
ZymoGenetics, Inc.

Dated: August 18, 2008
Public Version: August 25, 2008

I, LISA KOBIALKA, declare:

1. I am an attorney with the law firm of King & Spalding LLP, counsel of record for Plaintiff ZymoGenetics, Inc. I have personal knowledge of the facts set forth in this declaration and can testify competently to those facts.

2. Attached hereto as Exhibit 1 is a true and correct copy of page 37 from the transcript of the deposition of David Smolin, taken on July 18, 2007.

3. Attached hereto as Exhibit 2 is a true and correct copy of pages 13 and 73-74 from the transcript of the deposition of William Brady, taken on September 13, 2007.

4. Attached hereto as Exhibit 3 is a true and correct copy of page 61 from the deposition of Steven Nadler, taken on September 20, 2007.

5. Attached hereto as Exhibit 4 is a true and correct copy of excerpts from Bristol-Myers Squibb's Biological License Application for Orencia®, bearing Bates number BMS001290163.

6. Attached hereto as Exhibit 5 is a true and correct copy of the CTLA4Ig Development History, bearing Bates numbers BMS001011656-68.

7. Attached hereto as Exhibit 6 is a true and correct copy of a Model of Abatacept, submitted to the FDA as part of the Biological License Application for Orencia®, bearing Bates number BMS001290844.

8. Attached hereto as Exhibit 7 is a true and correct copy of an article entitled "A Nursing Guide to Infusion Therapy with Abatacept for the Treatment of Rheumatoid Arthritis," J. Infus. Nurs. 30(2):96-104 (2007), bearing Bates numbers BMS004295550-59.

9. Attached hereto as Exhibit 8 is a true and correct copy of a presentation entitled "Mechanism of Disease and Mechanism of Action of Orencia® (abatacept)," bearing Bates numbers BMS004294468-501.

10. Attached hereto as Exhibit 9 is a true and correct copy of U.S. Patent No. 5,770,197 entitled "Methods for regulating the immune response using B7 binding molecules and IL-4 binding molecules."

11. Attached hereto as Exhibit 10 is a true and correct copy of excerpts from "Communication in response to December 1, 1992 Office Action and Petition for two month extension" bearing Bates numbers BMS001163836-854.

12. Attached hereto as Exhibit 11 is a true and correct copy of pages 36-37, 111-112, and 116-117 from the transcript of the deposition of Nicholas Gascoigne, taken on April 29, 2008.

13. Attached hereto as Exhibit 12 is a true and correct copy of a technical report entitled "Additional Characterization Testing of Abatacept Drug Substance from Syracuse and Lonza Biologics" bearing Bates numbers BMS004257885-903.

14. Attached hereto as Exhibit 13 is a true and correct copy of a letter from the FDA to Bristol dated December 23, 2005, bearing Bates numbers BMS001785288-95.

15. Attached hereto as Exhibit 14 is a true and correct copy of an article by Arend, et al., entitled "Characterization of Two Species of Fc Fragments Obtained From Rat IgG2a By Prolonged Papain Digestion," J. Immunol. Vol. 118: 388-394, 1977.

16. Attached hereto as Exhibit 15 is a true and correct copy of an article by Thies, et al., entitled "Folding and Association of the Antibody Domain C_H3: Prolyl Isomerization Proceeds Dimerization," J. Mol. Biol. 293: 67-79, 1999.

17. Attached hereto as Exhibit 16 is a true and correct copy of a letter from the FDA to Bristol dated June 14, 2005, bearing Bates numbers BMS001009186-190.

I declare under penalty of perjury under the laws of the State of California and the United States that each of the above statements is true and correct.

Executed on August 18, 2008 in Redwood Shores, California.

Lisa Kobialka

IN THE UNITED STATES DISTRICT COURT
FOR THE DISTRICT OF DELAWARE

CERTIFICATE OF SERVICE

I, Philip A. Rovner, hereby certify that on August 25, 2008, the within document was filed with the Clerk of the Court using CM/ECF which will send notification of such filing(s) to the following; that the document was served on the following counsel as indicated; and that the document is available for viewing and downloading from CM/ECF.

BY HAND DELIVERY AND E-MAIL

Frederick L. Cottrell, III, Esq.
Kelly E. Farnan, Esq.
Richard Layton & Finger, P.A.
One Rodney Square
P. O. Box 551
Wilmington, DE 19899
cottrell@rlf.com
farnan@rlf.com

I hereby certify that on August 25, 2008 I have sent by E-mail the foregoing document to the following non-registered participant:

Christopher P. Borello, Esq.
Colleen Tracy, Esq.
Fitzpatrick Cella Harper & Scinto
30 Rockefeller Plaza
New York, NY 10112
cborello@fchs.com
ctracy@fchs.com

/s/ Philip A. Rovner
Philip A. Rovner (#3215)
Potter Anderson & Corroon LLP
Hercules Plaza
P. O. Box 951
Wilmington, DE 19899
(302) 984-6000
provner@potteranderson.com

748348

EXHIBIT 1

THIS EXHIBIT HAS BEEN REDACTED IN ITS ENTIRETY

EXHIBIT 2

THIS EXHIBIT HAS BEEN REDACTED IN ITS ENTIRETY

EXHIBIT 3

THIS EXHIBIT HAS BEEN REDACTED IN ITS ENTIRETY

EXHIBIT 4

THIS EXHIBIT HAS BEEN REDACTED IN ITS ENTIRETY

EXHIBIT 5

THIS EXHIBIT HAS BEEN REDACTED IN ITS ENTIRETY

EXHIBIT 6

THIS EXHIBIT HAS BEEN REDACTED IN ITS ENTIRETY

EXHIBIT 7

THIS EXHIBIT HAS BEEN REDACTED IN ITS ENTIRETY

EXHIBIT 8

THIS EXHIBIT HAS BEEN REDACTED IN ITS ENTIRETY

EXHIBIT 9

US005770197A

United States Patent [19]

Linsley et al.

[11] Patent Number: 5,770,197

[45] Date of Patent: *Jun. 23, 1998

[54] **METHODS FOR REGULATING THE IMMUNE RESPONSE USING B7 BINDING MOLECULES AND IL4-BINDING MOLECULES**

[75] Inventors: **Peter S. Linsley; Jeffrey A. Ledbetter,** both of Seattle; **Nitin K. Damle,** Renton; **William Brady,** Bothell; **Philip M. Wallace,** Seattle, all of Wash.

[73] Assignee: **Bristol-Myers Squibb Company,** Princeton, N.J.

[*] Notice: The term of this patent shall not extend beyond the expiration date of Pat. No. 5,434,131.

[21] Appl. No.: **8,898**

[22] Filed: **Jan. 22, 1993**

Related U.S. Application Data

[63] Continuation-in-part of Ser. No. 723,617, Jul. 27, 1991, abandoned.

[51] **Int. Cl.**[6] **A61K 39/395**; C07K 14/705; C07K 16/46

[52] **U.S. Cl.** **424/134.1**; 424/139.1; 424/144.1; 424/192.1; 424/810; 530/350; 530/388.7; 530/868; 435/69.7

[58] **Field of Search** 435/69.7; 530/386, 530/378.1, 387.3, 350, 388.7, 868; 536/23.5; 935/10; 514/2; 424/85.8, 134.1, 139.1, 144.1, 192.1, 810

[56] **References Cited**

U.S. PATENT DOCUMENTS

4,399,216	8/1983	Axel et al.	435/6
4,683,195	7/1987	Mullis et al.	435/6
4,683,202	7/1987	Mullis	435/91
5,434,131	7/1995	Linsley et al.	514/2

FOREIGN PATENT DOCUMENTS

WO 92/15671	9/1992	WIPO .
WO 93/00431	1/1993	WIPO .

OTHER PUBLICATIONS

Schwartz, Constimulation of T Lymphocytes: The Role of CD28, CTLA–4, and B7/BB1 in Interleukin–2 Production and Immunotherapy, Cell 71, pp. 1065–1068. 1992.

Tan et al., Induction of Alloantigen–specific Hyporesponsiveness in Human T Lymphocytes by Blocking Interaction of CD28 with Its Natural Ligand B7/BB1, J. Exp. Med, 177, pp. 165–173, 1993.

Sechzer, The Role of Animals in Biomedical Research "The Use of Short Term in Vitro adn Submammalian Tests as Alternatives to Large Scale Animal Bioassays" (1993) The New Academy of Sciences, at pp.68–73.

Long–Term Animal Studies, Their Predictive Value for Man, Edited by Stuart R. Walker and Anthony D. Dayan, 1986, Chapter 1,3, pp. 17–22.

Janeway, "Approaching the Asymptote? Evolution and Revolution in Immunology", *Cold Spring Harbor Symp. Quant. Biol.*LIV:1–13 (1989).

Shaw and Shimuzu, "Two Molecular Pathways of Human T Cell Adhesion ; Establishment of Receptor–Ligand Relationship", *Current Opinion in Immunology*. Eds. Kindt and Long, 1:92–97 (1988).

Hemler, "Adhesive Protein Receptors on Hematopoietic Cells", *Immunology Today*9:109–113 (1988).

Kakiuchi et al., "B Cells as Antigen–Presenting Cells : The Requirement for B Cell Activation", *J. Immunol.* 131:109–114 (1983).

Krieger et al., "Antigen Presentation by Splenic B Cells: Resting B Cells are Ineffective, Whereas Activated B Cells are Effective Accessory Cells for T Cells Responses", *J. Immunol.* 135:2937–2945 (1985).

McKenzie, "Alloantigen Presentation by B Cells—Requirement for IL–1 and IL–6". *J. Immunol.* 141:2907–2911 (1988).

Hawrylowicz and Unanue, "Regulation of Antigen–Presentation–I IFN–γ Induces Antigen–Presenting Properties on B Cells", *J. Immunol.* 141:4083–4088 (1988).

Springer et al., "The Lymphocyte Function–Associated LFA–1, CD2, and LFA–3 Molecules: Cell Adhesion Receptors of the Immune System", *A. Rev. Immunol.* 5:223–252 (1987).

Dinarello and Mier, "Current Concepts –Lymphokines", *New Engl. Jour. Med.* 317:940–945 (1987).

Weiss et al., "The Role of the T3/Antigen Receptor Complex in T–Cell Activation", *Ann. Rev. Immunol.* 4:593–619 (1986).

McMichael, Ed., "Non–Lineage, LFA–1 Family, and Leucocyte Common Antigens: New and Previously Defined Clusters", *Leukocyte Typing III,*Oxford Univ. Press, Oxford, UK (1987).

Moingeon et al., "CD2–mediated Adhesion Facilitates T Lymphocyte Antigen Recognition Function", *Nature*339:312–314 (1988).

Makgoba et al., ICAM–1 A Ligand for LFA–1–Dependent Adhesion of B, T and Myeloid Cells. *Nature*331:86–88 (1988).

Staunton et al., "Functional Clonging of ICAM–2 A Cell Adhesion Ligand for LFA–1 Homologous t ICAM–1", *Nature*339:61–64 (1989).

Norment et al., "Cell–Cell Adhesion Mediated by CD8 and MHC Class I Molecules", *Nature*336:79–81 (1988).

Doyle and Strominger, "Interaction Between CD4 and Class II MHC Molecules Mediates Cell Adhesion", *Nature*330:256–259 (1987).

Stoolman, "Adhesion Molecules Controlling Lymphocyte Migration", *Cell*56:907–910 (1989).

(List continued on next page.)

Primary Examiner—Lorraine M. Spector
Attorney, Agent, or Firm—Merchant, Gould, Smith, Edell, Welter & Schmidt

[57] **ABSTRACT**

The invention identifies the CTLA4 receptor as a ligand for the B7 antigen. The complete amino acid sequence encoding human CTLA4 receptor gene is provided. Methods are provided for expressing CTLA4 as an immunoglobulin fusion protein, for preparing hybrid CTLA4 fusion proteins, and for using the soluble fusion proteins, fragments and derivatives thereof, including monoclonal antibodies reactive with B7 and CTLA4, to regulate T cell interactions and immune responses mediated by such interactions.

11 Claims, 15 Drawing Sheets

Digitized by Google

OTHER PUBLICATIONS

Brescher and Cohn, "A Theory of Self–Nonself Discrimination", *Science*169:1042–1049 (1970).

Freeman et al., "B7 A New Member of the Ig Superfamily with Unique Expression on Activated and Neoplastic B Cells", *J. Immunol.* 143(8):2714–2722 (1989).

Freedman et al., "B7 A B Cell–Restricted Antigen that Identifies Preactivated B Cells", *J. Immunol.* 138:3260–3267 (1987).

Clark et al., "Polypeptides on Human B Lymphocytes Associated with Cell Activation", *Human Immunol.* 16:100–113 (1986).

Yokochi et al., "B Lymphoblast Antigen (BB–1) Expressed on Epstein–Barr Virus–Activated B Cells Blasts, B Lymphoblastoid Cell Lines, and Burkitt's Lymphomas", *J. Immunol.* 128:823–827 (1981).

Weiss, "Structure and Function of the T Cell Antigen Receptor", *J. Clin, Invest.* 86:1015–1022 (1990).

Allen, "Antigen Processing at the Molecular Level", *Immunol. Today*8:270–273 (1987).

Schwartz, "A Cell Culture Model for T Lymphocytes Clonal Anergy", *Science*248:1349–1356 (1990).

Weaver and Unanue, "The Costimulatory Function of Antigen–Presenting Cells", *Immunol. Today*11:49–55.

Aruffo and Seed, "Molecular Cloning of a CD28 cDNA by a High–Efficiency COS Cell Expression System", *Proc. Natl. Acad. Sci.* 84:8573–8577 (1987).

Damle et al., "Alloantigen–Sepcific Cytotoxic and Suppressor T Lymphocytes are Derived from Phenotypically Distinct Precursors", *J. Immunol.* 131:2296–2300 (1983).

June et al., "T–Cell Proliferation Involving the CD28 Pathway is Associated with Cyclosporine–Resistant Interleukin 2 Gene Expression", *Mol. Cell. Biol.* 7:4472–4481 (1987).

Thompson et al., "CD28 Activation Pathway Regulates the Production of Multiple T–Cell–Derived Lymphokines/Cytokines", *Proc. Natl. Acad. Sci.* 86:1333–1337 (1989).

Lindsten et al. "Regulation of Lymphokine Messenger RNA Stability by a Surface–Mediated T Cell Activation Pathway", *Science*244:339–343 (1989).

Damle et al., "Monoclonal Antibody Analysis of Human T Lymphocyte Subpopulations Exhibiting Antologous Mixed Lymphocyte Reaction", *Proc. Natl. Acad. Sci.* 78:5096–5098 (1981).

Lesslauer et al., "T90/44 (9.3 Antigen). A Cell Surface Molecule with a Function in Human T Cell Activation", *Eur. J. Immunol.* 16:1289–1296 (1986).

Linsley et al., "T–Cell Antigen CD28 Mediates Adhesion with B Cells by Interacting with Activation Antigen B7/BB–1", *Proc. Natl. Acad. Sci. USA,* 87:5031–5035 (1990).

Linsley et al., "Binding of the B Cell Activation Antigen B7 to CD28 Costimulates T Cell Proliferation and Interleukin 2 mRNA Accumulation ", *J. Exp. Med.* 173:721–730 (1991).

Kohno et al., CD28 Molecule as a Receptor–Like Function for Accessory Signals in Cell–Mediated Augmentation of IL–2 Production, *Cell Immunol.* 131:1–10 (1990).

Brunet et al., "A New Member of the Immunoglobulin Superfamiluy –CTLA–4", *Nature*328:267–270 (1987).

Brunet et al., "A Differential Molecular Biology Search for Genes Preferentially Expressed in Function T Lymphocytes: The CTLA Genes", *Immunol. Rev.*103:21–36 (1988).

Dariavach et al., "Human Ig Superfamily CTLA–4 Gene: Chromosomal Localization and Identity of Protein Sequence Between Murine and Human CTLA–4 Cytoplasmic Domains, " *Eur. J. Immunol.* 18:1901–1905 (1988).

Lafage–Pochitaloff et al., "Human CD28 and CTLA–4 Ig Superfamily Genes are Located on Chromosome 2 at Bands q33–q34", *Immunogenetics*31:198–201 (1990).

Capon et al., "Designing CD4 Immunoadhesins for AIDS Therapy", *Nature*337:525–531 (1989).

Mullis & Faloona, *Methods Enzymol.* 154:335–350 (1987).

Fiers, et al., *Nature* 273:113 (1987) (Exhibit 46).

Karin, et al., *Nature* 299:797–802 (1982).

Toyama and Okayama, *FEBS* 268:217–221 (1990).

Hitzeman et al., *J. Biol. Chem.* 255:12073 (1980).

Goeddel et al., *Nucleic Acids Res.* 8:4057 (1980).

Shimatake et al., *Nature* 292:128 (1981).

Sanger et al., *Proc. Natl. Acad. Sci. USA*74:5463 (1977).

Messing et al., *Nucleic Acids Res.* 9:309 (1981)..

Maxam et al., *Methods Enzymol.* 65:499 (1980).

Kohler and Milstein (see Kohler and Milstein, *Nature,* 256:495–497 (1975).

Zola et al., in *Monoclonal Hybridoma Antibodies: Techniques and Applications,* Hurell (ed.) pp. 51–52 (CRC Press, 1982).

Fink et al., *Prog. Clin. Pathol.,* 9:121–133 (1984), Fig. 6–1 at p. 123).

Rousseaux et al., in *Methods Enzymol.,* 121:663–669, Academic Press (1986).

Storb, *Blood*68:119–125 (1986).

Storb and Thomas, *Immunol. Rev.* 88:215–238 (1985).

Freireich E.J., et al. (Quantitative Comparison of Toxicity of Anticancer Agents in Mouse, Rat, Hamster, Dog, Monkey, and Man. Cancer Chemother, Rep. 50, No. 4, 219–244, May 1966).

Seed and Aruffo (*Proc. Natl. Acad. Sci.* 84:3365 1987.

Linsley et al., *Proc. Natl. Acad.* Sci. USA 87:5031 (1990).

Hansen et al., *Immunogenetics*10:247 (1980).

Ledbetter et al., *Proc. Natl. Acad. Sci.* 84:1384–1388 (1987).

Ledbetter et al., *Blood*75:1531 (1990).

Wysocki and Sato, *Proc Natl. Acad. Sci.* 75:2844 (1978).

Volkman et al., *Proc. Natl. Acad. Sci. USA* 78:2528 (1981).

Vitetta et al., *J. Exp. Med.* 134:242 (1971).

Damle et al., *J. Immunol.* 140:1753–1761 (1988).

Schnek et al., *Cell* 56:47 (1989).

Recny et al., *J. Biol. Chem.* 265:8542 (1990).

Clayton et al., *Nature* 339:548 (1988).

Alzari et al., *Ann. Rev. Immuno.* 6:555 (1988).

June et al., *Immunology Today* 11:211 (1989).

C. Ricordi et al. Transplantation 52:519 (1991).

A.G. Tzakis et al. Lancet 336:402 (1990).

C. Ricordi, P.E. Lacy, E. H. Finke, B.J. Olack, D. W. Scharp, Diabetes 37:413 (1988).

D. Faustman and C. Coe, Science 252:1700 (1991).

Y. J. Zeng et al. Transplantation 53:277 (1992).

S. M. Hsu, L. Raine, H. Fanger, J. Histochem, Cytochem, 29:577 (1981).

P. S. Linsley et al., Science 257:792 (1992).

T. Yokochi, R. D. Holly, E. A. Clark, J. Immunol. 128:823 (1982).

Ohara, J., and W. E. Paul 1985, Production of a monoclonal antibody to and molecular characterization of B–Cell stimulatory factor–1 Nature 315:333) (Verax (Lebanon, NH)).

William C. Fanslow et al. "Regulation of Alloreactivity in vivo by IL–4 and the soluble I1–4 receptor"J. Immunol. 147:535–540 (1991).

Digitized by Google

J.Cohen Science 257:751 Aug. 7, 1992.
D.J. Lenschow et al. Science 257:789 Aug. 7, 1992.
L.A. Turka et al. PNAS 89:11102–5 Nov. 1992.
C.R. Maliszewski et al. Cell Immunol. 143:434–448 Sep. 1992.
J.M. Doutrelepont et al. Clin. Exp. Immunol. 83: 133–136 1991.
S.P. Umland et al. Clin. Immunol & Immunopath. 63:66 1992.

Digitized by Google

FIG. 1

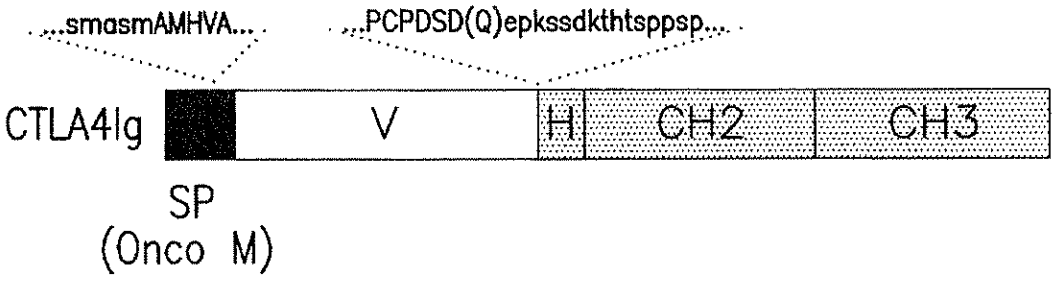

Digitized by Google

FIG. 2

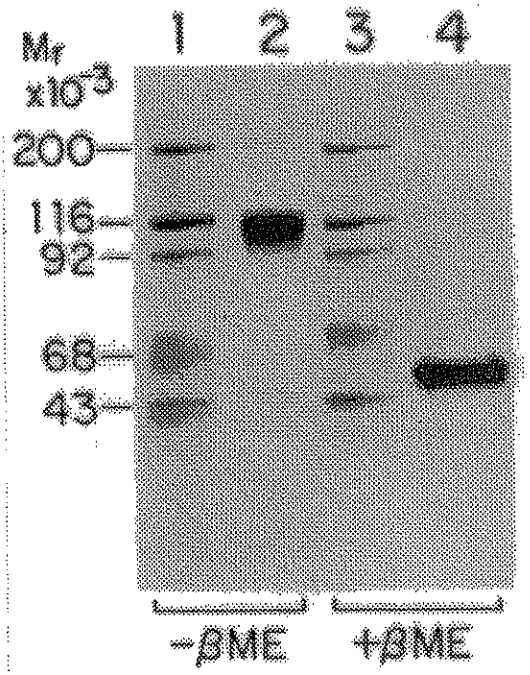

FIG. 8

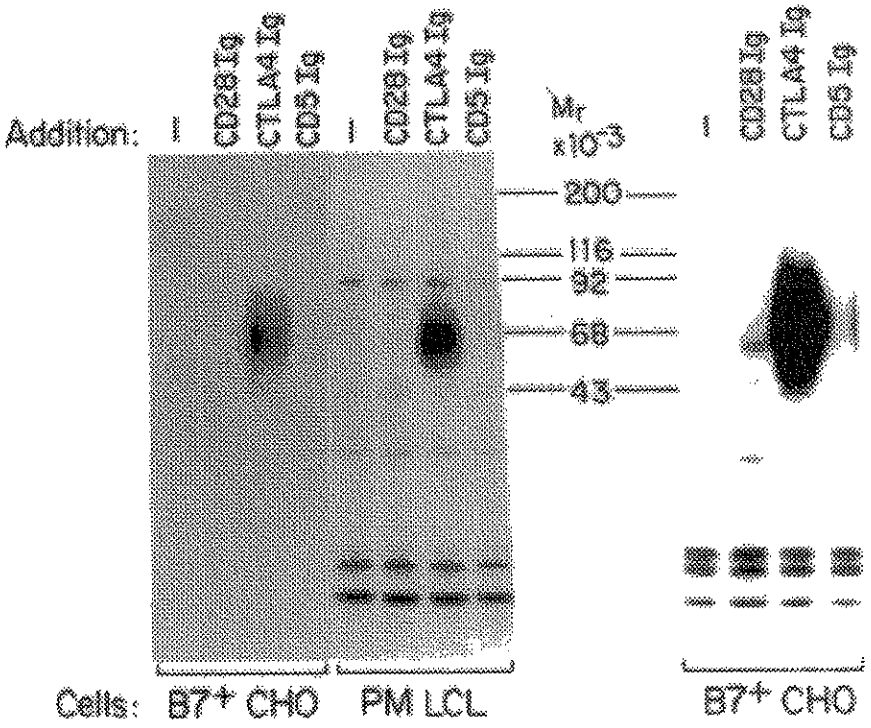

Digitized by Google

FIG. 3

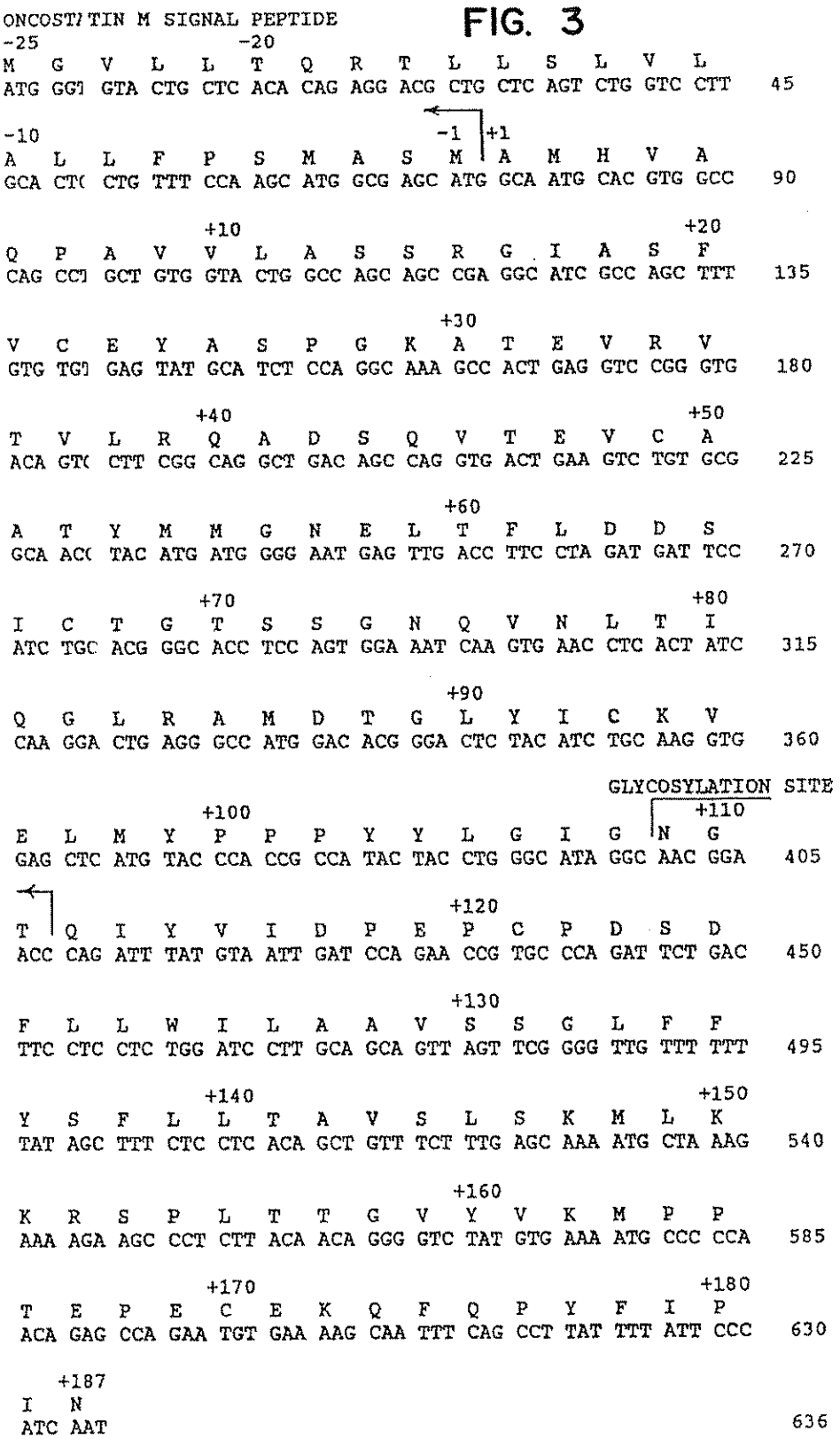

Digitized by Google

FIG. 4

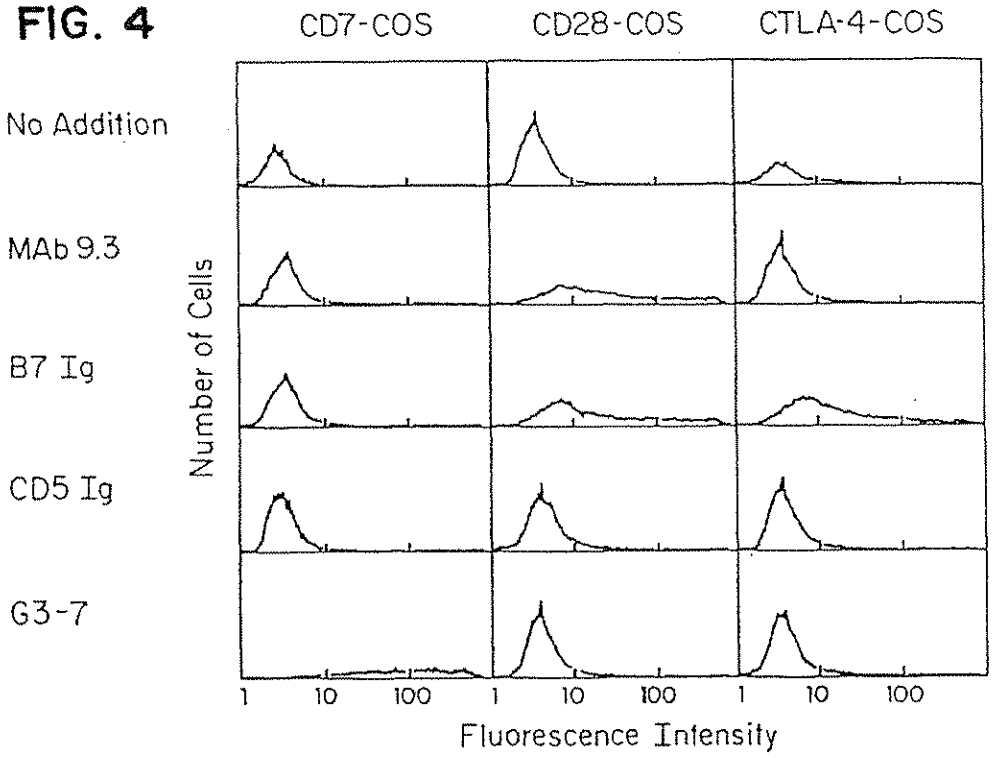

FIG. 5

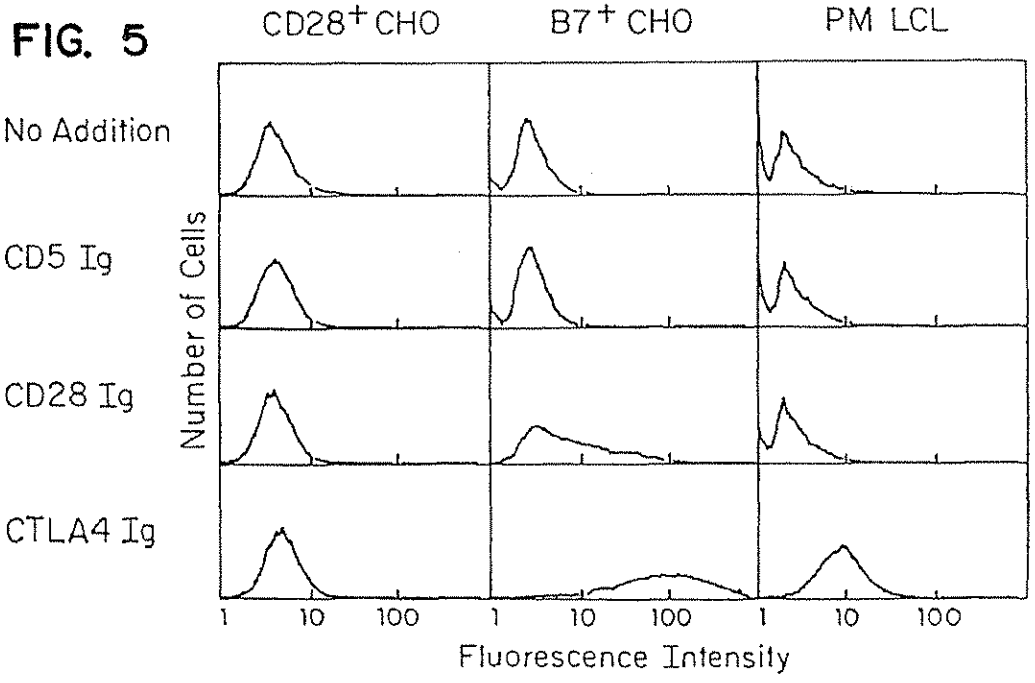

Digitized by Google

FIG. 6

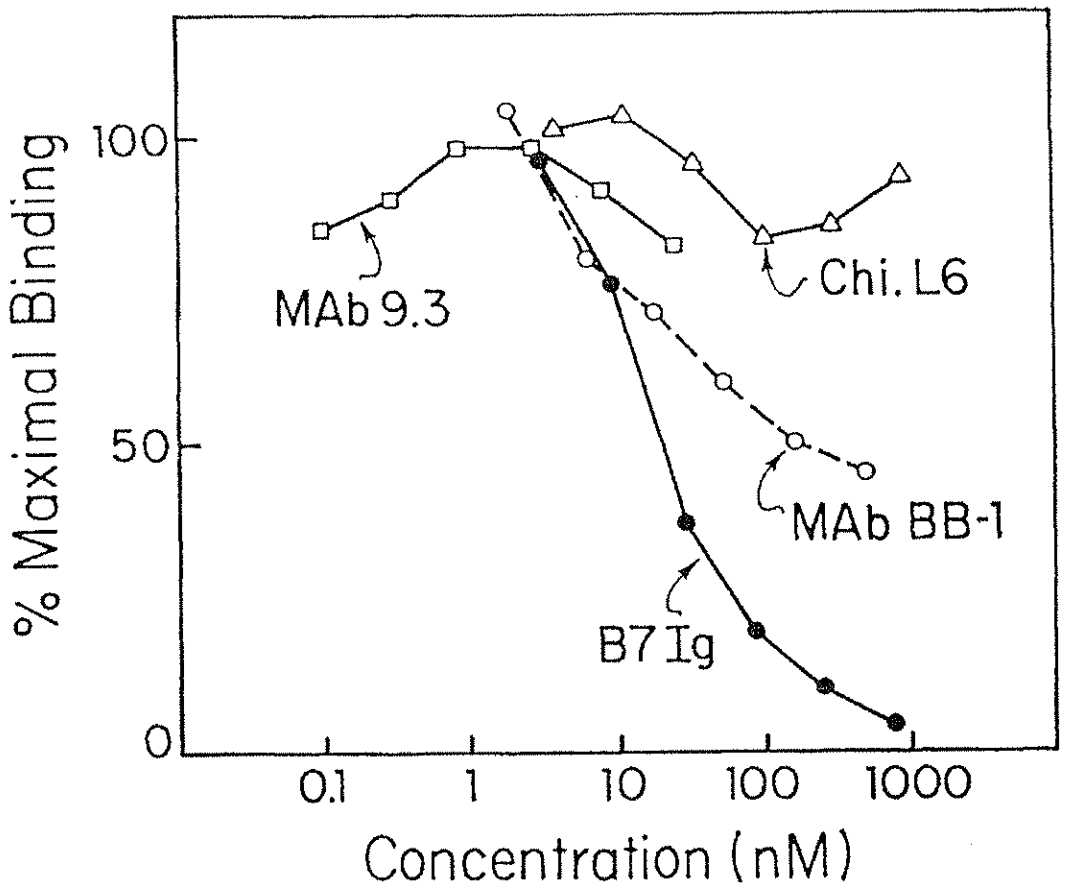

Digitized by Google

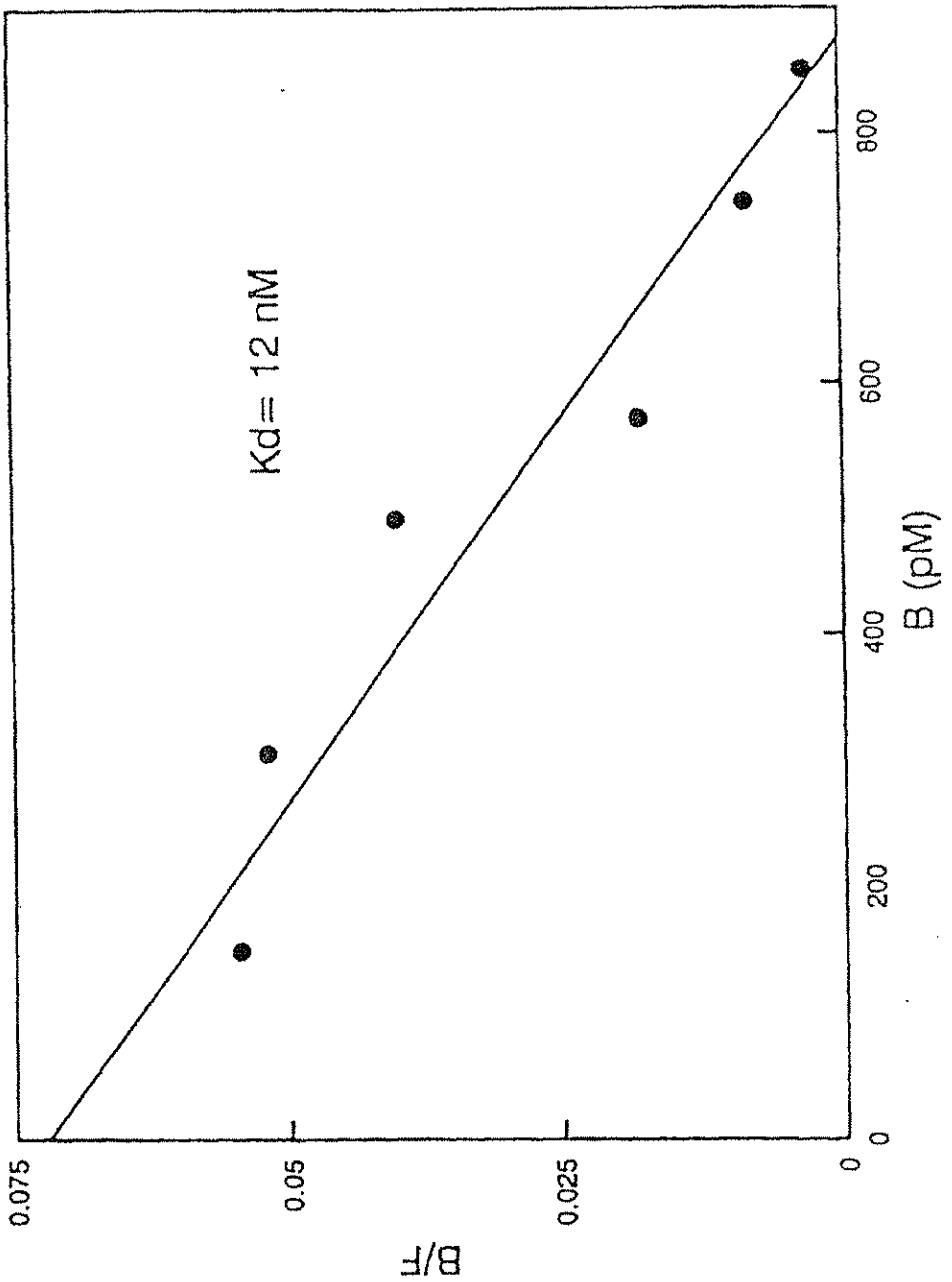

FIG. 7

Digitized by Google

FIG. 9

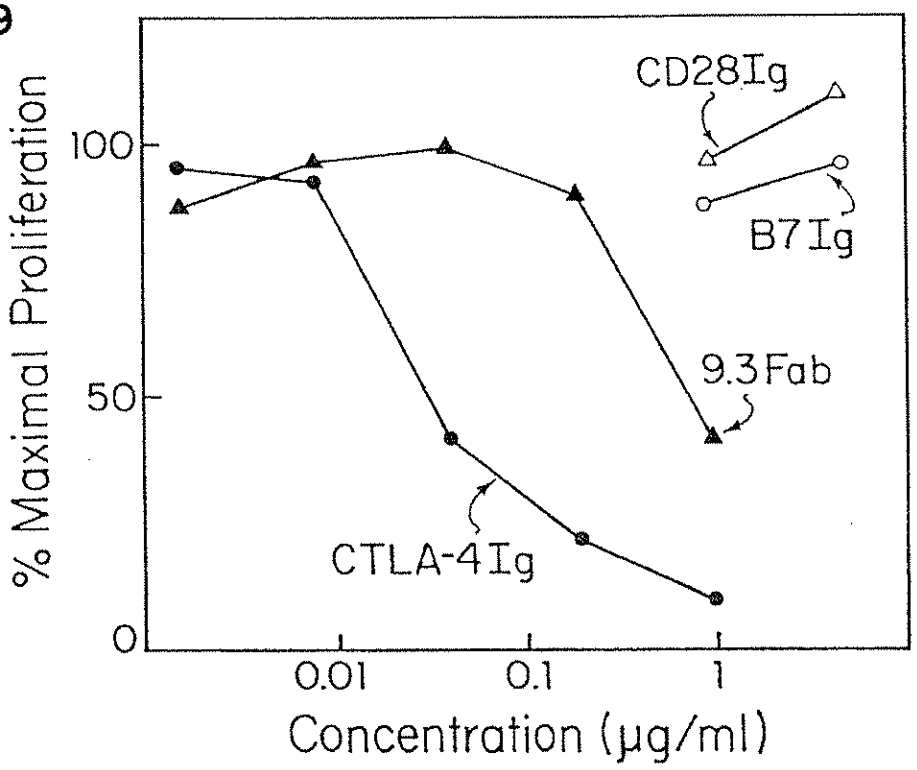

FIG. 10

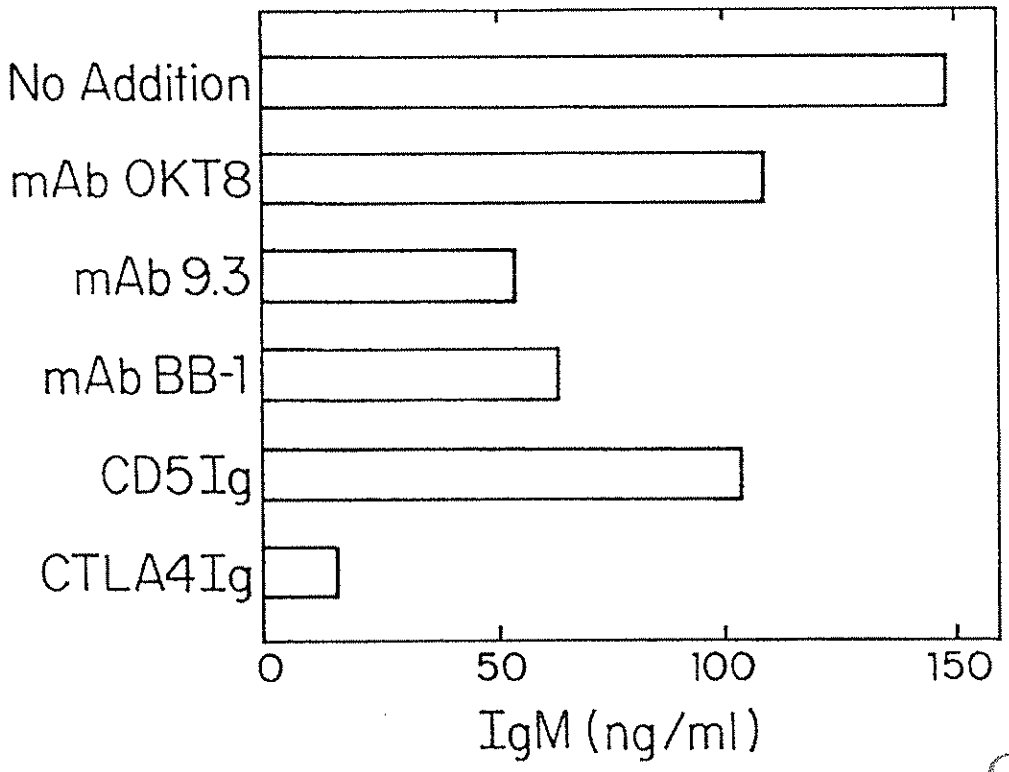

Digitized by Google

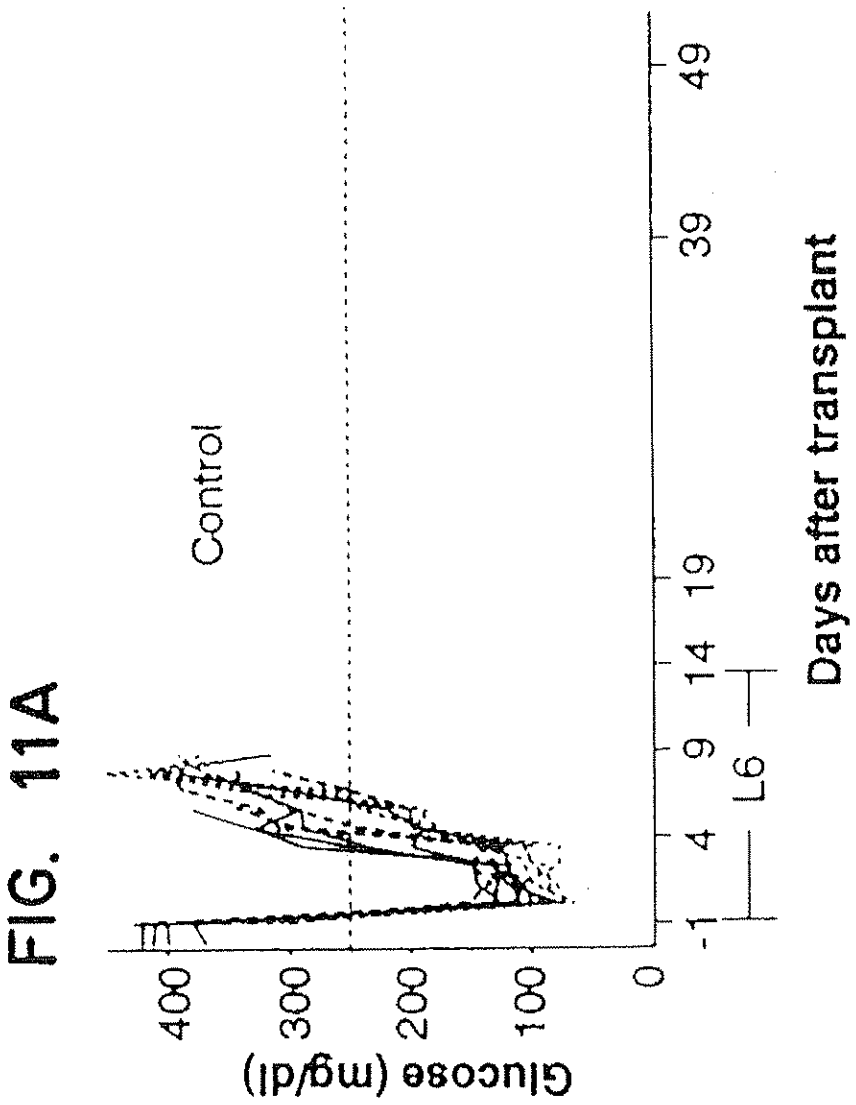

FIG. 11A

Digitized by Google

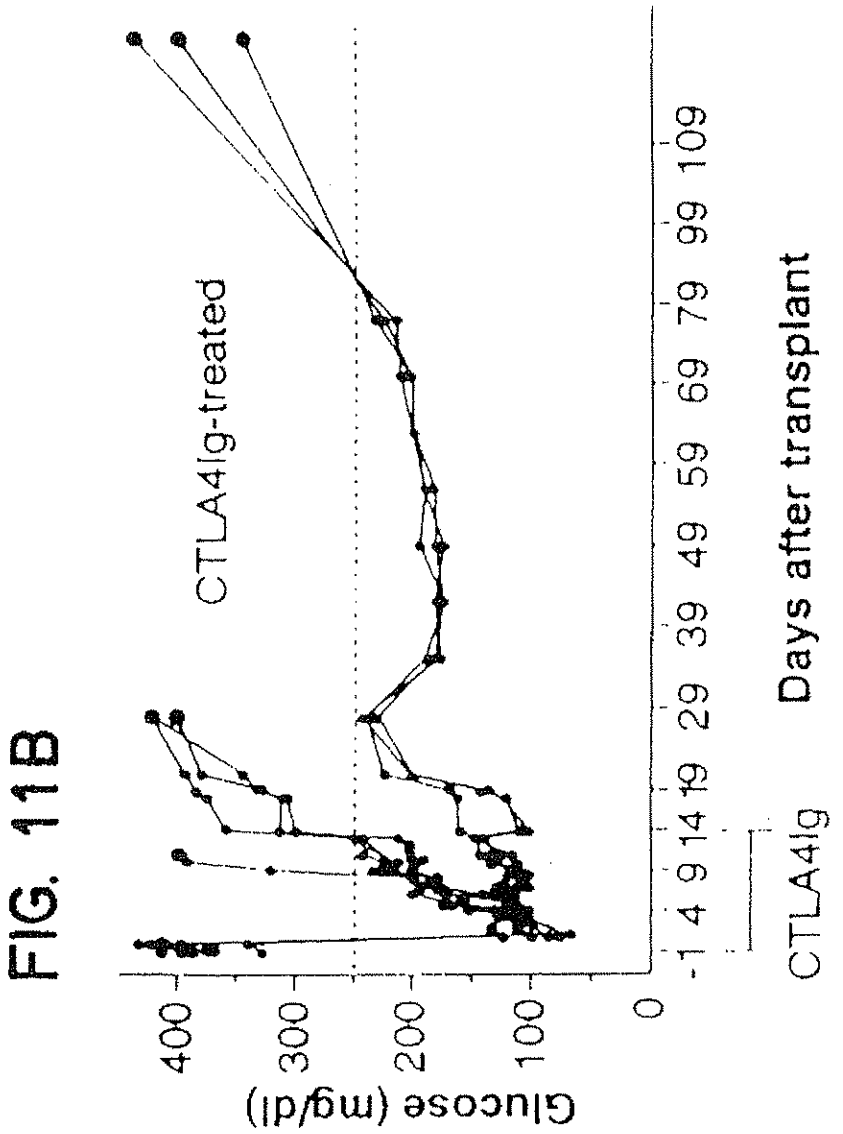

FIG. 11B

Digitized by Google

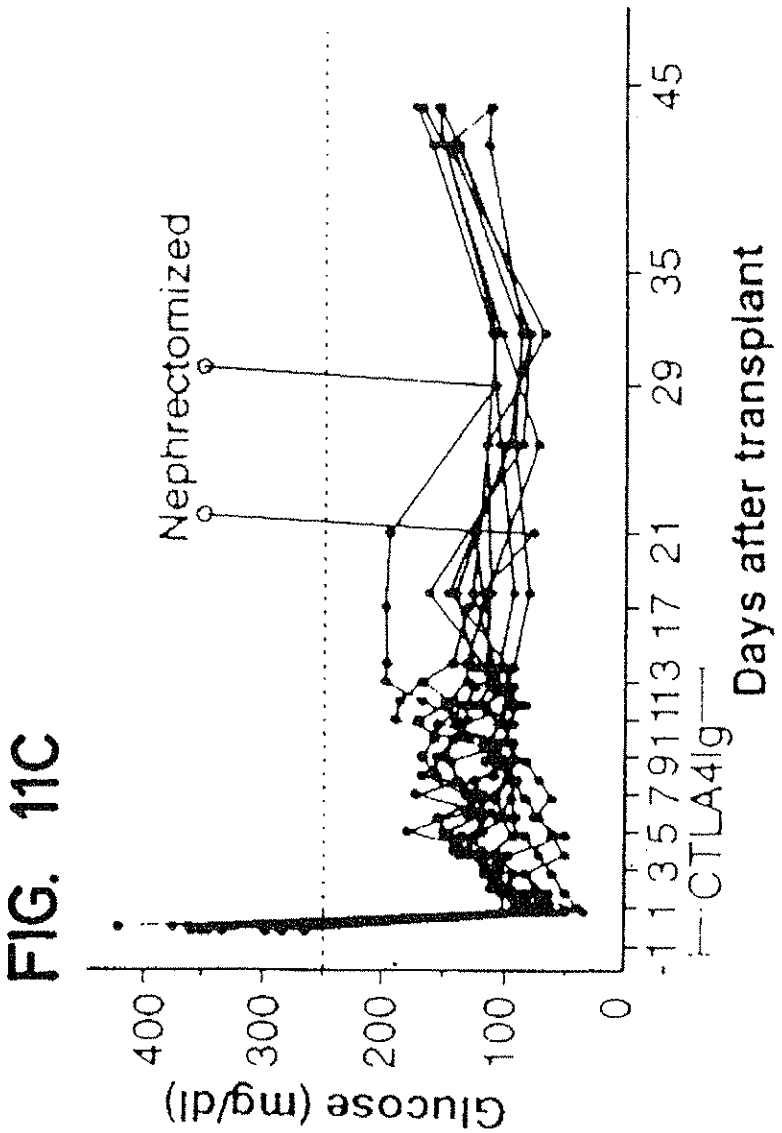

FIG. 11C

Digitized by Google

FIG. 12A

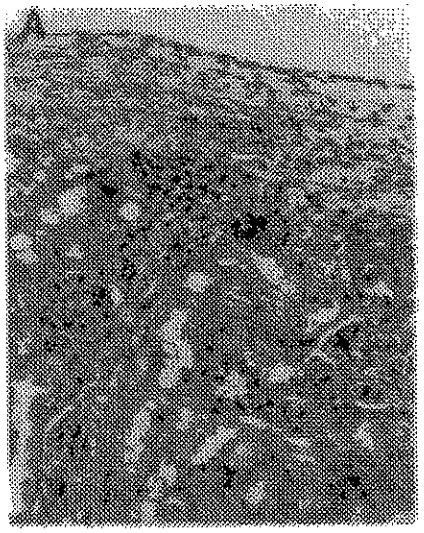

FIG. 12B



FIG. 12



FIG. 12D

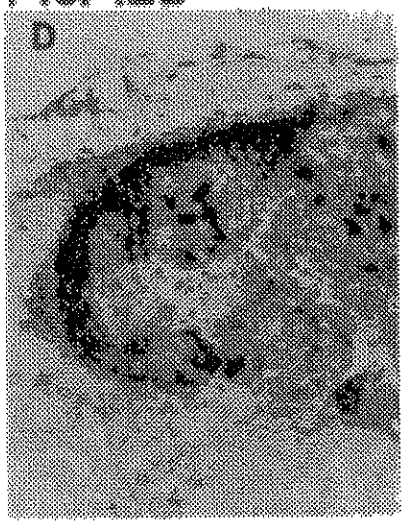

Digitized by Google

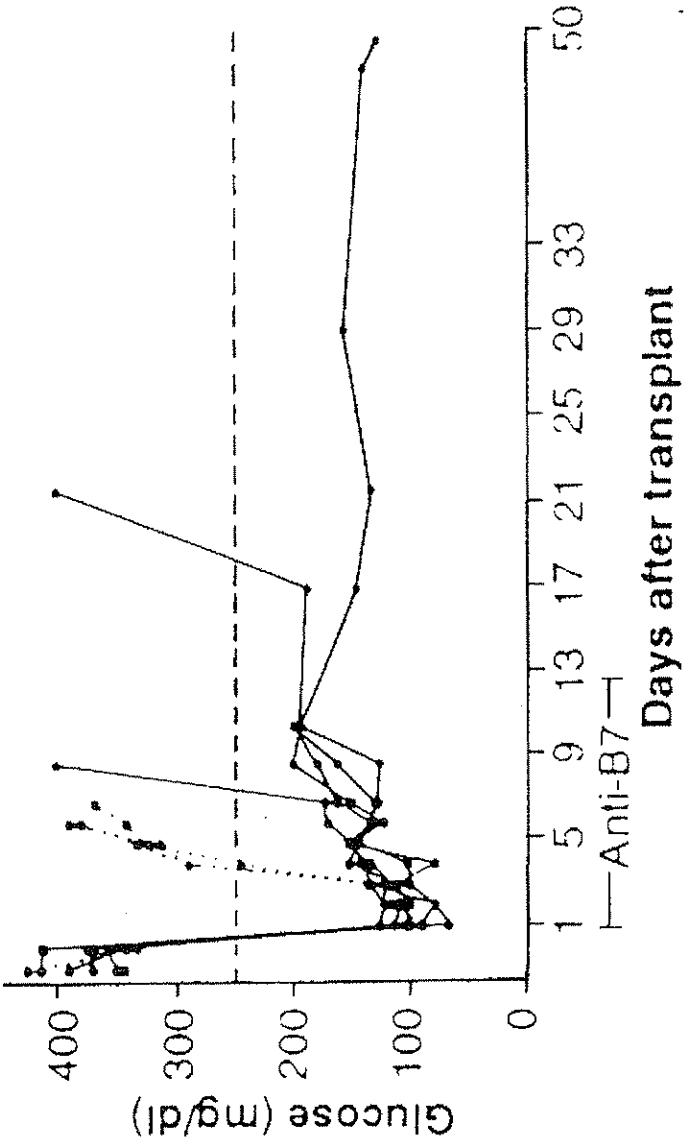

FIG. 13

Digitized by Google

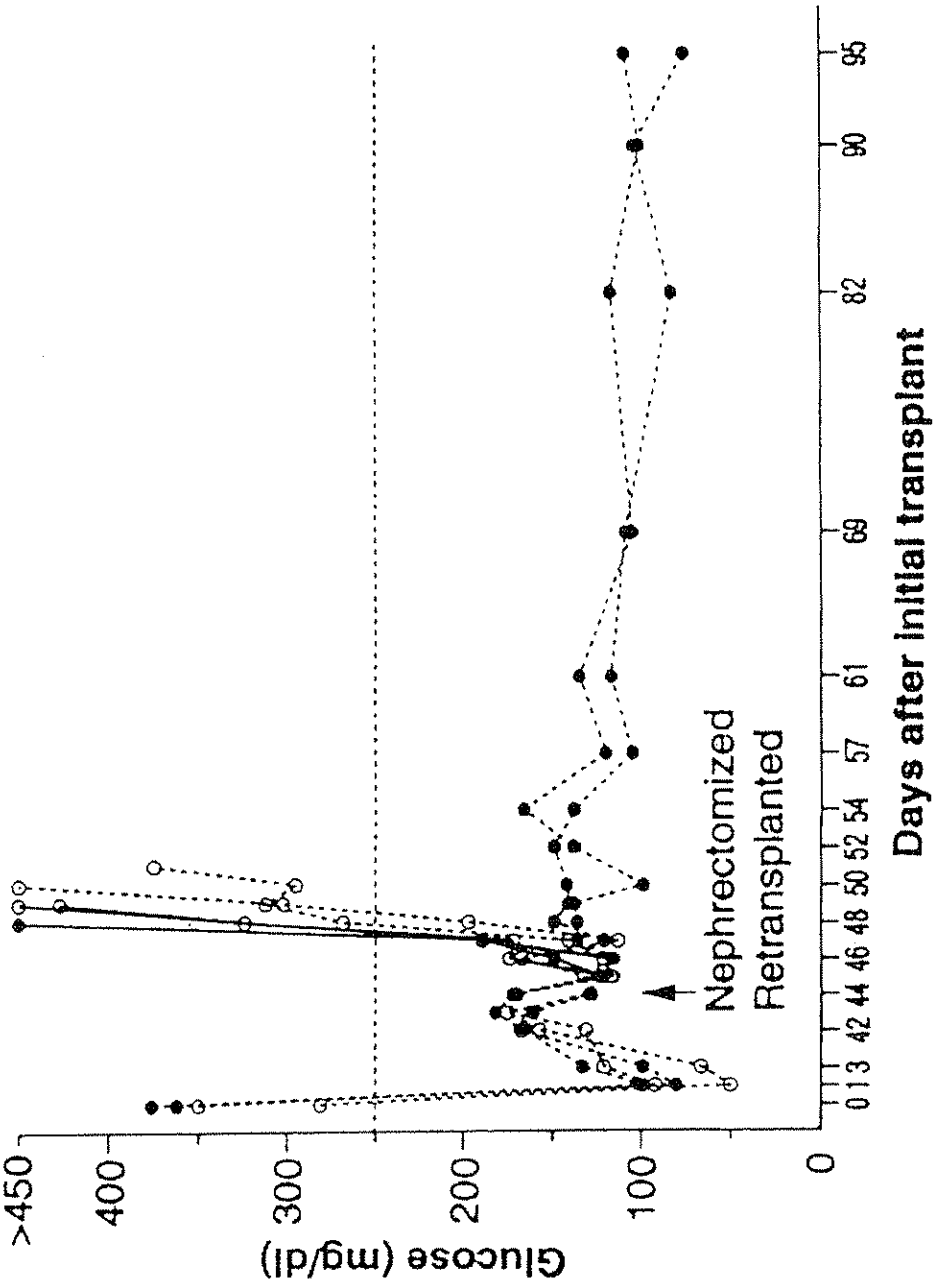

FIG. 14

Digitized by Google

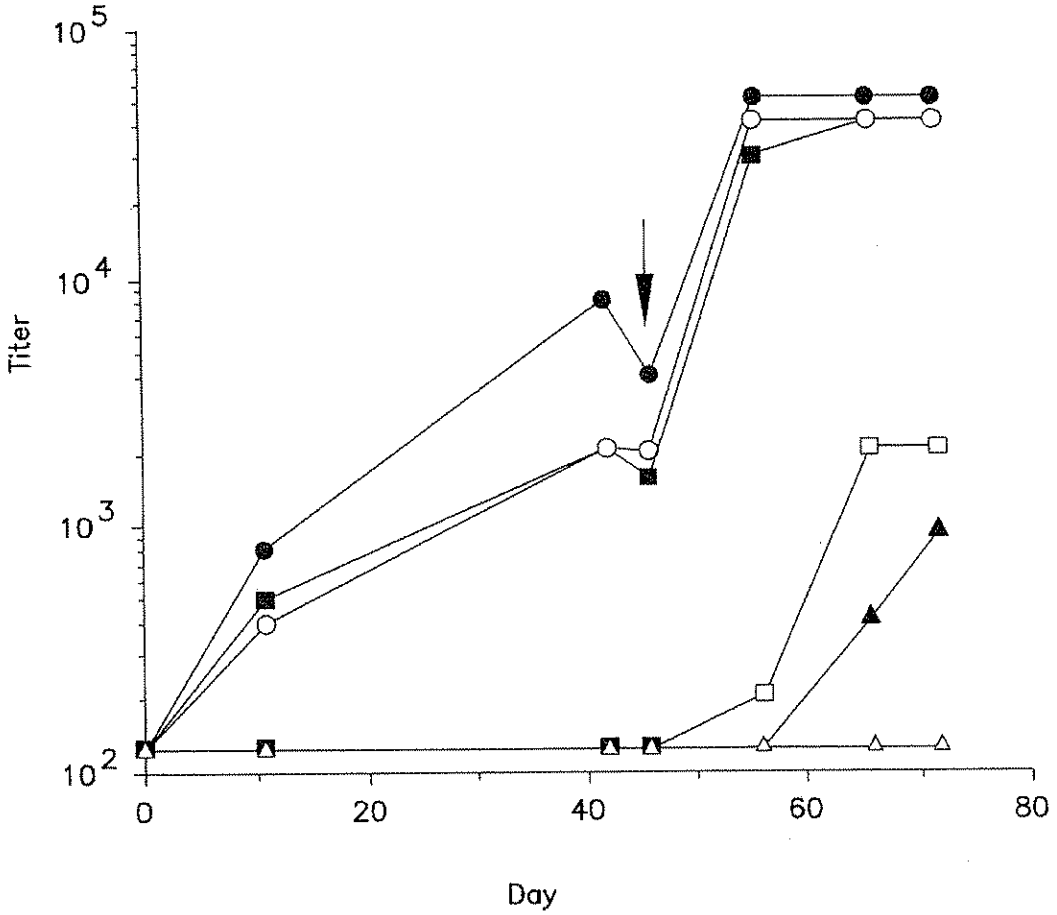

FIG. 15

Digitized by Google

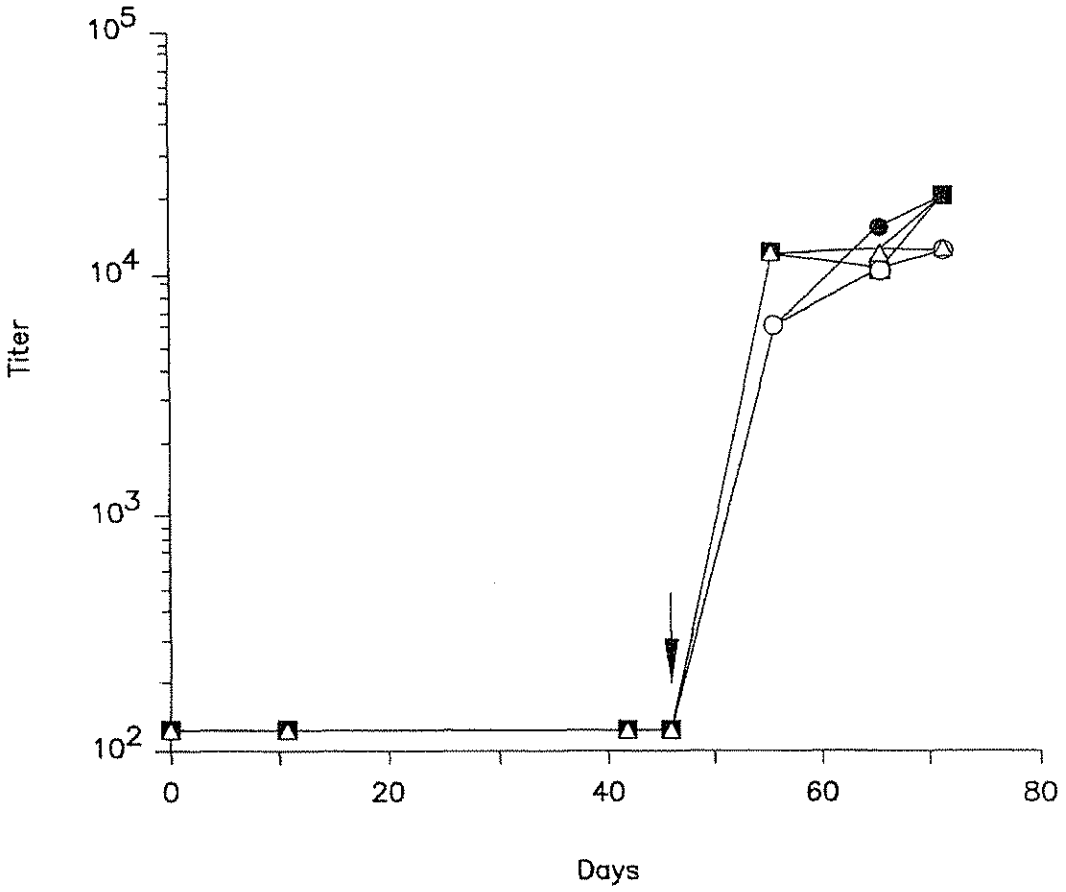

FIG. 16

Digitized by Google

METHODS FOR REGULATING THE IMMUNE RESPONSE USING B7 BINDING MOLECULES AND IL4-BINDING MOLECULES

This application is a continuation-in-part of U.S. Ser. No. 723,617, filed Jul. 27, 1991, the contents of which are incorporated by reference into the present application

Throughout this application various publications are referenced. The disclosures of these publications in their entireties are hereby incorporated by reference into this application in order to more fully describe the state of the art to which this invention pertains.

The present invention relates to expression of the CTLA4 receptor gene, identification of the interaction between the receptor and cells expressing B7 antigen, and to methods for regulating cellular interactions involving the CTLA4 receptor and the B7 antigen.

BACKGROUND OF THE INVENTION

The hallmark of a vertebrate immune system is the ability to discriminate "self" from "non-self" (foreign). This property has led to the evolution of a system requiring multiple signals to achieve optimal immune activation (Janeway, *Cold Spring Harbor Symp. Quant. Biol.* 54:1–14 (1989)). T cell-B cell interactions are essential to the immune response. Levels of many cohesive molecules found on T cells and B cells increase during an immune response (Springer et al., (1987), supra; Shaw and Shimuzu, *Current Opinion in Immunology*, Eds. Kindt and Long, 1:92–97 (1988)); and Hemler *Immunology Today* 9:109–113 (1988)). Increased levels of these molecules may help explain why activated B cells are more effective at stimulating antigen-specific T cell proliferation than are resting B cells (Kaiuchi et al., *J. Immunol.* 131:109–114 (1983); Kreiger et al., *J. Immunol.* 135:2937–2945 (1985); McKenzie, *J. Immunol.* 141:2907–2911 (1988); and Hawrylowicz and Unanue, *J. Immunol.* 141:4083–4088 (1988)).

The generation of a T lymphocyte ("T cell") immune response is a complex process involving cell-cell interactions (Springer et al., *A. Rev. Immunol.* 5:223–252 (1987)), particularly between T and accessory cells such as B cells, and production of soluble immune mediators (cytokines or lymphokines) (Dinarello and Mier, *New Engl. Jour. Med* 317:940–945 (1987)). This response is regulated by several T-cell surface receptors, including the T-cell receptor complex (Weiss et al., *Ann. Rev. Immunol.* 4:593–619 (1986)) and other "accessory" surface molecules (Springer et al., (1987) supra). Many of these accessory molecules are naturally occurring cell surface differentiation (CD) antigens defined by the reactivity of monoclonal antibodies on the surface of cells (McMichael, Ed., *Leukocyte Typing III*, Oxford Univ. Press, Oxford, N.Y. (1987)).

Antigen-independent intercellular interactions involving lymphocyte accessory molecules are essential for an immune response (Springer et al., (1987), supra). For example, binding of the T cell-associated protein, CD2, to its ligand LFA-3, a widely expressed glycoprotein (reviewed in Shaw and Shimuzu, supra), is important for optimizing antigen-specific T cell activation (Moingeon et al., *Nature* 339:314 (1988)).

An important adhesion system involves binding of the LFA-1 glycoprotein found on lymphocytes, macrophages, and granulocytes (Springer et al., (1987), supra; Shaw and Shimuzu (1988), supra) to its ligands ICAM-1 (Makgoba et al., *Nature* 331:86–88 (1988)) and ICAM-2 (Staunton et al., *Nature* 339:61–64 (1989)). The T cell accessory molecules CD8 and CD4 strengthen T cell adhesion by interaction with MHC class I (Norment et al., *Nature* 336:79–81 (1988)) and class II (Doyle and Strominger, *Nature* 330:256–259 (1987)) molecules, respectively. "Homing receptors" are important for control of lymphocyte migration (Stoolman, *Cell* 56:907–910 (1989)).

The VLA glycoproteins are integrins which appear to mediate lymphocyte functions requiring adhesion to extracellular matrix components (Hemler, supra). The CD2/LFA-3, LFA-1/ICAM-1 and ICAM-2, and VLA adhesion systems are distributed on a wide variety of cell types (Springer et al., (1987), supra; Shaw and Shimuzu, (1988,) supra and Hemler, (1988), supra).

Numerous in vitro studies have demonstrated that cytokines are involved in the generation of alloreactive effector cells. For example, membrane bound IL-4 and soluble IL-4 receptor were administered separately to mice and were shown to augment the lymphoproliferative response (William C. Fanslow et al. "Regulation of Alloreactivity in vivo by IL-4 and the soluble Il-4 receptor" J. Immunol. 147:535–540 (1991)). Specifically, administration of IL-4 to BALB\c mice resulted in slight augmentation of the lymphoproliferative response. In contrast, the soluble IL-4 receptor suppressed this response to allogeneic cells in a dose dependent manner. Moreover, a neutralizing antibody against IL-4 and another against soluble IL-4 receptor were effective inhibitors of the lymphoproliferative response.

It was proposed many years ago that B lymphocyte activation requires two signals (Bretscher and Cohn, *Science* 169:1042–1049 (1970)) and now it is believed that all lymphocytes require two signals for their optimal activation, an antigen specific or clonal signal, as well as a second, antigen non-specific signal (Janeway, supra). Freeman et al. (*J. Immunol.* 143(8):2714–2722 (1989)) isolated and sequenced a cDNA clone encoding a B cell activation antigen recognized by mAb B7 (Freeman et al., *J. Immunol.* 138:3260 (1987)). COS cells transfected with this cDNA have been shown to stain by both labeled mAb B7 and mAb BB-1 (Clark et al., *Human Immunol.* 16:100–113 (1986); Yokochi et al., *J. Immunol.* 128:823 (1981)); Freeman et al., (1989) supra; and Freedman et al., (1987), supra)). In addition, expression of this antigen has been detected on cells of other lineages, such as monocytes (Freeman et al., supra).

The signals required for a T helper cell (T_h) antigenic response are provided by antigen-presenting cells (APC). The first signal is initiated by interaction of the T cell receptor complex (Weiss, *J. Clin. Invest.* 86:1015 (1990)) with antigen presented in the context of class II major histocompatibility complex (MHC) molecules on the APC (Allen, *Immunol. Today* 8:270 (1987)). This antigen-specific signal is not sufficient to generate a full response, and in the absence of a second signal may actually lead to clonal inactivation or anergy (Schwartz, *Science* 248:1349 (1990)). The requirement for a second "costimulatory" signal provided by the MHC has been demonstrated in a number of experimental systems (Schwartz, supra; Weaver and Unanue, *Immunol. Today* 11:49 (1990)). The molecular nature of this second signal(s) is not completely understood, although it is clear in some cases that both soluble molecules such as interleukin (IL)-1 (Weaver and Unanue, supra) and membrane receptors involved in intercellular adhesion (Springer, *Nature* 346:425 (1990)) can provide costimulatory signals.

CD28 antigen, a homodimeric glycoprotein of the immunoglobulin superfamily (Aruffo and Seed, *Proc. Natl. Acad.*

Google

Sci. 84:8573–8577 (1987)), is an accessory molecule found on most mature human T cells (Damle et al., *J. Immunol.* 131:2296–2300 (1983)). Current evidence suggests that this molecule functions in an alternative T cell activation pathway distinct from that initiated by the T-cell receptor complex (June et al., *Mol. Cell. Biol.* 7:4472–4481 (1987)). Monoclonal antibodies (mAbs) reactive with CD28 antigen can augment T cell responses initiated by various polyclonal stimuli (reviewed by June et al., supra). These stimulatory effects may result from mAb-induced cytokine production (Thompson et al., *Proc. Natl. Acad. Sci* 86:1333–1337 (1989); and Lindsten et al., *Science* 244:339–343 (1989)) as a consequence of increased mRNA stabilization (Lindsten et al., (1989), supra). Anti-CD28 mAbs can also have inhibitory effects, i.e., they can block autologous mixed lymphocyte reactions (Damle et al., *Proc. Natl. Acad. Sci.* 78:5096–6001 (1981)) and activation of antigen-specific T cell clones (Lesslauer et al., *Eur. J. Immunol.* 16:1289–1296 (1986)).

Studies have shown that CD28 is a counter-receptor for the B cell activation antigen, B7/BB-1 (Linsley et al, *Proc. Natl. Acad. Sci. USA* 87:5031–5035 (1990)). For convenience the B7/BB-1 antigen is hereafter referred to as the "B7 antigen".

Interactions between CD28 and B7 antigen have been characterized using genetic fusions of the extracellular portions of B7 antigen and CD28 receptor, and Immunoglobulin (Ig) Cγ1 (constant region heavy chains) (Linsley et al, *J. Exp. Med.* 173:721–730 (1991)). Immobilized B7Ig fusion protein, as well as B7 positive CHO cells, have been shown to costimulate T cell proliferation.

T cell stimulation with B7 positive CHO cells also specifically stimulates increased levels of transcripts for IL-2. Additional studies have shown that anti-CD28 mAb inhibited IL-2 production induced in certain T cell leukemia cell lines by cellular interactions with a B cell leukemia line (Kohno et al., *Cell. Immunol.* 131-1-10 (1990)).

CD28 has a single extracellular variable region (V)-like domain (Aruffo and Seed, supra). A homologous molecule, CTLA4 has been identified by differential screening of a murine cytolytic-T cell cDNA library (Brunet et al., *Nature* 328:267–270 (1987)).

Transcripts of the CTLA4 molecule have been found in T cell populations having cytotoxic activity, suggesting that CTLA4 might function in the cytolytic response (Brunet et al., supra; and Brunet et al., *Immunol. Rev.* 103-21-36 (1988)). Researchers have reported the cloning and mapping of a gene for the human counterpart of CTLA4 (Dariavach et al., *Eur. J. Immunol.* 18:1901–1905 (1988)) to the same chromosomal region (2q33-34) as CD28 (Lafage-Pochitaloff et al., *Immunogenetics* 31:198–201 (1990)).

Sequence comparison between this human CTLA4 DNA and that encoding CD28 proteins reveals significant homology of sequence, with the greatest degree of homology in the juxtamembrane and cytoplasmic regions (Brunet et al., 1988, supra; Dariavach et al., 1988, supra).

The high degree of homology between CD28 and CTLA4, together with the co-localization of their genes, raises questions as to whether these molecules are also functionally related. However, since the protein product of CTLA4 has not yet been successfully expressed, these questions remain unanswered.

Expression of soluble derivatives of cell-surface glycoproteins in the immunoglobulin gene superfamily has been achieved for CD4, the receptor for HIV-1, and CD28 and B7 receptors, using hybrid fusion molecules consisting of DNA sequences encoding amino acids corresponding to portions of the extracellular domain of CD4 receptor fused to antibody domains (immunoglobulin γ1 (Capon et al., *Nature* 337:525–531 (1989) (CD4) and Linsley et al., *J. Exp. Med.*, supra (CD28 and B7)).

There is a need for the present invention. At present, the major therapies to prevent the rejection of organ transplants rely on panimmunosuppressive drugs, such as cyclosporine A or monoclonal antibodies (MAbs) to CD3. These drugs must frequently be taken for the life of the individual, depress the entire immune system, and often result in secondary health ailments such as increased frequency of infections and cancer.

SUMMARY OF THE INVENTION

Accordingly, the present invention provides the complete and correct DNA sequence encoding the amino acid sequence corresponding to the CTLA4 receptor protein, and identifies B7 antigen as a natural ligand for the CTLA4 receptor. The invention also provides a method for expressing the DNA as a CTLA4 immunoglobulin (Ig) fusion protein product. Embodiments of the invention include CTLA4Ig fusion protein, and hybrid fusion proteins including CD28Ig/CTLA4Ig fusion proteins. Also provided are methods for using the CTLA4 fusion protein, B7Ig fusion protein, hybrid fusion proteins, and fragments and/or derivatives thereof, such as monoclonal antibodies reactive with CTLA4 and the B7 antigen, to regulate cellular interactions and immune responses.

The human CTLA receptor protein of the invention is encoded by 187 amino acids and includes a newly identified N-linked glycosylation site.

The CTLA4Ig fusion protein of the invention binds the B7 antigen expressed on activated B cells, and cells of other lineages, a ligand for CD28 receptor on T cells. The CTLA4Ig binds B7 antigen with significantly higher affinity than B7 binding to the CD28 receptor. The CTLA4Ig construct has a first amino acid sequence corresponding to the extracellular domain of the CTLA4 receptor fused to a second amino acid sequence corresponding to the human Ig Cγ1 domain. The first amino acid sequence contains amino acid residues from about position 1 to about position 125 of the amino acid sequence corresponding to the extracellular domain of CTLA4 joined to a second amino acid sequence containing amino acid residues corresponding to the hinge, CH2 and CH3 regions of human IgCγ1. The fusion protein is preferably produced in dimeric form. Soluble CTLA4Ig is a potent inhibitor in vitro of T and B lymphocyte responses.

Also contemplated in the invention are hybrid fusion proteins such as CD28Ig/CTLA4Ig fusion proteins having a first amino acid sequence corresponding to fragments of the extracellular domain of CD28 joined to a second amino acid sequence corresponding to fragments of the extracellular domain of CTLA4Ig and a third amino acid sequence corresponding to the hinge, CH2 and CH3 regions of human IgCγ1. One embodiment of the hybrid fusion proteins is a CD28Ig/CTLA4Ig fusion construct having a first amino acid sequence containing amino acid residues from about position 1 to about position 94 of the amino acid sequence corresponding to the extracellular domain of CD28, joined a second amino acid sequence containing amino acid residues from about position 94 to about position 125 of the amino acid sequence corresponding to the extracellular domain of CTLA4, joined to a third amino acid sequence containing amino acids residues corresponding to the hinge, CH2 and CH3 regions of human IgCγ1.

Digitized by Google

Also included in the invention is a method for regulating T cell interactions with other cells by inhibiting the interaction of CTLA4-positive T cells with B7 positive cells by reacting the T cells with ligands for the CTLA4 receptor. The ligands include B7Ig fusion protein, a monoclonal antibody reactive with CTLA4 receptor, and antibody fragments.

The invention also provides a method for regulating T cell interactions with B7 positive cells, using a ligand for the B7 antigen. Such a ligand is the CTLA4Ig fusion protein of the invention, its fragments or derivatives, the CD28Ig/CTLA4Ig fusion protein hybrid, or a monoclonal antibody reactive with the B7 antigen.

The invention further includes a method for treating immune system diseases mediated by T cell interactions with B7 positive cells by administering a ligand reactive with B7 antigen to regulate T cell interactions with B7 positive cells. The ligand is the CTLA4Ig fusion protein, or the CD28Ig/CTLA4Ig fusion protein hybrid, or a monoclonal antibody reactive with B7 antigen.

A monoclonal antibody reactive with the CTLA4Ig fusion protein and a monoclonal antibody reactive with CD28Ig/CTLA4Ig fusion protein are described for use in regulating cellular interactions.

A novel Chinese Hamster Ovary cell line stably expressing the CTLA4Ig fusion protein is also disclosed.

Further, the present invention provides a method for blocking B7 interaction so as to regulate the immune response. This method comprises contacting lymphocytes with a CTLA4-binding molecule and an IL4-binding molecule.

Additionally, the present invention provides a method for regulating an immune response which comprises contacting B7-positive lymphocytes with a CTLA4-binding molecule and an IL4-binding molecule.

Also, the invention provides method for inhibiting tissue transplant rejection by a subject, the subject being a recipient of transplanted tissue. This method comprises administering to the subject a CTLA4-binding molecule and an IL4-binding molecule.

The present invention further provides a method for inhibiting graft versus host disease in a subject which comprises administering to the subject a CTLA4-binding molecule and an IL4-binding molecule.

BRIEF DESCRIPTION OF THE FIGURES

FIG. **1** is a diagrammatic representation of CTLA4Ig fusion constructs as described in Example 2, infra.

FIG. **2** is a photograph of a gel obtained from SDS-PAGE chromatographic purification of CTLA4Ig as described in Example 2, infra.

FIG. **3** depicts the complete amino acid sequence encoding human CTLA4 receptor (SEQ ID NOs: 13 and 14) fused to the oncostatin M signal peptide (position −25 to −1), and including the newly identified N-linked glycosylation site (position 109–111), as described in Example 3, infra.

FIG. **4** depicts the results of FACS® analysis of binding of the B7Ig fusion protein to CD28- and CTLA4-transfected COS cells as described in Example 4, infra.

FIG. **5** depicts the results of FACS® analysis of binding of purified CTLA4Ig on B7 antigen-positive ($B7^+$) CHO cells and on a lymphoblastoid cell line (PM LCL) as described in Example 4, infra.

FIG. **6** is a graph illustrating competition binding analysis of ^{125}I labeled B7Ig to immobilized CTLA4Ig as described in Example 4, infra.

FIG. **7** is a graph showing the results of Scatchard analysis of ^{125}I-labeled B7Ig binding to immobilized CTLA4Ig as described in Example 4, infra.

FIG. **8** is a photograph of a gel from SDS-PAGE chromatography of immunoprecipitation analysis of B7 positive CHO cells and PM LCL cells surface-labeled with ^{125}I as described in Example 4, infra.

FIG. **9** is a graph depicting the effects on proliferation of T cells of CTLA4Ig as measured by [^3H]-thymidine incorporation as described in Example 4, infra.

FIG. **10** is a bar graph illustrating the effects of CTLA4Ig on helper T cell (T_h)-induced immunoglobulin secretion by human B cells as determined by enzyme immunoassay (ELISA) as described in Example 4, infra.

FIGS. **11A**, **11B**, and **11C** are line graphs showing the survival of human pancreatic islet xenografts.

FIGS. **12A**, **12B**, **12C**, and **12D** are photographs of histopathology slides of human islets transplanted under the kidney capsule of B10 mice.

FIG. **13** is a line graph showing the prolongation of islet graft survival with MAb to human B7.

FIG. **14** is a line graph showing induction of donor-specific unresponsiveness to islet graft antigens by CTLA4Ig.

FIG. **15** is a line graph showing antibody serum titer levels of mice injected with sheep red blood cells (SRBC), mAb L6 and rat Ig, mAb L6 and anti-IL4, CTLA4Ig and rat Ig, CTLA4Ig and anti-IL4. The X axis measures the antibody-serum titer. The Y axis measures time in days. The closed box represents mice injected with SRBC at day 0 and day 46. The open box represents mice injected with SRBC at day 46. The closed circle represents mice injected with mAb L6 and rat immunoglobulin. The open circle represents mice injected with mAb L6 and anti-IL4 antibody. The closed triangle represents mice injected with CTLA4Ig and rat immunoglobulin. The open triangle represents mice injected with CTLA4Ig and anti-IL4 antibody.

FIG. **16** is a line graph showing antibody serum titer levels of mice injected with KLH, mAb L6 and rat Ig, mAb L6 and anti-IL4, CTLA4Ig and rat Ig, CTLA4Ig and anti-IL4. The X axis measures the antibody-serum titer. The Y axis measures time in days. The closed box represents mice injected with keyhole limpet hemocyanin (KLH) at day 46. The closed circle represents mice injected with mAb L6 and rat immunoglobulin. The open circle represents mice injected with mAb L6 and anti-IL4 antibody. The closed triangle represents mice injected with CTLA4Ig and rat immunoglobulin. The open triangle represents mice injected with CTLA4Ig and anti-IL4 antibody.

DETAILED DESCRIPTION OF THE INVENTION

Definition

As used in this application, the following words or phrases have the meanings specified.

As used herein "blocking B7 interaction" means to interfere with the binding of the B7 antigen to its ligands such as CD28 and CTLA4 thereby obstructing T cell and B cell interaction.

As used herein a "B7-binding molecule" means any molecule which will bind the B7 antigen.

As used herein an "IL4-binding molecule" means any molecule which will recognize and bind to IL4.

In order that the invention herein described may be more fully understood, the following description is set forth.

Google

This invention is directed to the isolation and expression of the human CTLA4 receptor found on T cell surfaces, which binds to the B7 antigen expressed on activated B cells, and cells of other lineages, and to expression of soluble fusion protein products of the CTLA4 receptor gene. The invention also provides methods for using the expressed CTLA4 receptor to regulate cellular interactions, including T cell interactions with B7 positive cells.

In a preferred embodiment, the complete and correct DNA sequence encoding the amino acid sequence corresponding to human CTLA4 receptor protein of the invention is cloned using PCR. The cDNA containing the complete predicted coding sequence of CTLA4 was assembled from two PCR fragments amplified from H38 RNA, and inserted into the expression vector, CDM8 as described in detail in the Examples, infra. Isolates were transfected into COS cells and tested for binding of B7Ig, a soluble fusion protein having an amino acid sequence corresponding to the extracellular domain of B7 and a human immunoglobulin (Ig) Cγ1 region, as described by Linsley et al., *J. Exp. Med.* 173:721–730 (1991).

The DNA sequence of one isolate, designated as OMCTLA4, was then determined and found to correspond exactly to the predicted human CTLA4 sequence, fused at the N-terminus to the signal peptide from oncostatin M. The CTLA4 receptor is encoded by 187 amino acids (exclusive of the signal peptide and stop codons) and includes a newly identified N-linked glycosylation site at amino acid positions 109–111 (see FIG. 3, infra). The CTLA4 receptor is expressed using the oncostatin M signal peptide.

In another preferred embodiment, soluble forms of the protein product of the CTLA4 receptor gene (CTLA4Ig) are prepared using fusion proteins having a first amino acid sequence corresponding to the extracellular domain of CTLA4 and a second amino acid sequence corresponding to the human IgCγ1 domain. Cloning and expression plasmids (CDM8 and πLN) were constructed containing cDNAs encoding portions of the amino acid sequence corresponding to human CTLA4 receptor based on the cDNA sequence described herein, where the cDNA encoding a first amino acid sequence corresponding to a fragment of the extracellular domain of the CTLA4 receptor gene is joined to DNA encoding a second amino acid sequence corresponding to an IgC region that permits the expression of the CTLA4 receptor gene by altering the solubility of the expressed CTLA4 protein. Thus, soluble CTLA4Ig fusion protein is encoded by a first amino acid sequence containing amino acid residues from about position 1 to about position 125 of the amino acid sequence corresponding to the extracellular domain of CTLA4 joined to a second amino acid sequence containing amino acid residues corresponding to the hinge, CH2 and CH3 regions of human IgCγ1. The fusion protein is preferably produced in dimeric form. The construct was then transfected into COS or CHO cells, and CTLA4Ig was purified and identified as a dimer.

In accordance with the practice of this invention, CTLA4Ig and the CTL4Ig/CD28 fusion protein hybrid may have amino acid substitutions in the amino acid sequence corresponding to the external domain of CTLA4 so as to produce molecules which would retain the functional property of CTLA4, namely, the molecule having such substitutions will still bind the B7 antigen. These amino acid substitutions include, but are not necessarily limited to, amino acid substitutions known in the art as "conservative".

For example, it is a well-established principle of protein chemistry that certain amino acid substitutions, entitled "conservative amino acid substitutions," can frequently be made in a protein without altering either the conformation or the function of the protein. Such changes include substituting any of isoleucine (I), valine (V), and leucine (L) for any other of these hydrophobic amino acids; aspartic acid (D) for glutamic acid (E) and vice versa; glutamine (Q) for asparagine (N) and vice versa; and serine (S) for threonine (T) and vice versa. Other substitutions can also be considered conservative, depending on the environment of the particular amino acid and its role in the three-dimensional structure of the protein. For example, glycine (G) and alanine (A) can frequently be interchangeable, as can alanine and valine (V).

Methionine (M), which is relatively hydrophobic, can frequently be interchanged with leucine and isoleucine, and sometimes with valine. Lysine (K) and arginine (R) are frequently interchangeable in locations in which the significant feature of the amino acid residue is its charge and the differing pK's of these two amino acid residues are not significant. Still other changes can be considered "conservative" in particular environments.

In fact, using the methodologies disclosed herein, mutants of the CTLA4-binding molecule were produced. One mutant comprises (1) a sequence beginning with the amino acid at position 1 and ending with the amino acid at position 95 of the CD28 receptor protein (Aruffo and Seed 1987); (2) a sequence beginning with the amino acid at position 95 and ending with amino acid at position 125 of the extracellular domain of CTLA4 (Brunet et al. 1987); and (3) a sequence corresponding to the human IgCγ1 domain.

The second mutant comprises (1) a sequence beginning with the amino acid at position 1 and ending with the amino acid at position 95 of the CD28 receptor protein (Aruffo and Seed 1987); (2) a sequence beginning with the amino acid at position 95 and ending with amino acid at position 120 of the extracellular domain of CTLA4 (Brunet et al. 1987); and (3) a sequence corresponding to the human IgCγ1 domain.

The present invention provides a method for blocking B7 interaction so as to regulate the immune response which comprises contacting lymphocytes with a B7-binding molecule and an IL4-binding molecule. The lymphocytes may be B7 positive lymphocytes.

Further, the present invention provides a method for regulating an immune response which comprises contacting B7-positive lymphocytes with a B7-binding molecule and an IL4-binding molecule.

The immune response may be a B cell response resulting in the inhibition of antibody production. Additionally, the immune response may be a T cell response resulting in inhibition of cell mediated immunity. Further, the immune response may be an inhibition of lymphocyte proliferation.

Also, the present invention provides a method for inhibiting tissue transplant rejection by a subject, the subject being a recipient of transplanted tissue. This method can comprise administering to the subject a CTLA4-binding molecule and an IL4-binding molecule.

The invention further provides a method for inhibiting graft versus host disease in a subject which comprises administering to the subject a CTLA4-binding molecule and an IL4-binding molecule.

In accordance with the practice of this invention, the CTLA4-binding molecule may be a CTLA4Ig fusion protein. For example, the CTLA4Ig fusion protein may be a fusion protein having a first amino acid sequence containing amino acid residues from about position 1 to about position 125 of the amino acid sequence corresponding to the extracellular domain of CTLA4 and a second amino acid

Digitized by Google

sequence containing amino acid residues corresponding to the hinge, CH2 and CH3 regions of human immunoglobulin Cγ1.

Alternatively, the CTLA4-binding molecule may be a CD28Ig/CTLA4Ig fusion protein hybrid. For example, the CD28Ig/CTLA4Ig fusion protein hybrid may be a fusion protein hybrid having a first amino acid sequence corresponding to a portion of the extracellular domain of CD28 receptor fused to a second amino acid sequence corresponding to a portion of the extracellular domain of CTLA4 receptor and a third amino acid sequence corresponding to the hinge, CH2 and CH3 regions of human immunoglobulin Cγ1.

Further, the IL4-binding molecule may be a monoclonal antibody which specifically recognizes and binds to IL4. Alternatively, the IL4-binding molecule is a soluble IL4 receptor which recognizes and binds to IL4 (Fanslow et al. 1991).

DNA encoding the amino acid sequence corresponding to the CTLA4Ig fusion protein has been deposited with the American Type Culture Collection (ATCC) in Rockville, Md., under the provisions of the Budapest Treaty on May 31, 1991 and has been accorded ATCC accession number: 68629.

The present invention provides the first protein product of CTLA4 transcripts in the form of a soluble fusion protein. The CTLA4Ig protein forms a disulfide-linked dimer having two subunits, each of which has an M_r of approximately 50,000 indicating that native CTLA4 probably exists on the T cell surface as a disulfide-linked homodimer.

B7 antigen has been shown to be a ligand for CD28 receptor on T cells (Linsley et al., *Proc. Natl. Acad. Sci. USA*, supra). The CTLA4 receptor molecule appears functionally and structurally related to the CD28 receptor; both are receptors for the B cell activation antigen, B7, while CTLA4 appears to have higher affinity for B7, among the highest yet reported for lymphoid adhesion systems. However, CTLA4Ig was shown to bind more strongly to B7 positive ($B7^+$) cell lines than CD28Ig. Other experiments demonstrated that CTLA4 is a higher affinity receptor for B7 antigen than CD28 receptor. Additionally, CTLA4Ig was shown to bind a single protein on lymphoblastoid cells which is similar in size to the B7 antigen. CTLA4Ig inhibited T cell proliferation and inhibited T_h-induced IgM production.

In another preferred embodiment, hybrid fusion proteins having amino acid sequences corresponding to fragments of different receptor proteins were constructed. For example, amino acid sequences corresponding to selected fragments of the extracellular domains of CD28 and CTLA4 were linked to form CD28Ig/CTLA4Ig hybrid fusion proteins. Thus, a CD28Ig/CTLA4Ig fusion protein was obtained having a first amino acid sequence containing amino acid residues corresponding to a fragment of the extracellular domain of CD28 joined to a second amino acid sequence corresponding to a fragment of the extracellular domain of CTLA4Ig and to a third amino acid sequence corresponding to the hinge, CH2 and CH3 regions of human IgCγ1. One embodiment of the hybrid fusion proteins is a CD28Ig/CTLA4Ig fusion construct having a first amino acid sequence containing amino acid residues from about position 1 to about position 94 of the amino acid sequence corresponding to the extracellular domain of CD28, joined to a second amino acid sequence containing amino acid residues from about position 94 to about position 125 of the amino acid sequence corresponding to the extracellular domain of CTLA4, joined to a third amino acid sequence corresponding to the hinge, CH2 and CH3 regions of human IgCγ1.

The techniques for cloning and expressing DNA sequences encoding the amino acid sequences corresponding to the CTLA4 receptor protein, soluble fusion proteins and hybrid fusion proteins, e.g synthesis of oligonucleotides, PCR, transforming cells, constructing vectors, expression systems, and the like are well-established in the art, and most practitioners are familiar with the standard resource materials for specific conditions and procedures. However, the following paragraphs are provided for convenience and notation of modifications where necessary, and may serve as a guideline.

Cloning and Expression of Coding Sequences for Receptors and Fusion Proteins

Fusion protein constructs corresponding to CD28IgCγ1 and B7IgCγ1 for characterizing the CTLA4Ig of the present invention, and for preparing CD28Ig/CTLA4Ig fusion hybrids, were prepared as described by Linsley et al., *J. Exp. Med.* 173:721–730 (1991), incorporated by reference herein. Alternatively, cDNA clones may be prepared from RNA obtained from cells expressing B7 antigen and CD28 receptor based on knowledge of the published sequences for these proteins (Aruffo and Seed, and Freeman, supra) using standard procedures.

CTLA4Ig fusions consisting of DNA encoding amino acid sequences corresponding to the extracellular domain of CTLA4 and the hinge, CH2 and CH3 regions of human IgCγ1 were constructed by ligation of PCR fragments. The cDNA encoding the amino acid sequences is amplified using the polymerase chain reaction ("PCR") technique (see U.S. Pat. Nos. 4,683,195 and 4,683,202 to Mullis et al. and Mullis & Faloona, *Methods Enzymol.* 154:335–350 (1987)). CTLA4Ig fusion polypeptides were obtained having DNA encoding amino acid sequences containing amino acid residues from about position 1 to about position 125 of the amino acid sequence corresponding to the extracellular domain of CTLA4 and DNA encoding amino acid sequences corresponding to the hinge, CH2 and CH3 regions of Ig Cγ1.

Because the expression of CTLA4 receptor protein in human lymphoid cells has not been previously reported, it was necessary to locate a source of CTLA4 mRNA. PCR cDNA made from the total cellular RNA of several human leukemia cell lines was screened, using as primers, oligonucleotides from the published sequence of the CTLA4 gene (Dariavach et al., supra). Of the cDNA tested, H38 cells (an HTLV II-associated leukemia line) provided the best yield of PCR products having the expected size. Since a signal peptide for CTLA4 was not identified in the CTLA4 gene, the N terminus of the predicted sequence of CTLA4 was fused to the signal peptide of oncostatin M (Malik et al., *Molec. and Cell. Biol.* 9:2847 (1989)) in two steps using oligonucleotides as described in the Examples, infra. The product of the PCR reaction was ligated with cDNA encoding the amino acid sequences corresponding to the hinge, CH2 and CH3 regions of Ig Cγ1 into a expression vector, such as CDM8 or πLN.

To obtain DNA encoding full length human CTLA4, a cDNA encoding the transmembrane and cytoplasmic domains of CTLA4 was obtained by PCR from H38 cells and joined with a fragment from CTLA4Ig, obtained as described above, encoding the oncostatin M signal peptide fused to the N terminus of CTLA4, using oligonucleotide primers as described in the Examples, infra. PCR fragments were ligated into the plasmid CDM8, resulting in an expression plasmid encoding the full length CTLA4 gene, and designated OMCTLA4.

Digitized by Google

For construction of DNA encoding the amino acid sequence corresponding to hybrid fusion proteins, DNA encoding amino acids corresponding to portions of the extracellular domain of one receptor gene is joined to DNA encoding amino acids corresponding to portions of the extracellular domain of another receptor gene, and to DNA encoding the amino acid sequences corresponding to the hinge, CH2 and CH3 regions of human IgCγ1 using procedures as described above for the B7Ig, CD28Ig and CTLA4Ig constructs. Thus, for example, DNA encoding amino acid residues from about position 1 to about position 94 of the amino acid sequence corresponding to the extracellular domain of the CD28 receptor is joined to DNA encoding amino acid residues from about position 94 to about position 125 of the amino acid sequence corresponding to the extracellular domain of the CTLA4 receptor and to DNA encoding the amino acid sequences corresponding to the hinge, CH2 and CH3 regions of human IgCγ1.

To produce large quantities of cloned DNA, vectors containing DNA encoding the fusion constructs of the invention are transformed into suitable host cells, such as the bacterial cell line *E. coli* strain MC1061/p3 (Invitrogen Corp., San Diego, Calif.) using standard procedures, and colonies are screened for the appropriate plasmids.

The clones containing DNA encoding fusion constructs obtained as described above are then transfected into suitable host cells for expression. Depending on the host cell used, transfection is performed using standard techniques appropriate to such cells. For example, transfection into mammalian cells is accomplished using DEAE-dextran mediated transfection, $CaP0_4$ co-precipitation, lipofection, electroporation, or protoplast fusion, and other methods known in the art including: lysozyme fusion or erythrocyte fusion, scraping, direct uptake, osmotic or sucrose shock, direct microinjection, indirect microinjection such as via erythrocyte-mediated techniques, and/or by subjecting host cells to electric currents. The above list of transfection techniques is not considered to be exhaustive, as other procedures for introducing genetic information into cells will no doubt be developed.

Expression in eukaryotic host cell cultures derived from multicellular organisms is preferred (see *Tissue Cultures*, Academic Press, Cruz and Patterson, Eds. (1973)). These systems have the additional advantage of the ability to splice out introns and thus can be used directly to express genomic fragments. Useful host cell lines include Chinese hamster ovary (CHO), monkey kidney (COS), VERO and HeLa cells. In the present invention, cell lines stably expressing the fusion constructs are preferred.

Expression vectors for such cells ordinarily include promoters and control sequences compatible with mammalian cells such as, for example, CMV promoter (CDM8 vector) and avian sarcoma virus (ASV) (πLN vector). Other commonly used early and late promoters include those from Simian Virus 40 (SV 40) (Fiers, et al., *Nature* 273:113 (1973)), or other viral promoters such as those derived from polyoma, Adenovirus 2, and bovine papilloma virus. The controllable promoter, hMTII (Karin, et al., *Nature* 299:797–802 (1982)) may also be used. General aspects of mammalian cell host system transformations have been described by Axel (U.S. Pat. No. 4,399,216 issued Aug. 16, 1983). It now appears, that "enhancer" regions are important in optimizing expression; these are, generally, sequences found upstream or downstream of the promoter region in non-coding DNA regions. Origins of replication may be obtained, if needed, from viral sources. However, integration into the chromosome is a common mechanism for DNA replication in eukaryotes.

Although preferred host cells for expression of the fusion constructs include eukaryotic cells such as COS or CHO cells, other eukaryotic microbes may be used as hosts. Laboratory strains of *Saccharomyces cerevisiae*, Baker's yeast, are most used although other strains such as *Schizosaccharomyces pombe* may be used. Vectors employing, for example, the 2μ origin of replication of Broach, *Meth. Enz.* 101:307 (1983), or other yeast compatible origins of replications (see, for example, Stinchcomb et al., *Nature* 282:39 (1979)); Tschempe et al., *Gene* 10:157 (1980); and Clarke et al., *Meth. Enz.* 101:300 (1983)) may be used. Control sequences for yeast vectors include promoters for the synthesis of glycolytic enzymes (Hess et al., *J. Adv. Enzyme Reg.* 7:149 (1968); Holland et al., *Biochemistry* 17:4900 (1978)). Additional promoters known in the art include the CMV promoter provided in the CDM8 vector (Toyama and Okayama, *FEBS* 268:217–221 (1990); the promoter for 3-phosphoglycerate kinase (Hitzeman et al., *J. Biol. Chem.* 255:2073 (1980)), and those for other glycolytic enzymes. Other promoters, which have the additional advantage of transcription controlled by growth conditions are the promoter regions for alcohol dehydrogenase 2, isocytochrome C, acid phosphatase, degradative enzymes associated with nitrogen metabolism, and enzymes responsible for maltose and galactose utilization. It is also believed terminator sequences are desirable at the 3' end of the coding sequences. Such terminators are found in the 3' untranslated region following the coding sequences in yeast-derived genes.

Alternatively, prokaryotic cells may be used as hosts for expression. Prokaryotes most frequently are represented by various strains of *E. coli*; however, other microbial strains may also be used. Commonly used prokaryotic control sequences which are defined herein to include promoters for transcription initiation, optionally with an operator, along with ribosome binding site sequences, include such commonly used promoters as the beta-lactamase (penicillinase) and lactose (lac) promoter systems (Chang et al., *Nature* 198: 1056 (1977)), the tryptophan (trp) promoter system (Goeddel et al., *Nucleic Acids Res.* 8:4057 (1980)) and the lambda derived P_L promoter and N-gene ribosome binding site (Shimatake et al., *Nature* 292:128 (1981)).

The nucleotide sequences encoding CD28Ig and CTLA4Ig proteins, and fusion hybrid proteins such as CD28Ig/CTLA4Ig, may be expressed in a variety of systems as set forth below. The cDNA may be excised by suitable restriction enzymes and ligated into suitable prokaryotic or eukaryotic expression vectors for such expression. Because CD28 and CTLA4 receptor proteins occur in nature as dimers, it is believed that successful expression of these proteins requires an expression system which permits these proteins to form as dimers. Truncated versions of these proteins (i.e. formed by introduction of a stop codon into the sequence at a position upstream of the transmembrane region of the protein) appear not to be expressed. The expression of CD28 and CTLA4 receptors as fusion proteins permits dimer formation of these proteins. Thus, expression of CTLA4 protein as a fusion product is preferred in the present invention.

A stable CHO line of the invention, designated Chinese Hamster Ovary Cell Line CTLA4Ig-24, is preferred for expression of CTLA4Ig and has been deposited with the ATCC under the terms of the Budapest Treaty on May 31, 1991, and accorded ATCC accession number 10762.

Expression of the CTLA4 receptor of the invention is accomplished transfecting a cell line such as COS cells, and detecting expression by binding of the CTLA4-transfected

Google

cells to a ligand for the CTLA4 receptor, for example by testing for binding of the cells to B7Ig fusion protein.

Sequences of the resulting constructs are confirmed by DNA sequencing using known procedures, for example as described by Sanger et al., *Proc. Natl. Acad. Sci. USA* 74:5463 (1977), as further described by Messing et al., *Nucleic Acids Res.* 9:309 (1981), or by the method of Maxam et al. *Methods Enzymol.* 65:499 (1980)).

Recovery of Protein Products

As noted above, CD28 and CTLA4 receptor genes are not readily expressed as mature proteins using direct expression of DNA encoding the truncated protein. To enable homodimer formation, DNA encoding the amino acid sequence corresponding to the extracellular domains of CD28 and CTLA4, and including the codons for a signal sequence such as that of oncostatin M in cells capable of appropriate processing, is fused with DNA encoding the amino acid sequence corresponding to the Fc domain of a naturally dimeric protein. Purification of these fusion protein products after secretion from the cells is thus facilitated using antibodies reactive with the anti-immunoglobulin portion of the fusion proteins. When secreted into the medium, the fusion protein product is recovered using standard protein purification techniques, for example by application to protein A columns.

USE

CTLA4Ig fusion protein and/or fragments of the fusion protein may be used to react with B7 positive cells, such as B cells, to regulate immune responses mediated by T cell interactions with the B7 antigen positive cells.

CTLA4Ig fusion protein and CTLA4Ig/CD28Ig hybrid proteins, and/or fragments and derivatives of these proteins, may also be used to react with B7 positive cells, including B cells, to regulate immune responses mediated by T cell dependent B cell responses. The term "fragment" as used herein means a portion of the amino acid sequence encoding the protein referred to as "CTLA4". A fragment of the CTLA4Ig fusion protein that may be used is a polypeptide having an amino acid sequence corresponding to some portion of the amino acid sequence corresponding to the CTLA4 receptor used to obtain the CTLA4Ig fusion protein as described herein.

The B7 antigen expressed on activated B cells and cells of other lineages, and the CD28 receptor expressed on T cells, can directly bind to each other, and this interaction can mediate cell-cell interaction. Such interactions directly trigger the CD28 activation pathway in T cells, leading to cytokine production, T cell proliferation, and B cell differentiation into immunoglobulin producing cells. The activation of B cells that occurs, can cause increased expression of B7 antigen and further CD28 stimulation, leading to a state of chronic inflammation such as in autoimmune diseases, allograft rejection, graft versus host disease or chronic allergic reactions. Blocking or inhibiting this reaction may be effective in preventing T cell cytokine production and thus preventing or reversing inflammatory reactions.

CTLA4Ig is shown herein to be a potent inhibitor of in vitro lymphocyte functions requiring T and B cell interaction. This indicates the importance of interactions between the B7 antigen and its counter-receptors, CTLA4 and/or CD28. The cytoplasmic domains of murine and human CTLA4 are similar (Dariavach et al., supra, 1988), suggesting that this region has important functional properties. The cytoplasmic domains of CD28 and CTLA4 also share homology.

CTLA4 is a more potent inhibitor in vitro of lymphocyte responses than either anti-BB1, or anti-CD28 mAbs. CTLA4Ig does not have direct stimulatory effects on T cell proliferation to counteract its inhibitory effects. Therefore, the CTLA4Ig fusion protein may perform as a better inhibitor in vivo than anti-CD28 monoclonal antibodies. The immunosuppressive effects of CTLA4Ig in vitro suggests its use in therapy for treatment of autoimmune disorders involving abnormal T cell activation or Ig production.

The CTLA4Ig fusion protein is expected to exhibit inhibitory properties in vivo. Thus, it is expected that CTLA4Ig will act to inhibit T cells in a manner similar to the effects observed for the anti-CD28 antibody, under similar conditions in vivo. Under conditions where T cell/B cell interactions are occurring as a result of contact between T cells and B cells, binding of introduced CTLA4Ig to react with B7 antigen positive cells, for example B cells, may interfere, i.e. inhibit, the T cell/B cell interactions resulting in regulation of immune responses. Because of this exclusively inhibitory effect, CTLA4Ig is expected to be useful in vivo as an inhibitor of T cell activity, over non-specific inhibitors such as cyclosporine and glucosteroids.

In one embodiment, the CTLA4Ig fusion protein or CTLA4Ig/CD28Ig hybrid proteins, may be introduced in a suitable pharmaceutical carrier in vivo, i.e. administered into a human subject for treatment of pathological conditions such as immune system diseases or cancer.

Introduction of the fusion protein in vivo is expected to result in interference with T cell interactions with other cells, such as B cells, as a result of binding of the ligand to B7 positive cells. The prevention of normal T cell interactions may result in decreased T cell activity, for example, decreased T cell proliferation. In addition, administration of the fusion protein in vivo is expected to result in regulation of in vivo levels of cytokines, including, but not limited to, interleukins, e.g. interleukin ("IL")-2, IL-3, IL-4, IL-6, IL-8, growth factors including tumor growth factor ("TGF"), colony stimulating factor ("CSF"), interferons ("IFNs"), and tumor necrosis factor ("TNF") to promote desired effects in a subject. For example, when the fusion protein is introduced in vivo, it may block production of cytokines, which contribute to malignant growth, for example of tumor cells. The fusion protein may also block proliferation of viruses dependent on T cell activation, such as the virus that causes AIDS, HTLV1.

Under some circumstances, as noted above, the effect of administration of the CTLA4Ig fusion protein or its fragments in vivo is inhibitory, resulting from blocking by the fusion protein of the CTLA4 and CD28 triggering resulting from T cell/B cell contact. For example, the CTLA4Ig protein may block T cell proliferation. Introduction of the CTLA4Ig fusion protein in vivo will thus produce effects on both T and B cell-mediated immune responses. The fusion protein may also be administered to a subject in combination with the introduction of cytokines or other therapeutic reagents.

In an additional embodiment of the invention, other reagents, including derivatives reactive with the CTLA4Ig fusion protein or the CTLA4 receptor are used to regulate T cell interactions. For example, antibodies, and/or antibody fragments reactive with the CTLA4 receptor may be screened to identify those capable of inhibiting the binding of the CTLA4Ig fusion protein to the B7 antigen. The antibodies or antibody fragments such as Fab or $F(ab')_2$ fragments, may then be used to react with the T cells, for example, to inhibit T cell proliferation.

Digitized by Google

Monoclonal antibodies reactive with CTLA4 receptor, may be produced by hybridomas prepared using known procedures, such as those introduced by Kohler and Milstein (see Kohler and Milstein, *Nature,* 256:495–97 (1975)), and modifications thereof, to regulate cellular interactions.

These techniques involve the use of an animal which is primed to produce a particular antibody. The animal can be primed by injection of an immunogen (e.g. the B7Ig fusion protein, CTLA4Ig fusion protein or CD28Ig/CTLA4Ig hybrid fusion protein) to elicit the desired immune response, i.e. production of antibodies from the primed animal. A primed animal is also one which is expressing a disease. Lymphocytes derived from the lymph nodes, spleens or peripheral blood of primed, diseased animals can be used to search for a particular antibody. The lymphocyte chromosomes encoding desired immunoglobulins are immortalized by fusing the lymphocytes with myeloma cells, generally in the presence of a fusing agent such as polyethylene glycol (PEG). Any of a number of myeloma cell lines may be used as a fusion partner according to standard techniques; for example, the P3-NS1/1-Ag4-1, P3-x63-Ag8.653, Sp2/0-Ag14, or HL1-653 myeloma lines. These myeloma lines are available from the ATCC, Rockville, Md.

The resulting cells, which include the desired hybridomas, are then grown in a selective medium such as HAT medium, in which unfused parental myeloma or lymphocyte cells eventually die. Only the hybridoma cells survive and can be grown under limiting dilution conditions to obtain isolated clones. The supernatants of the hybridomas are screened for the presence of the desired specificity, e.g. by immunoassay techniques using the CTLA4Ig protein that has been used for immunization. Positive clones can then be subcloned under limiting dilution conditions, and the monoclonal antibody produced can be isolated.

Various conventional methods can be used for isolation and purification of the monoclonal antibodies so as to obtain them free from other proteins and contaminants. Commonly used methods for purifying monoclonal antibodies include ammonium sulfate precipitation, ion exchange chromatography, and affinity chromatography (see Zola et al., in *Monoclonal Hybridoma Antibodies: Techniques and Applications*, Hurell (ed.) pp. 51–52 (CRC Press, 1982)). Hybridomas produced according to these methods can be propagated in vitro or in vivo (in ascites fluid) using techniques known in the art (see generally Fink et al., *Prog. Clin. Pathol.,* 9:121–33 (1984), FIG. 6-1 at p. 123).

Generally, the individual cell line may be propagated in vitro, for example, in laboratory culture vessels, and the culture medium containing high concentrations of a single specific monoclonal antibody can be harvested by decantation, filtration, or centrifugation.

In addition, fragments of these antibodies containing the active binding region reactive with the extracellular domain of CTLA4 receptor, such as Fab, $F(ab')_2$ and Fv fragments may be produced. Such fragments can be produced using techniques well established in the art (see e.g. Rousseaux et al., in *Methods Enzymol.,* 121:663–69, Academic Press (1986)).

Anti-B7 monoclonal antibodies prepared as described above may be used to bind to B7 antigen to inhibit interactions of CD28-positive or CTLA4-positive T cells with B7 positive cells. Anti-CTLA4 monoclonal antibodies may be used to bind to CTLA4 receptor to inhibit the interaction of CTLA4-positive T cells with other cells.

In another embodiment, the CTLA4Ig fusion protein may be used to identify additional compounds capable of regulating the interaction between CTLA4 and the B7 antigen. Such compounds may include small naturally occurring molecules that can be used to react with B cells and/or T cells. For example, fermentation broths may be tested for the ability to inhibit CTLA4/B7 interactions. In addition, derivatives of the CTLA4Ig fusion protein as described above may be used to regulate T cell proliferation. For example, the fragments or derivatives may be used to block T cell proliferation in graft versus host (GVH) disease which accompanies allogeneic bone marrow transplantation.

The CD28-mediated T cell proliferation pathway is cyclosporine-resistant, in contrast to proliferation driven by the CD3/Ti cell receptor complex (June et al., 1987, supra). Cyclosporine is relatively ineffective as a treatment for GVH disease (Storb, *Blood* 68:119–125 (1986)). GVH disease is thought to be mediated by T lymphocytes which express CD28 antigen (Storb and Thomas, *Immunol. Rev.* 88:215–238 (1985)). Thus, the CTLA4Ig fusion protein may be useful alone, or in combination with immunosuppressants such as cyclosporine, for blocking T cell proliferation in GVH disease.

Regulation of CTLA4-positive T cell interactions with B7 positive cells, including B cells, by the methods of the invention may thus be used to treat pathological conditions such as autoimmunity, transplantation, infectious diseases and neoplasia.

The CTLA4-binding molecules and IL4-binding molecules described herein may be in a variety of dosage forms which include, but are not limited to, liquid solutions or suspensions, tablets, pills, powders, suppositories, polymeric microcapsules or microvesicles, liposomes, and injectable or infusible solutions. The preferred form depends upon the mode of administration and the therapeutic application.

The most effective mode of administration and dosage regimen for the molecules of the present invention depends upon the severity and course of the disease, the subject's health and response to treatment and the judgment of the treating physician. Accordingly, the dosages of the molecules should be titrated to the individual subject.

The interrelationship of dosages for animals of various sizes and species and humans based on mg/m^2 of surface area is described by Freireich, E. J., et al. (Quantitative Comparison of Toxicity of Anticancer Agents in Mouse, Rat, Hamster, Dog, Monkey and Man. Cancer Chemother, Rep., 50, No.4, 219–244, May 1966).

Adjustments in the dosage regimen may be made to optimize the growth inhibiting response. Doses may be divided and administered on a daily basis or the dose may be reduced proportionally depending upon the situation. For example, several divided doses may be administered daily or the dose may be proportionally reduced as indicated by the specific therapeutic situation.

In accordance with the practice of the invention an effective amount for treating a subject may be between about 0.1 and about 10 mg/kg body weight of subject. Also, the effective amount may be an amount between about 1 and about 10 mg/kg body weight of subject.

Advantages of the Invention: The subject invention overcomes the problems associated with current therapies directed to preventing the rejection of tissue or organ transplants. In contrast to present therapies, the present invention affects only immunological responses mediated by B7 interactions.

For example, the present invention affects the transplant antigen-specific T cells, thus inducing donor-specific and

Digitized by Google

antigen-specific tolerance. The binding of CD28 by its ligand, B7/BB1 (B7), during T cell receptor engagement is critical for proper T cell signaling in some systems (M. K. Jenkins, P. S. Taylor, S. D. Norton, K. B. Urdahl, J. Immunol. 147:2461 (1991); C. H. June, J. A. Ledbetter, P. S. Linsley, C. B. Thompson, Immunol. Today 11:211 (1990); H. Reiser, G. J. Freeman, Z. Razi-Wolf, C. D. Gimmi, B. Benacerraf, L. M. Nadler, Proc. Natl. Acad. Sci. U.S.A. 89:271 (1992); N. K. Damie, K. Klussman, P. S. Linsley, A. Aruffo, J. Immunol. 148:1985 (1992)).

When the interaction of CD28 with its ligand is blocked, antigen-specific T cells are inappropriately induced into a state of antigen-specific T cell anergy (M. K. Jenkins, P. S. Taylor, S. D. Norton, K. B. Urdahl, J. Immunol. 147:2461 (1991); F. A. Harding, J. G. McArthur, J. A. Gross, D. H. Raulet, J. P. Allison, Nature 356:607 (1992)).

CTLA4Ig fusion protein binds to both human and murine B7 (with a 20-fold greater affinity than CD28), blocks the binding of CD28 to B7, inhibits T cell activation, and induces T cell unresponsiveness in vitro (F. A. Harding, J. G. McArthur, J. A. Gross, D. H. Raulet, J. P. Allison, Nature 356:607 (1992); P. S. Linsley et al., J. Exp. Med. 174:561 (1991).

Moreover, the present invention would be useful to obtain expression of a soluble protein product of the heretofore unexpressed CTLA4 gene, and to identify a natural ligand for CTLA4 that is involved in functional responses of T cells. The soluble protein product could then be used to regulate T cell responses in vivo to treat pathological conditions.

The following examples are presented to illustrate the present invention and to assist one of ordinary skill in making and using the same. The examples are not intended in any way to otherwise limit the scope of the invention.

EXAMPLE 1

Preparation of B7Ig and CD28Ig Fusion Proteins

Receptor-immunoglobulin C gamma (IgCγ) fusion proteins B7Ig and CD28Ig were prepared as described by Linsley et al., in *J. Exp. Med.* 173:721–730 (1991), incorporated by reference herein. Briefly, DNA encoding amino acid sequences corresponding to the respective receptor protein (e.g. B7) was joined to DNA encoding amino acid sequences corresponding to the hinge, CH2 and CH3 regions of human IgCγ1. This was accomplished as follows.

Polymerase Chain Reaction (PCR).

For PCR, DNA fragments were amplified using primer pairs as described below for each fusion protein. PCR reactions (0.1 ml final volume) were run in Taq polymerase buffer (Stratagene, La Jolla, Calif.), containing 20 μmoles each of dNTP; 50–100 pmoles of the indicated primers; template (1 ng plasmid or cDNA synthesized from ≦1 μg total RNA using random hexamer primer, as described by Kawasaki in PCR Protocols, Academic Press, pp. 21–27 (1990), incorporated by reference herein); and Taq polymerase (Stratagene). Reactions were run on a thermocycler (Perkin Elmer Corp., Norwalk, Conn.) for 16–30 cycles (a typical cycle consisted of steps of 1 min at 94° C., 1–2 min at 50° C. and 1–3 min at 72° C.).

Plasmid Construction.

Expression plasmids containing cDNA encoding CD28, as described by Aruffo and Seed, *Proc. Natl. Acad. Sci. USA* 84:8573 (1987)), were provided by Drs. Aruffo and Seed (Mass General Hospital, Boston, Mass.). Plasmids containing cDNA encoding CD5, as described by Aruffo, *Cell* 61:1303 (1990)), were provided by Dr. Aruffo. Plasmids containing cDNA encoding B7, as described by Freeman et al., *J. Immunol.* 143:2714 (1989)), were provided by Dr. Freeman (Dana Farber Cancer Institute, Boston, Mass.). For initial attempts at expression of soluble forms of CD28 and B7, constructs were made (OMCD28 and OMB7) as described by Linsley et al., *J. Exp. Med.*, supra, in which stop codons were introduced upstream of the transmembrane domains and the native signal peptides were replaced with the signal peptide from oncostatin M (Malik et al., *Mol. Cell Biol.* 9:2847 (1989)). These were made using synthetic oligonucleotides for reconstruction (OMCD28) or as primers (OMB7) for PCR. OMCD28, is a CD28 cDNA modified for more efficient expression by replacing the signal peptide with the analogous region from oncostatin M. CD28Ig and B7Ig fusion constructs were made in two parts. The 5' portions were made using OMCD28 and OMB7 as templates and the oligonucleotide, CTAGCCACTGAAGCTTCACCATGGGTGTACTGCTCACAC (SEQ ID NO:1), (encoding the amino acid sequence corresponding to the oncostatin M signal peptide) as a forward primer, and either TGGCATGGGCTCCTGATCAGGCTTAGAAGGTCCGGGAAA (SEQ ID NO:2), or, TTTGGGCTCCTGATCAGGAAAATGCTCTTGCTTGGTTGT (SEQ ID NO:3) as reverse primers, respectively. Products of the PCR reactions were cleaved with restriction endonucleases (Hind III and BclI) as sites introduced in the PCR primers and gel purified.

The 3' portion of the fusion constructs corresponding to human IgCγ1 sequences was made by a coupled reverse transcriptase (from Avian myeloblastosis virus; Life Sciences Associates, Bayport, N.Y.)-PCR reaction using RNA from a myeloma cell line producing human-mouse chimeric mAb L6 (provided by Dr. P. Fell and M. Gayle, Bristol-Myers Squibb Company, Pharmaceutical Research Institute, Seattle, Wash.) as template. The oligonucleotide, AAGCAAGAGCATTTTCCTGATCAGGAGCCCAAATCTTCTGACAAAACTCACACATCCCCACCGTCCCCAGCACCTGAACTCCTG (SEQ ID NO:4), was used as forward primer, and CTTCGACCAGTCTAGAAGCATCCTCGTGCGACCGCGAGAGC (SEQ ID NO:5) as reverse primer. Reaction products were cleaved with BclI and XbaI and gel purified. Final constructs were assembled by ligating HindIII/BclI cleaved fragments containing CD28 or B7 sequences together with BclI/XbaI cleaved fragment containing IgCγ1 sequences into HindIII/XbaI cleaved CDM8. Ligation products were transformed into MC1061/p3 *E. coli* cells and colonies were screened for the appropriate plasmids. Sequences of the resulting constructs were confirmed by DNA sequencing.

The construct encoding B7 contained DNA encoding amino acids corresponding to amino acid residues from approximately position 1 to approximately position 215 of the extracellular domain of B7. The construct encoding CD28 contained DNA encoding amino acids corresponding to amino acid residues from approximately position 1 to approximately position 134 of the extracellular domain of CD28.

CD5Ig was constructed in identical fashion, using CATTGCACAGTCAAGCTTCCATGCCCATGGGTTCTCTGGCCACCTTG (SEQ ID NO:6), as forward primer and ATCCACAGTGCAGTGATCATTTGGATCCTGGCATGTGAC (SEQ ID NO:7) as reverse primer. The PCR product was restriction endonuclease digested and ligated with the IgCγ1 fragment as described above. The resulting construct (CD5Ig) encoded a mature protein having an amino acid sequence containing amino acid residues from position 1 to position 347 of the sequence corresponding to CD5, two amino acids introduced by the

Digitized by Google

construction procedure (amino acids DQ), followed by DNA encoding amino acids corresponding to the IgCγ1 hinge region.

Cell Culture and Transfections.

COS (monkey kidney cells) were transfected with expression plasmids expressing CD28 and B7 using a modification of the protocol of Seed and Aruffo (*Proc. Natl. Acad. Sci.* 84:3365 (1987)), incorporated by reference herein. Cells were seeded at 10^6 per 10 cm diameter culture dish 18–24 h before transfection. Plasmid DNA was added (approximately 15 μg/dish) in a volume of 5 mls of serum-free DMEM containing 0.1 mM chloroquine and 600 μg/ml DEAE Dextran, and cells were incubated for 3–3.5 h at 37° C. Transfected cells were then briefly treated (approximately 2 min) with 10% dimethyl sulfoxide in PBS and incubated at 37° C. for 16–24 h in DMEM containing 10% FCS. At 24 h after transfection, culture medium was removed and replaced with serum-free DMEM (6 ml/dish). Incubation was continued for 3 days at 37° C., at which time the spent medium was collected and fresh serum-free medium was added. After an additional 3 days at 37° C., the spent medium was again collected and cells were discarded.

CHO cells expressing CD28, CD5 or B7 were isolated as described by Linsley et al., (1991) supra, as follows: Briefly, stable transfectants expressing CD28, CD5, or B7, were isolated following cotransfection of dihydrofolate reductase-deficient Chinese hamster ovary ($dhfr^-$ CHO) cells with a mixture of the appropriate expression plasmid and the selectable marker, pSV2dhfr (Linsley et al., *Proc. Natl. Acad. Sci. USA* 87:5031 (1990)), incorporated by reference herein. Transfectants were then grown in increasing concentrations of methotrexate to a final level of 1 μM and were maintained in DMEM supplemented with 10% fetal bovine serum (FBS), 0.2 mM proline and 1 μM methotrexate. CHO lines expressing high levels of CD28 ($CD28^+$ CHO) or B7 ($B7^+$ CHO) were isolated by multiple rounds of fluorescence-activated cell sorting (FACS®) following indirect immunostaining with mAbs 9.3 or BB-1. Amplified CHO cells negative for surface expression of CD28 or B7 ($dhfr^+$ CHO) were also isolated by FACS® from CD28-transfected populations.

Immunostaining and FACS® Analysis.

Transfected CHO or COS cells or activated T cells were analyzed by indirect immunostaining. Before staining, CHO cells were removed from their culture vessels by incubation in PBS containing 10 mM EDTA. Cells were first incubated with murine mAbs 9.3 (Hansen et al., *Immunogenetics* 10:247 (1980)) or BB-1 (Yokochi et al., *J. Immunol.* 128:823 (1981)), or with Ig fusion proteins (all at 10 μg/ml in DMEM containing 10% FCS) for 1–2 h at 4° C. Cells were then washed, and incubated for an additional 0.5–2 h at 4° C. with a FITC-conjugated second step reagent (goat anti-mouse Ig serum for murine mAbs, or goat anti-human Ig Cγ serum for fusion proteins (Tago, Inc., Burlingame, Calif.)). Fluorescence was analyzed on a FACS IV® cell sorter (Becton Dickinson and CO., Mountain View, Calif.) equipped with a four decade logarithmic amplifier.

Purification of Ig Fusion Proteins.

The first, second and third collections of spent serum-free culture media from transfected COS cells were used as sources for the purification of Ig fusion proteins. After removal of cellular debris by low speed centrifugation, medium was applied to a column (approximately 200–400 ml medium/ml packed bed volume) of immobilized protein A (Repligen Corp., Cambridge, Mass.) equilibrated with 0.05M sodium citrate, pH 8.0. After application of the medium, the column was washed with 1M potassium phosphate, pH 8, and bound protein was eluted with 0.05M sodium citrate, pH 3. Fractions were collected and immediately neutralized by addition of 1/10 volume of 2M Tris, pH 8. Fractions containing the peak of A_{280} absorbing material were pooled and dialyzed against PBS before use. Extinction coefficients of 2.4 and 2.8 ml/mg for CD28Ig and B7Ig, respectively, were determined by amino acid analysis of solutions of known absorbance. The recovery of purified CD28Ig and B7Ig binding activities was nearly quantitative as judged by FACS® analysis after indirect fluorescent staining of $B7^+$ and $CD28^+$ CHO cells.

EXAMPLE 2

Preparation of CTLA4Ig Fusion Protein

A soluble genetic fusion encoding CTLA4Ig between the extracellular domain of CTLA4 and an IgCγ1 domain was constructed in a manner similar to that described above for the CD28Ig construct. The extracellular domain of the CTLA4 gene was cloned by PCR using synthetic oligonucleotides corresponding to the published sequence (Dariavach et al., *Eur. Journ. Immunol.* 18:1901–1905 (1988)).

Because a signal peptide for CTLA4 was not identified in the CTLA4 gene, the N-terminus of the predicted sequence of CTLA4 was fused to the signal peptide of oncostatin M (Malik et al., *Mol. and Cell. Biol.* 9:2847 (1989)) in two steps using overlapping oligonucleotides. For the first step, the oligonucleotide, CTCAGTCTGGTCCTTGCACTCCT-GTTTCCAAGCATGGCGAGCATGGCAATG-CACGTGGCCCAGCC (SEQ ID NO:8) (which encoded the C terminal 15 amino acids from the oncostatin M signal peptide fused to the N terminal 7 amino acids of CTLA4) was used as forward primer, and TTTGGGCTCCTGATCA-GAATCTGGGCACGGTTG (SEQ ID NO:9) (encoding amino acid residues 119–125 of the amino acid sequence encoding CTLA4 receptor and containing a Bcl I restriction enzyme site) as reverse primer. The template for this step was cDNA synthesized from 1 μg of total RNA from H38 cells (an HTLV II infected T cell leukemic cell line provided by Drs. Salahudin and Gallo, NCI, Bethesda, Md.). A portion of the PCR product from the first step was reamplified, using an overlapping forward primer, encoding the N terminal portion of the oncostatin M signal peptide and containing a Hind III restriction endonuclease site, CTAGC-CACTGAAGCTTCACCAATGGGTGTACT-GCTCACACAGAGGACGCTGCTCAGTCTG-GTCCTTGCACTC (SEQ ID NO:10) and the same reverse primer. The product of the PCR reaction was digested with Hind III and Bcl I and ligated together with a Bcl 1/Xba I cleaved cDNA fragment encoding the amino acid sequences corresponding to the hinge, CH2 and CH3 regions of IgCγ1 into the Hind III/Xba I cleaved expression vector, CDM8 or Hind III/Xba I cleaved expression vector πLN (provided by Dr. Aruffo).

A map of the resulting CTLA4Ig fusion construct is shown in FIG. 1. Sequences displayed in this figure show the junctions between CTLA4 (upper case letters, unshaded regions) and the signal peptide, SP, of oncostatin M (dark shaded regions), and the hinge, H, of IgCγ1 (stippled regions). The amino acid in parentheses was introduced during construction. Asterisks (*) indicate cysteine to serine mutations introduced in the IgCγ hinge region. The immunoglobulin superfamily V-like domain present in CTLA4 is indicated, as are the CH2 and CH3 domains of IgCγ1.

Expression plasmids, CDM8, containing CTLA4Ig were then transfected into COS cells using DEAE/dextran transfection by modification (Linsley et al., 1991, supra) of the protocol described by Seed and Aruffo, 1987, supra.

Google

Expression plasmid constructs (πLN or CDM8) containing cDNA encoding the amino acid sequence of CTLA4Ig, was transfected by lipofection using standard procedures into dhfr⁻ CHO lines to obtain novel cell lines stably expressing CTLA4Ig.

DNA encoding the amino acid sequence corresponding to CTLA4Ig has been deposited with the ATCC under the Budapest Treaty on May 31, 1991, and has been accorded ATCC accession number 68629.

A preferred stable transfectant, expressing CTLA4Ig, designated Chinese Hamster Ovary Cell Line, CTLA4Ig-24, was made by screening B7 positive CHO cell lines for B7 binding activity in the medium using immunostaining. Transfectants were maintained in DMEM supplemented with 10% fetal bovine serum (FBS), 0.2 mM proline and 1 μM methotrexate.

The CTLA4Ig-24 CHO cell line has been deposited with the ATCC under the Budapest Treaty on May 31, 1991 and has been accorded accession number ATCC 10762.

CTLA4Ig was purified by protein A chromatography from serum-free conditioned supernatants (FIG. 2). Concentrations of CTLA4Ig were determined assuming an extinction coefficient at 280 nm of 1.6 (experimentally determined by amino acid analysis of a solution of known absorbance). Molecular weight standards (lanes 1 and 3, FIG. 2) and samples (1 μg) of CTLA4Ig (lanes 2 and 4) were subjected to SDS-PAGE (4–12% acrylamide gradient) under non-reducing conditions (−βME, lanes 1 and 2) or reducing conditions (+βME, lanes 3 and 4) Proteins were visualized by staining with Coomassie Brilliant Blue.

Under non-reducing conditions, CTLA4Ig migrated as a M_r approximately 100,000 species, and under reducing conditions, as a M_r approximately 50,000 species (FIG. 2). Because the IgC γ hinge disulfides were eliminated during construction, CTLA4Ig, like CD28Ig, is a dimer presumably joined through a native disulfide linkage.

EXAMPLE 3

CTLA4 Receptor

To reconstruct DNA encoding the amino acid sequence corresponding to the full length human CTLA4 gene, cDNA encoding amino acids corresponding to a fragment of the transmembrane and cytoplasmic domains of CTLA4 was cloned by PCR and then joined with cDNA encoding amino acids corresponding to a fragment from CTLA4Ig that corresponded to the oncostatin M signal peptide fused to the N-terminus of CTLA4. Procedures for PCR, and cell culture and transfections were as described above in Example 1 using COS cells and DEAE-dextran transfection.

Because the expression of CTLA4 receptor protein in human lymphoid cells has not been previously reported, it was necessary to locate a source of CTLA4 mRNA. PCR cDNA reverse transcribed from the total cellular RNA of H38 cells, as noted above, was used for cloning by PCR. For this purpose, the oligonucleotide, GCAATGCACGTGGCCCAGCCTGCTGTGGTAGTG (SEQ ID NO:11), (encoding the first 11 amino acids in the predicted coding sequence) was used as a forward primer, and TGATGTAACATGTCTAGATCAATTGATGGGAATAAAATAAGGCTG (SEQ ID NO:12) (homologous to the last 8 amino acids in CTLA4 and containing a Xba I site) as reverse primer. The template again was a cDNA synthesized from 1 μg RNA from H38 cells. Products of the PCR reaction were cleaved with the restriction endonucleases Nco I and Xba I and the resulting 316 bp product was gel purified. A 340 bp Hind III/Nco I fragment from the CTLAIg fusion described above was also gel-purified, and both restriction fragments were ligated into Hind III/Xba I cleaved CDM8 to form OMCTLA.

The resulting construct corresponded to full length CTLA4 (SEQ ID NOs: 13 and 14) and the oncostatin M signal peptide. The construct is shown in FIG. 3 and was designated OMCTLA4. The sequence for CTLA4 shown in FIG. 3 differs from the predicted human CTLA4 DNA sequence (Dariavach et al., supra) by a base change such that the previously reported alanine at amino acid position 111 of the amino acid sequence shown, encodes a threonine. This threonine is part of a newly identified N-linked glycosylation site that may be important for successful expression of the fusion protein.

Ligation products were transformed into MC1061/p3 *E. coli* cells and colonies were screened for the appropriate plasmids. Sequences of the resulting constructs were confirmed by DNA sequence analysis.

EXAMPLE 4

Characterization of CTLA4Ig

To characterize the CTLA4Ig constructs, several isolates, CD28Ig, B7Ig, and CD5Ig, were prepared as described above and were transfected into COS cells as described in Examples 2 and 3, and were tested by FACS® analysis for binding of B7Ig. In addition to the above-mentioned constructs, CDM8 plasmids containing cDNAs encoding CD7 as described by Aruffo and Seed, (*EMBO Jour.* 6:3313–3316 (1987)), incorporated by reference herein, were also used.

mAbs. Murine monoclonal antibodies (mAbs) 9.3 (anti-CD28) and G19-4 (anti-CD3), G3-7 (anti-CD7), BB-1 (anti-B7 antigen) and rat mAb 187.1 (anti-mouse K chain) have been described previously (Ledbetter et al., *Proc. Natl. Acad. Sci.* 84:1384–1388 (1987); Ledbetter et al., *Blood* 75:1531 (1990); Yokochi et al., supra) and were purified from ascites before use. The hybridoma producing mAb OKT8 was obtained from the ATCC, Rockville, Md., and the mAb was also purified from ascites before use. mAb 4G9 (anti-CD19) was provided by Dr. E. Engleman, Stanford University, Palo Alto, Calif.). Purified human-mouse chimeric mAb L6 (having human Cγ1 Fc portion) was a gift of Dr. P. Fell and M. Gayle (Bristol-Myers Squibb Pharmaceutical Research Institute, Seattle, Wash.).

Immunostaining and FACS® Analysis.

Prior to staining, COS or CHO cells were removed from their culture vessels by incubation in PBS containing 10 mM EDTA. Cells were first incubated with mAbs or Ig fusion proteins at 10 μg/ml in DMEM containing 10% FBS for 1–2 hr at 4° C. Cells were then washed, and incubated for an additional 0.5–2 hrs at 4° C. with FITC-conjugated goat anti-mouse immunoglobulin or with FITC-conjugated goat anti-human Ig C γ serum (both from Tago, Burlingame, Calif.). When binding of both mAbs and Ig fusion proteins were measured in the same experiment, FITC-conjugated anti-mouse and anti-human second step reagents were mixed together before use. Fluorescence on a total of 10,000 cells was then analyzed by FACS®.

Peripheral Blood Lymphocyte Separation and Stimulation.

Peripheral blood lymphocytes (PBLs) were isolated by centrifugation through Lymphocyte Separation Medium (Litton Bionetics, Kensington, Md.). Alloreactive T cells were isolated by stimulation of PBL in a primary mixed lymphocyte reaction (MLR). PBL were cultured at 10^6/ml irradiated (5000 rad) T51 LCL. EBV-transformed lymphoblastoid cell lines (LCL), PM (Bristol-Myers Squibb Co.) and T51 (Bristol-Myers Squibb Co.) were maintained in RPMI supplemented with 10% FBS. After 6 days, alloreactive "blasts" cells were cryopreserved. Secondary MLR were conducted by culturing thawed alloreactive blasts together with fresh irradiated T51 LCL in the presence and

Google

absence of mAbs and Ig fusion proteins. Cells were cultured in 96 well flat bottom plates (4×10^4 alloreactive blasts and 1×10^4 irradiated T51 LCL cells/well, in a volume of 0.2 ml) in RPMI containing 10% FBS. Cellular proliferation of quadruplicate cultures was measured by uptake of [^{3}H]-thymidine during the last 6 hours of a 2–3 day culture.

PHA-activated T cells were prepared by culturing PBLs with 1 μg/ml PHA (Wellcome, Charlotte, N.C.) for five days, and one day in medium lacking PHA. Viable cells were collected by sedimentation through Lymphocyte Separation Medium before use. Cells were stimulated with mAbs or transfected CHO cells for 4–6 hr at 37° C., collected by centrifugation and used to prepare RNA.

CD4$^+$ T cells were isolated from PBLs by separating PBLs from healthy donors into T and non-T cells using sheep erythrocyte rosetting technique and further separating T cells by panning into CD4$^+$ cells as described by Damle et al., *J. Immunol.* 139:1501 (1987), incorporated by reference herein. B cells were also purified from peripheral blood by panning as described by Wysocki and Sato, *Proc. Natl. Acad. Sci.* 75:2844 (1978), incorporated by reference herein, using anti-CD19 mAb 4G9. To measure T_A-induced Ig production, 10^6 CD4$^+$ T cells were mixed with 10^6 CD19$^+$ B cells in 1 ml of RPMI containing 10% FBS. Following culture for 6 days at 37° C., production of human IgM was measured in the culture supernatants using solid phase ELISA as described by Volkman et al., *Proc. Natl. Acad. Sci. USA* 78:2528 (1981), incorporated by reference herein. Briefly, 96-well flat bottom microtiter ELISA plates (Corning, Corning, N.Y.) were coated with 200 μl/well of sodium carbonate buffer (pH 9.6) containing 10 μg/ml of affinity-purified goat anti-human IgG or IgM antibody (Tago, Burlingame, Calif.), incubated overnight at 4° C., and then washed with PBS and wells were further blocked with 2% BSA in PBS (BSA-PBS). Samples to be assayed were added at appropriate dilution to these wells and incubated with 200 μl/well of 1:1000 dilution of horseradish peroxidase (HRP)-conjugated F(ab')$_2$ fraction of affinity-purified goat anti-human IgG or IgM antibody (Tago). The plates were then washed, and 100 μl/well of o-phenylenediamine (Sigma Chemical Co., St. Louis, Mo.) solution (0.6 mg/ml in citrate-phosphate buffer with pH 5.5 and 0.045% hydrogen peroxide). Color development was stopped with 2N sulfuric acid. Absorbance at 490 nm was measured with an automated ELISA plate reader. Test and control samples were run in triplicate and the values of absorbance were compared to those obtained with known IgG or IgM standards run simultaneously with the supernatant samples to generate the standard curve using which the concentrations of Ig in the culture supernatant were quantitated. Data are expressed as ng/ml of Ig±SEM of either triplicate or quadruplicate cultures.

Immunoprecipitation Analysis and SDS PAGE.

Cells were surface-labeled with ^{125}I and subjected to immunoprecipitation analysis. Briefly, PHA-activated T cells were surface-labeled with ^{125}I using lactoperoxidase and H_2O_2 as described by Vitetta et al., *J. Exp. Med.* 134:242 (1971), incorporated by reference herein. SDS-PAGE chromatography was performed on linear acrylamide gradients gels with stacking gels of 5% acrylamide. Gels were stained with Coomassie Blue, destained, and photographed or dried and exposed to X ray film (Kodak XAR-5).

Binding Assays.

B7Ig was labeled with ^{125}I to a specific activity of approximately 2×10^6 cpm/pmole. Ninety-six well plastic dishes were coated for 16–24 hrs with a solution containing CTLA4Ig (0.5 μg in a volume of 0.05 ml of 10 mM Tris, pH 8). Wells were blocked with binding buffer (DMEM containing 50 mM BES (Sigma Chemical Co.), pH 6.8, 0.1% BAS, and 10% FCS) before addition of a solution (0.09 ml) containing ^{125}I B7Ig (approximately 5×10^5 cpm) in the presence or absence of competitor. Following incubation for 2–3 hrs at 23° C., wells were washed once with binding buffer, and four times with PBS. Bound radioactivity was then solubilized by addition of 0.5N NaOH, and quantified by gamma counting.

Binding to B7Ig.

The functional activity of the OMCTLA4 construct encoding the complete human CTLA4 DNA gene, is shown in the experiment shown in FIG. 4. COS cells were transfected with expression plasmids CD7, OMCD28 and OMCTLA4 as described above. Forty-eight hours following transfection, cells were collected and incubated with medium only (no addition) or with mAbs 9.3, B7Ig, CD5Ig or G3-7. Cells were then washed and binding was detected by a mixture of FITC-conjugated goat anti-mouse Ig and FITC-conjugated goat anti-human Ig second step reagents. Transfected cells were tested for expression of the appropriate cell surface markers by indirect immunostaining and fluorescence was measured using FACS® analysis as described above.

As shown in FIG. 4, mAb 9.3 bound to CD28-transfected COS cells, but not to CTLA4-transfected cells. In contrast, the B7Ig fusion protein (but not control CD5Ig fusion protein) bound to both CD28- and CTLA4-transfected cells. CD7-transfected COS cells bound neither mAb 9.3 nor either of the fusion proteins. This indicates that CD28 and CTLA4 both bind the B cell activation antigen, B7. Furthermore, mAb 9.3 did not detectably bind CTLA4.

Binding of CTLA4Ig on B7 Positive CHO cells.

To further characterize the binding of CTLA4Ig and B7, the binding activity of purified CTLA4Ig on B7$^+$ CHO cells and on a lymphoblastoid cell line (PM LCL) was measured in the experiment shown in FIG. 5. Amplified transfected CHO cell lines and PM LCLs were incubated with medium only (no addition) or an equivalent concentration of human IgCγ1-containing proteins (10 μg/ml) of CD5Ig, CD28Ig or CTLA4Ig. Binding was detected by FACS® following addition of FITC-conjugated goat anti-human Ig second step reagents. A total of 10,000 stained cells were analyzed by FACS®.

As shown in FIG. 5, CD28Ig bound to B7$^+$ CHO cells but not to PM LCL, a cell line which expresses relatively low levels of the B7 antigen (Linsley et al., supra, 1990). CTLA4Ig bound more strongly to both cell lines than did CD28Ig, suggesting that it bound with higher affinity. Neither CD28Ig nor CTLA4Ig bound to CD28$^+$ CHO cells.

Affinity of Binding of CTLA4Ig and B7Ig.

The apparent affinity of interaction between CTLA4Ig and B7Ig was then measured using a solid phase competition binding assay. Ninety-six well plastic dishes were coated with CTLA4Ig as described above. B7Ig was radiolabeled with ^{125}I (5×10^5 cpm, 2×10^6 cpm/pmole), and added to a concentration of 4 nM in the presence of the indicated concentrations (see FIG. 6) of unlabeled chimeric mAb L6, mAb 9.3, mAb BB-1 or B7Ig. Plate-bound radioactivity was determined and expressed as a percentage of radioactivity bound to wells treated without competitor (28,300 cpm). Each point represents the mean of duplicate determinations; replicates generally varied from the mean by ≦20%. Concentrations were calculated based on a M_r of 75,000 per binding site for mAbs and 51,000 per binding site for B7Ig.

As shown in FIG. 6, only mAb BB-1 and unlabeled B7Ig competed significantly for ^{125}I-B7Ig binding (half-maximal

Digitized by Google

effects at approximately 22 nM and approximately 175 nM, respectively). Neither chimeric mAb L6, nor mAb 9.3 competed effectively at the concentrations tested. In other experiments, the concentrations of mAb 9.3 used were sufficient to inhibit binding of ^{125}I-B7Ig to immobilized CD28Ig or to cell surface expressed CD28 by ≧90%.

When the competition data from FIG. **6** were plotted in a Scatchard representation, a dissociation constant, K_d, of approximately 12 nM was calculated for binding of ^{125}I-B7 to immobilized CTLA4Ig (FIG. **7**). This value is approximately 20 fold lower than the previously determined K_d of binding between ^{125}I-B7Ig and CD28 (approximately 200 nM) (Linsley et al, (1991), supra) indicating that CTLA4 is a higher affinity receptor for the B7 antigen than CD28 receptor.

To identify the molecule(s) on lymphoblastoid cells which bound CTLA4Ig (FIG. **7**), ^{125}I-surface labeled cells were subjected to immunoprecipitation analysis (FIG. **8**). B7$^+$ CHO and PM LCL cells were surface-labeled with ^{125}I, and extracted with a non-ionic detergent solution as described above. Aliquots of extracts containing approximately 1.5× 10^7 cpm in a volume of 0.1 ml were subjected to immunoprecipitation analysis as described above with no addition, or 2 μg each of CD28Ig, CTLA4Ig or CD5Ig. Washed immunoprecipitates were then analyzed by SDS-PAGE (10–20% acrylamide gradient) under reducing conditions. The gel was then dried and subjected to autoradiography. The left panel of FIG. **8** shows an autoradiogram obtained after a 1 day exposure. The right panel of FIG. **8** shows an autoradiogram of the same gel after a 10 day exposure. The autoradiogram in the center panel of FIG. **8** was also exposed for 10 days. Positions of molecular weight standard are also indicated in this figure.

As shown by FIG. **8**, a diffusely migrating (M_r approximately 50,000–75,000; center at approximately 60,000) radiolabeled protein was immunoprecipitated by CTLA4Ig, but not by CD28Ig or CD5Ig. This molecule co-migrated with B7 immunoprecipitated from B7$^+$ CHO cells by CTLA4Ig, and much more weakly, by CD28Ig. These findings indicate that CTLA4Ig binds a single protein on lymphoblastoid cells which is similar in size to the B7 antigen.

Inhibition of Immune Responses In Vitro by CTLA4Ig

Inhibition of Proliferation. Previous studies have shown that the anti-CD28 mAb, mAb 9.3, and the anti-B7 mAb, mAb BB-1, inhibit proliferation of alloantigen specific T_h cells, as well as immunoglobulin secretion by alloantigen-presenting B Cells (Damle, et al., *Proc. Natl. Acad. Sci.* 78:5096 (1981); Lesslauer et al., *Eur. J. Immunol.* 16:1289 (1986)). Because CTLA4 is a high affinity receptor for the B7 antigen as demonstrated herein, soluble CTLA4Ig was tested for its ability to inhibit these responses. The effects of CTLA4Ig on T cell proliferation were examined in the experiment shown in FIG. **9**.

Primary mixed lymphocyte reaction (MLR) blasts were stimulated with irradiated T51 lymphoblastoid cells (LC) in the absence or presence of concentrations of murine mAb 9.3 Fab fragments, or B7Ig, CD28Ig or CTLA4Ig immunoglobulin Cγ fusion proteins. Cellular proliferation was measured by [^{3}H]-thymidine incorporation after 4 days and is expressed as the percentage of incorporation by untreated cultures (21,000 cpm). FIG. **9** shows the means of quadruplicate determinations (SEM ≦10%).

As shown in FIG. **9**, CTLA4Ig inhibited the MLR reaction in a dose-dependant fashion by a maximum of >90% with a ½ maximal response at approximately 30 ng/ml (approximately 0.8 nM). The Fab fragment of mAb 9.3, which previously was shown to be a more potent inhibitor of MLR than whole mAb 9.3 (Damle et al., *J. Immunol.* 140:1753–1761 (1988)), also inhibited the MLR, but at higher concentrations (approximately 800 ng/ml or approximately 30 nM for ½ maximal response). B7Ig and CD28Ig did not significantly inhibit the MLR even at higher concentrations. In another experiment, addition of B7Ig together with CTLA4Ig partially overcame the inhibition of MLR by CTLA4Ig, indicating that the inhibition was specifically due to interactions with B7 antigen.

Inhibition of Immunoglobulin Secretion.

The effects of CTLA4Ig on helper T cell (T_h)-induced immunoglobulin secretion were also examined (FIG. **10**). CD4$^+$ T cells were mixed with allogeneic CD19$^+$ B cells in the presence or absence of the indicated immunoglobulin molecules as described above. Murine mAbs OKT8, 9.3 and BB-1 were added at 20 μg/ml, and Ig fusion proteins at 10 μg/ml. After 6 days of culture, concentrations of human IgM (SEM <5%) in culture supernatants were determined by enzyme immunoassay (ELISA) as described above. IgM production by B cells cultured in the absence of CD4$^+$ T cells was 11 ng/ml.

As shown in FIG. **10**, CD4$^+$ T cells stimulated IgM production by allogenic CD19$^+$ B Cells (in the absence of CD4$^+$ T cells, IgM levels were reduced by 93%). mAbs 9.3 and BB-1 significantly inhibited T_h-induced IgM production (63% and 65% inhibition, respectively). CTLA4Ig was even more effective as an inhibitor (89% inhibition) than were these mAbs. Inhibition by control Ig molecules, mAb OKT8 and CD5Ig, was much less (≦30% inhibition). None of these molecules significantly inhibited Ig production measured in the presence of *Staphylococcal aureus* enterotoxin B. Similar results were obtained with CD4$^+$ T cells and B cells derived from other donors. These results indicate that the inhibition by CTLA4Ig is specific.

The above data also demonstrate that the CTLA4 and CD28 receptors are functionally as well as structurally related. Like CD28, CTLA4 is also a receptor for the B cell activation antigen, B7. CTLA4Ig bound ^{125}I-B7 with an affinity constant, K_d, of approximately 12 nM, a value some 20 fold higher than the affinity between CD28 and B7Ig (approximately 200 nM). Thus, CTLA4 and CD28 may be thought of as high and low affinity receptors, respectively, for the same ligand, the B7 antigen.

The apparent affinity between CD28 and B7 is similar to the affinity reported for binding of soluble alloantigen to the T cell receptor of a murine T cell hybridoma (approximately 100 nM; Schnek et al., *Cell* 56:47 (1989)), and is higher affinity than interactions between CD2 and LFA3 (Recny et al., *J. Biol. Chem.* 265:8542 (1990)), or CD4 and MHC class II molecules (Clayton et al., *Nature* 339:548 (1989)). The apparent affinity constant, K_d, between CTLA4 and B7 is even greater, and compares favorably with higher affinity mAbs (K_d 2–10,000 nM; Alzari et al., *Ann. Rev. Immuno.* 6:555 (1988)). The K_d between CTLA4 and B7 is similar to or greater than K_d values of integrin receptors and their ligands (10–2000 nM; Hautanen et al., *J. Biol. Chem.* 264:1437–1442 (1989); Di Minno et al., *Blood* 61:140–148 (1983); Thiagarajan and Kelley, *J. Biol. Chem.* 263:035–3038 (1988)). The affinity of interaction between CTLA4 and B7 is thus among the highest yet reported for lymphoid adhesion systems.

These results demonstrate the first expression of a functional protein product of CTLA4 transcripts. CTLA4Ig, a fusion construct containing the extracellular domain of CTLA4 fused to an IgCγ1 domain, forms a disulfide-linked dimer of M_r approximately 50,000 subunits (FIG. **1**).

Google

Because no interchain disulfides would be predicted to form in the Ig portion of this fusion, it seems likely that cysteines from CTLA4 are involved in disulfide bond formation. The analogous CD28Ig fusion protein (Linsley et al, supra, 1991) also contains interchain disulfide linkage(s). These results suggest that CTLA4 receptor, like CD28 (Hansen et al., *Immunogenetics* 10:247–260 (1980)), exists on the T cell surface as a disulfide linked homodimer. Although CD28 and CTLA4 are highly homologous proteins, they are immunologically distinct, because the anti-CD28 mAb, mAb 9.3, does not recognize CTLA4 (FIGS. 4 and 5).

It is not known whether CTLA4 can activate T cells by a signalling pathway analogous to CD28. The cytoplasmic domains of murine and human CTLA4 are identical (Dariavach et al., supra 1988), suggesting that this region has important functional properties. The cytoplasmic domains of CD28 and CTLA4 also share homology, although it is unclear if this is sufficient to impart similar signaling properties to the two molecules.

CTLA4Ig is a potent inhibitor of in vitro lymphocyte functions requiring T cell and B cell collaboration (FIGS. 9 and 10). These findings, together with previous studies, indicate the fundamental importance of interactions between B7 antigen and its counter-receptors, CD28 and/or CTLA4, in regulating both T and B lymphocyte responses. CTLA4Ig should be a useful reagent for future investigations on the role of these interactions during immune responses. CTLA4Ig is a more potent inhibitor of in vitro lymphocyte responses than either mAb BB-1 or mAb 9.3 (FIGS. 9 and 10). The greater potency of CTLA4Ig over mAb BB-1 is most likely due to the difference in affinities for B7 between these molecules (FIG. 6). CTLA4Ig is also more potent than mAb 9.3, probably because, unlike the mAb, it does not also have direct stipulatory effects on T cell proliferation (June et al., *Immunology Today* 11:211 (1989)) to counteract its inhibitory effects. The immunosuppressive effects of CTLA4Ig in vitro suggest that future investigations are warranted into possible therapeutic effects of this molecule for treatment of autoimmune disorders involving aberrant T cell activation or Ig production.

As will be apparent to those skilled in the art to which the invention pertains, the present invention may be embodied in forms other than those specifically disclosed above without departing from the spirit or essential characteristics of the invention. The particular embodiments of the invention described above, are, therefore, to be considered as illustrative and not restrictive. The scope of the present invention is as set forth in the appended claims rather than being limited to the examples contained in the foregoing description.

EXAMPLE 5

Female BALB/c (H-2^d) and C57BL/6 (H-2^d)mice, 6 to 8 wk. of age were obtained from The Jackson Laboratory (Bar Harbor, Me.).

Human pancreatic islets cells were purified after collagenase digestion as described (C. Ricordi et al. Transplantation 52:519 (1991); A. G. Tzakis et al. Lancet 336:402 (1990); C. Ricordi, P. E. Lacy, E. H. Finke, B. J. Olack, D. W. Scharp, Diabetes 37:413 (1988)).

B6 or B10 mice, treated with streptozocin (175 mg per kilogram of body weight) 3 to 5 days before transplant and exhibiting nonfasting plasma glucose levels of greater than 280 mg/dl (with the majority over 300 mg/ml), were used as recipients.

Each animal received approximately 800 fresh human islets of 150 μm in diameter beneath the left renal capsule (D. Faustman and C. Coe, Science 252:1700 (1991); Y. J. Zeng et al. Transplantation 53:277 (1992)). Treatment was started immediately after transplantation.

Control animals were treated with PBS (solid lines) or L6 (dotted lines) at 50 μg every other day for 14 days immediately after transplantation (FIG. 11A). Islet transplants were considered rejected when glucose levels were greater than 250 mg/dl for three consecutive days. Animals treated with PBS (n=14) and L6 (n=8) had mean graft survivals of 5.6 and 6.4 days, respectively.

Animals were treated with 10 μg of CTLA4Ig for 14 consecutive days immediately after transplant (n=7) (FIG. 11B). Three out of seven animals maintained their grafts for >80 days. The remaining four animals had a mean graft survival of 12.75 days.

Animals were treated with 50 μg of CTLA4Ig every other day for 14 days immediately after human islet transplantation (FIG. 11C). All animals (n=12) treated with this dose maintained grafts throughout the analysis (FIG. 11C). Selected mice were nephrectomized on days 21 and 29 after the transplant to assess the graft's function (FIG. 11C).

Histology was performed on kidneys transplanted with human islet cells (FIGS. 12A, 12B, 12C, 12D). The slides were analyzed blindly.

Hematoxylin and eosin staining of a control human islet grafted mouse 29 days after transplantation showed a massive lymphocyte infiltration (FIG. 12A). The same tissue, stained for insulin, showed no detectable insulin production (FIG. 12B).

Histological examination of tissue from a CTLA4Ig-treated mouse 21 days after transplant showed intact islets under the kidney capsule with very few lymphocytes infiltrating the transplanted tissue (FIG. 12C). The tissue was stained with hematoxylin and eosin. The same tissue from the CTLA4Ig-treated mouse, stained for insulin, showed the production of insulin by the grafted islets (FIG. 12D). Similar results were observed in graft tissue examined at later time points. The upper, middle, and lower arrowheads identify the kidney capsule, islet transplant, and kidney parenchyma, respectively.

In the histopathology assay all tissues were fixed in 10% buffered formalin and processed, and 5-μm sections were stained either with hematoxylin and eosin or for insulin with the avidin-biotin-peroxidase method (S. M. Hsu, L. Raine, H. Fanger, J. Histochem, Cytochem, 29:577 (1981)). Magnification was ×122.

In FIG. 13 streptozotocin-treated animals were transplanted as described hereinabove for FIG. 11. The mice were treated either with PBS (dotted lines) or with MAb to human B7 (solid lines) at a dose of 50 μg every other day for 14 days (FIG. 13). Control animals (treated with PBS) (n=3) had a mean graft survival of 3.5 days, whereas anti-B7-treated animals (n=5) maintained grafts from 9 to >50 days (FIG. 13).

In FIG. 14 normal glycemic, CTLA4Ig-treated, transplanted mice (dotted lines) were nephrectomized on day 44 after transplant and immediately retransplanted with either 1000 first party donor islets (dotted lines, solid circles) or 1000 second party islets (dotted lines, open circles) beneath the remaining kidney capsule.

These islets, frozen at the time of the first transplant, were thawed and cultured for 3 days before transplant to ensure islet function. B10 mice that had been treated with streptozotocin and exhibited nonfasting glucose levels of greater than 280 mg/dl were used as controls (solid lines) (FIG. 14). No treatment was given after transplantation.

Digitized by Google

Control animals rejected both the first party (solid lines, closed circles) and the second party (solid lines, open circles) islet grafts by day 4 after transplant (FIG. 14). The CTLA4Ig-treated mice retransplanted with second party islets had a mean graft survival of 4.5 days, whereas animals retransplanted with first party donor islets maintained grafts for as long as analyzed (>80 days) (FIG. 14).

CTLA4Ig Significantly Prolongs Human Islet Graft Survival in Mice in a Donor-Specific Manner Thereby Providing an Approach to Immunosuppression

C57BL/6 (B6) or C57BL/10 (B10) mice were treated with streptozotocin to eliminate mouse pancreatic islet B dell function. Diabetic animals were grafted under the kidney capsule, and treatment was started immediately after surgery. Survival of the islet grafts was monitored by the analysis of blood glucose concentrations.

Transplanted control animals, treated with either phosphate-buffered saline (PBS)(n=14) or L6 (a human IgG1 chimeric MAb; n=8), had a mean graft survival of 5.6 and 6.4 days, respectively (FIG. 11A).

In contrast, islet rejection was delayed in animals treated with CTLA4Ig (10 μg per day for 14 days), with four out of the seven animals exhibiting moderately prolonged mean graft survival (12.75 days), whereas the remaining three animals maintained normal glucose levels for >80 days (FIG. 11B).

This eventual increase in glucose concentration may be a result of islet exhaustion because no evidence of active cellular rejection was observed.

In the three mice that maintained long-term islet grafts, the transient increase in glucose concentrations around day 21 after the transplant may have represented a self-limited rejection episode consistent with the pharmacokinetics of CTLA4Ig clearance after therapy (P. S. Linsley et al., Science 257:792 (1992)).

In subsequent experiments, the dose of CTLA4Ig was increased to 50 μg per animal every other day for about 14 days. This treatment resulted in 100% of the animals maintaining normal islet function throughout the experiment with no signs of a rejection crisis (FIG. 11C).

In order to confirm that insulin production originated from the transplanted islets and not from the native mouse pancreas, we nephrectomized selected animals at days 21 and 29 to remove the islet grafts (FIG. 11C). In these animals, glucose concentrations increased to above 350 mg/dl within 24 hours, which indicated that the islet xenograft was responsible for maintaining normal glucose levels. It appears that the blocking of the CD28-B7 interaction inhibits xenogenic islet graft rejection.

The effects of treatment with the soluble receptor, namely CTLAIg fusion protein, were not a result of Fc binding (L6 did not effect graft rejection) or general effects on T cell or B cell function in vivo.

Historical analyses of islet xenograft from control (PBS treated) and CTLA4Ig treated mice were done (FIGS. 12A, 12B, 12C, 12D). The islet tissue from the control animal demonstrated evidence of immune rejection, with a marked lymphocytic infiltrate into the graft and few remaining islets (FIG. 12A).

Immunohistochemical staining showed that insulin-positive cells were present only rarely, and no somatostatin-positive cells were present at all (FIG. 12B). In contrast, transplant tissue from the CTLA4Ig-treated mice was devoid of any lymphocytic infiltrate (FIG. 12C).

The grafts were intact, with many islets visible. In addition, the B cells observed in the human islet tissue produced human insulin (FIG. 12D) and somatostatin.

The human CTLA4Ig used in this study reacts with both murine and human B7. One advantage of the xenogeneic transplant model is the availability of a MAb to human B7 that does not react with mouse B7 (T. Yokochi, R. D. Holly, E. A. Clark, J. Immunol. 128:823 (1982)). Thus, the role of human B7-bearing antigen-presenting cells (APCs) could be directly examined.

The mice were transplanted as described and then treated with 50 μg of MAb to human B7 every other day for 14 days after transplant. This treatment prolonged graft survival in treated mice (9 to >50 days) in comparison to that for control mice (FIG. 13). The anti-B7 MAb is unable to block rejection as effectively as CTLA4Ig.

The CTLA4Ig therapy resulted in graft acceptance in the majority of mice. However, the animals may not be tolerant. Transient immunosuppression can lead to permanent islet graft acceptance because of graft adaptation (the loss of immunogenicity as a result of the loss of APC function) (L. Hao, Y. Wang, R. G. Gill, K. J. Lafferty, J. Immunol. 139:4022 (1987); K. J. Lafferty, S. J. Prowse, M. Simeonovic, Annu. Rev. Immunol. 1:143 (1983)).

In order to differentiate between these possibilities, we nephrectomized selected xenografted, CTLA4Ig-treated mice (day 40) and retransplanted them under the remaining kidney capsule with either the original donor islets (first party) or unrelated second party human islets (FIG. 14).

Streptozotocin-treated control animals, having never received an islet graft, were also transplanted with either first or second party islets. No treatment after the transplant was given. Control animals rejected the first and second party islets by day 4. The CTLA4Ig-treated animals that had received the second party islets rejected these islets by day 5, whereas animals receiving first party donor islets maintained the grafts for >80 days (FIG. 14).

These results suggest that the CTLA4Ig treatment resulted in prolonged donor-specific unresponsiveness to the xenogeneic islets. The ability of the murine immune response to distinguish differences among the human islet donors also supports the direct recognition of the polymorphic MHC products expressed on the human islet cells.

EXAMPLE 6

Female BALB/c (H-2^d) and C57BL/6 (H-2^d)mice, 6 to 8 wk. of age were obtained from The Jackson Laboratory (Bar Harbor, Me.).

Monoclonal antibody 11B11 is a rat IgGl anti-murine IL-4 (Ohara, J., and W. E. Paul, 1985, Production of a monoclonal antibody to and molecular characterization of B-cell stimulatory factor-1. Nature 315:333) (Verax (Lebanon, N.H.)).

BALB/c mice (five per group) were immunized intravenously with 10^8 SRBC alone or together with 200 μg chimeric L6 mAb or human CTLA4Ig fusion protein. The indicated groups were treated 2 hrs. prior to injection of SRBCs by intraperitoneal injection of 2 mls of either rat immunoglobulin or rat anti-murine IL-4 mAb 11B11 at 5 mg/ml. Treatment with chimeric L6 mAb or CTLA4Ig was repeated daily for 4 additional days.

All animals were given intravenous injections of SRBCs (FIG. 15) or KLH (FIG. 16) on day 46. Specifically, in FIG. 15, the closed box represents mice who were administered with only SRBC at day 0 and day 46. The open box represents mice administered with only SRBC at day 46. The remaining mice represented in FIG. 15 were further administered with SRBC at day 46. In contrast, in FIG. 16, the mice were administered with a different immunogen, KLH, at day 46 only.

Digitized by Google

Serum concentrations of mice measured as having antibodies directed against SRBCs or KLH were determined by ELISA as described (Linsley et al., Science 1992).

Serum antibody titers were calculated as the dilution giving an A_{450} of five times background. Serum antibody titer values from FIG. **15** were determined from pooled sera from five mice per group, while serum antibody titer values from FIG. **16** represents mean titers of five individual sera. Arrows indicate an SRBC or KLH injection at day 46.

FIGS. **15** and **16** show that the immunological response in mice injected concurrently with both CTLA4Ig and anti-IL4 (open triangle) is suppressed in an antigen-specific manner.

FIG. **15** shows that there is no rise in serum antibody titer (i.e. no primary or secondary immunological response) in mice injected concurrently with CTLA4Ig and anti-IL4 and injected with SRBC at day 0 and day 46. The combination of CTLA4Ig and anti-IL4 suppresses a primary and secondary immune response and induces long lasting immunological non-responsiveness to SRBC.

Additionally, FIG. **15** shows that there is no primary immunological response in mice injected concurrently with CTLA4Ig and the control rat Ig (Cappel, Organontecknika, Palo Alto, Calif.). However, these mice exhibit a secondary immunological response after injection with SRBC at day 46 (closed triangle, FIG. **15**).

FIG. **16** shows that administration of CTLA4Ig and anti-IL4, followed by a different immunogen, KLH, at day 46 in mice does not suppress a primary immune response to KLH in mice. Instead, these mice exhibited a primary immune response to KLH (open triangle, FIG. **16**). Thus, mice treated with CTLA4Ig and anti-IL4 exhibited a highly specific immune response depending on the antigen administered therein.

SEQUENCE LISTING

(1) GENERAL INFORMATION:

(i i i) NUMBER OF SEQUENCES: 14

(2) INFORMATION FOR SEQ ID NO:1:

(i) SEQUENCE CHARACTERISTICS:
(A) LENGTH: 39 base pairs
(B) TYPE: nucleic acid
(C) STRANDEDNESS: single
(D) TOPOLOGY: linear

(i i) MOLECULE TYPE: DNA (genomic)

(i i i) HYPOTHETICAL: NO

(i v) ANTI-SENSE: NO

(v i) ORIGINAL SOURCE:
(A) ORGANISM: Homo sapiens

(x i) SEQUENCE DESCRIPTION: SEQ ID NO:1:

CTAGCCACTG AAGCTTCACC ATGGGTGTAC TGCTCACAC 39

(2) INFORMATION FOR SEQ ID NO:2:

(i) SEQUENCE CHARACTERISTICS:
(A) LENGTH: 39 base pairs
(B) TYPE: nucleic acid
(C) STRANDEDNESS: single
(D) TOPOLOGY: linear

(i i) MOLECULE TYPE: DNA (genomic)

(i i i) HYPOTHETICAL: NO

(i v) ANTI-SENSE: NO

(v i) ORIGINAL SOURCE:
(A) ORGANISM: Homo sapiens

(x i) SEQUENCE DESCRIPTION: SEQ ID NO:2:

TGGCATGGGC TCCTGATCAG GCTTAGAAGG TCCGGGAAA 39

(2) INFORMATION FOR SEQ ID NO:3:

(i) SEQUENCE CHARACTERISTICS:
(A) LENGTH: 39 base pairs
(B) TYPE: nucleic acid

Digitized by Google

-continued

(C) STRANDEDNESS: single
(D) TOPOLOGY: linear

(i i) MOLECULE TYPE: DNA (genomic)

(i i i) HYPOTHETICAL: NO

(i v) ANTI-SENSE: NO

(v i) ORIGINAL SOURCE:
(A) ORGANISM: Homo sapiens

(x i) SEQUENCE DESCRIPTION: SEQ ID NO:3:

TTTGGGCTCC TGATCAGGAA AATGCTCTTG CTTGGTTGT 39

(2) INFORMATION FOR SEQ ID NO:4:

(i) SEQUENCE CHARACTERISTICS:
(A) LENGTH: 84 base pairs
(B) TYPE: nucleic acid
(C) STRANDEDNESS: single
(D) TOPOLOGY: linear

(i i) MOLECULE TYPE: DNA (genomic)

(i i i) HYPOTHETICAL: NO

(i v) ANTI-SENSE: NO

(v i) ORIGINAL SOURCE:
(A) ORGANISM: Homo sapiens

(x i) SEQUENCE DESCRIPTION: SEQ ID NO:4:

AAGCAAGAGC ATTTTCCTGA TCAGGAGCCC AAATCTTCTG ACAAAACTCA CACATCCCCA 60

CCGTCCCCAG CACCTGAACT CCTG 84

(2) INFORMATION FOR SEQ ID NO:5:

(i) SEQUENCE CHARACTERISTICS:
(A) LENGTH: 41 base pairs
(B) TYPE: nucleic acid
(C) STRANDEDNESS: single
(D) TOPOLOGY: linear

(i i) MOLECULE TYPE: DNA (genomic)

(i i i) HYPOTHETICAL: NO

(i v) ANTI-SENSE: NO

(v i) ORIGINAL SOURCE:
(A) ORGANISM: Homo sapiens

(x i) SEQUENCE DESCRIPTION: SEQ ID NO:5:

CTTCGACCAG TCTAGAAGCA TCCTCGTGCG ACCGCGAGAG C 41

(2) INFORMATION FOR SEQ ID NO:6:

(i) SEQUENCE CHARACTERISTICS:
(A) LENGTH: 47 base pairs
(B) TYPE: nucleic acid
(C) STRANDEDNESS: single
(D) TOPOLOGY: linear

(i i) MOLECULE TYPE: DNA (genomic)

(i i i) HYPOTHETICAL: NO

(i v) ANTI-SENSE: NO

(v i) ORIGINAL SOURCE:
(A) ORGANISM: Homo sapiens

Digitized by Google

-continued

(x i) SEQUENCE DESCRIPTION: SEQ ID NO:6:

CATTGCACAG TCAAGCTTCC ATGCCCATGG GTTCTCTGGC CACCTTG 47

(2) INFORMATION FOR SEQ ID NO:7:

(i) SEQUENCE CHARACTERISTICS:
(A) LENGTH: 39 base pairs
(B) TYPE: nucleic acid
(C) STRANDEDNESS: single
(D) TOPOLOGY: linear

(i i) MOLECULE TYPE: DNA (genomic)

(i i i) HYPOTHETICAL: NO

(i v) ANTI-SENSE: NO

(v i) ORIGINAL SOURCE:
(A) ORGANISM: Homo sapiens

(x i) SEQUENCE DESCRIPTION: SEQ ID NO:7:

ATCCACAGTG CAGTGATCAT TTGGATCCTG GCATGTGAC 39

(2) INFORMATION FOR SEQ ID NO:8:

(i) SEQUENCE CHARACTERISTICS:
(A) LENGTH: 65 base pairs
(B) TYPE: nucleic acid
(C) STRANDEDNESS: single
(D) TOPOLOGY: linear

(i i) MOLECULE TYPE: DNA (genomic)

(i i i) HYPOTHETICAL: NO

(i v) ANTI-SENSE: NO

(v i) ORIGINAL SOURCE:
(A) ORGANISM: Homo sapiens

(x i) SEQUENCE DESCRIPTION: SEQ ID NO:8:

CTCAGTCTGG TCCTTGCACT CCTGTTTCCA AGCATGGCGA GCATGGCAAT GCACGTGGCC 60

CAGCC 65

(2) INFORMATION FOR SEQ ID NO:9:

(i) SEQUENCE CHARACTERISTICS:
(A) LENGTH: 33 base pairs
(B) TYPE: nucleic acid
(C) STRANDEDNESS: single
(D) TOPOLOGY: linear

(i i) MOLECULE TYPE: DNA (genomic)

(i i i) HYPOTHETICAL: NO

(i v) ANTI-SENSE: NO

(v i) ORIGINAL SOURCE:
(A) ORGANISM: Homo sapiens

(x i) SEQUENCE DESCRIPTION: SEQ ID NO:9:

TTTGGGCTCC TGATCAGAAT CTGGGCACGG TTG 33

(2) INFORMATION FOR SEQ ID NO:10:

(i) SEQUENCE CHARACTERISTICS:
(A) LENGTH: 72 base pairs
(B) TYPE: nucleic acid
(C) STRANDEDNESS: single
(D) TOPOLOGY: linear

Digitized by Google

-continued

(i i) MOLECULE TYPE: DNA (genomic)

(i i i) HYPOTHETICAL: NO

(i v) ANTI-SENSE: NO

(v i) ORIGINAL SOURCE:
(A) ORGANISM: Homo sapiens

(x i) SEQUENCE DESCRIPTION: SEQ ID NO:10:

CTAGCCACTG AAGCTTCACC AATGGGTGTA CTGCTCACAC AGAGGACGCT GCTCAGTCTG 60

GTCCTTGCAC TC 72

(2) INFORMATION FOR SEQ ID NO:11:

(i) SEQUENCE CHARACTERISTICS:
(A) LENGTH: 33 base pairs
(B) TYPE: nucleic acid
(C) STRANDEDNESS: single
(D) TOPOLOGY: linear

(i i) MOLECULE TYPE: DNA (genomic)

(i i i) HYPOTHETICAL: NO

(i v) ANTI-SENSE: NO

(v i) ORIGINAL SOURCE:
(A) ORGANISM: Homo sapiens

(x i) SEQUENCE DESCRIPTION: SEQ ID NO:11:

GCAATGCACG TGGCCCAGCC TGCTGTGGTA GTG 33

(2) INFORMATION FOR SEQ ID NO:12:

(i) SEQUENCE CHARACTERISTICS:
(A) LENGTH: 45 base pairs
(B) TYPE: nucleic acid
(C) STRANDEDNESS: single
(D) TOPOLOGY: linear

(i i) MOLECULE TYPE: DNA (genomic)

(i i i) HYPOTHETICAL: NO

(i v) ANTI-SENSE: NO

(v i) ORIGINAL SOURCE:
(A) ORGANISM: Homo sapiens

(x i) SEQUENCE DESCRIPTION: SEQ ID NO:12:

TGATGTAACA TGTCTAGATC AATTGATGGG AATAAAATAA GGCTG 45

(2) INFORMATION FOR SEQ ID NO:13:

(i) SEQUENCE CHARACTERISTICS:
(A) LENGTH: 561 base pairs
(B) TYPE: nucleic acid
(C) STRANDEDNESS: single
(D) TOPOLOGY: linear

(i i) MOLECULE TYPE: DNA (genomic)

(i i i) HYPOTHETICAL: NO

(i v) ANTI-SENSE: NO

(v i) ORIGINAL SOURCE:
(A) ORGANISM: Homo sapiens

(i x) FEATURE:
(A) NAME/KEY: CDS

Digitized by Google

-continued

(B) LOCATION: 1..561

(x i) SEQUENCE DESCRIPTION: SEQ ID NO:13:

```
GCA ATG CAC GTG GCC CAG CCT GCT GTG GTA CTG GCC AGC AGC CGA GGC          48
Ala Met His Val Ala Gln Pro Ala Val Val Leu Ala Ser Ser Arg Gly
 1               5                  10                  15

ATC GCC AGC TTT GTG TGT GAG TAT GCA TCT CCA GGC AAA GCC ACT GAG          96
Ile Ala Ser Phe Val Cys Glu Tyr Ala Ser Pro Gly Lys Ala Thr Glu
            20                  25                  30

GTC CGG GTG ACA GTG CTT CGG CAG GCT GAC AGC CAG GTG ACT GAA GTC         144
Val Arg Val Thr Val Leu Arg Gln Ala Asp Ser Gln Val Thr Glu Val
        35                  40                  45

TGT GCG GCA ACC TAC ATG ATG GGG AAT GAG TTG ACC TTC CTA GAT GAT         192
Cys Ala Ala Thr Tyr Met Met Gly Asn Glu Leu Thr Phe Leu Asp Asp
    50                  55                  60

TCC ATC TGC ACG GGC ACC TCC AGT GGA AAT CAA GTG AAC CTC ACT ATC         240
Ser Ile Cys Thr Gly Thr Ser Ser Gly Asn Gln Val Asn Leu Thr Ile
65                  70                  75                  80

CAA GGA CTG AGG GCC ATG GAC ACG GGA CTC TAC ATC TGC AAG GTG GAG         288
Gln Gly Leu Arg Ala Met Asp Thr Gly Leu Tyr Ile Cys Lys Val Glu
                85                  90                  95

CTC ATG TAC CCA CCG CCA TAC TAC CTG GGC ATA GGC AAC GGA ACC CAG         336
Leu Met Tyr Pro Pro Pro Tyr Tyr Leu Gly Ile Gly Asn Gly Thr Gln
            100                 105                 110

ATT TAT GTA ATT GAT CCA GAA CCG TGC CCA GAT TCT GAC TTC CTC CTC         384
Ile Tyr Val Ile Asp Pro Glu Pro Cys Pro Asp Ser Asp Phe Leu Leu
        115                 120                 125

TGG ATC CTT GCA GCA GTT AGT TCG GGG TTG TTT TTT TAT AGC TTT CTC         432
Trp Ile Leu Ala Ala Val Ser Ser Gly Leu Phe Phe Tyr Ser Phe Leu
    130                 135                 140

CTC ACA GCT GTT TCT TTG AGC AAA ATG CTA AAG AAA AGA AGC CCT CTT         480
Leu Thr Ala Val Ser Leu Ser Lys Met Leu Lys Lys Arg Ser Pro Leu
145                 150                 155                 160

ACA ACA GGG GTC TAT GTG AAA ATG CCC CCA ACA GAG CCA GAA TGT GAA         528
Thr Thr Gly Val Tyr Val Lys Met Pro Pro Thr Glu Pro Glu Cys Glu
                165                 170                 175

AAG CAA TTT CAG CCT TAT TTT ATT CCC ATC AAT                             561
Lys Gln Phe Gln Pro Tyr Phe Ile Pro Ile Asn
            180                 185
```

(2) INFORMATION FOR SEQ ID NO:14:

(i) SEQUENCE CHARACTERISTICS:
(A) LENGTH: 187 amino acids
(B) TYPE: amino acid
(D) TOPOLOGY: linear

(i i) MOLECULE TYPE: protein

(x i) SEQUENCE DESCRIPTION: SEQ ID NO:14:

```
Ala Met His Val Ala Gln Pro Ala Val Val Leu Ala Ser Ser Arg Gly
 1               5                  10                  15

Ile Ala Ser Phe Val Cys Glu Tyr Ala Ser Pro Gly Lys Ala Thr Glu
            20                  25                  30

Val Arg Val Thr Val Leu Arg Gln Ala Asp Ser Gln Val Thr Glu Val
        35                  40                  45

Cys Ala Ala Thr Tyr Met Met Gly Asn Glu Leu Thr Phe Leu Asp Asp
    50                  55                  60

Ser Ile Cys Thr Gly Thr Ser Ser Gly Asn Gln Val Asn Leu Thr Ile
65                  70                  75                  80

Gln Gly Leu Arg Ala Met Asp Thr Gly Leu Tyr Ile Cys Lys Val Glu
```

Digitized by Google

-continued

```
                                85                  90                  95

Leu Met Tyr Pro Pro Pro Tyr Tyr Leu Gly Ile Gly Asn Gly Thr Gln
                100                 105                 110

Ile Tyr Val Ile Asp Pro Glu Pro Cys Pro Asp Ser Asp Phe Leu Leu
            115                 120                 125

Trp Ile Leu Ala Ala Val Ser Ser Gly Leu Phe Phe Tyr Ser Phe Leu
        130                 135                 140

Leu Thr Ala Val Ser Leu Ser Lys Met Leu Lys Lys Arg Ser Pro Leu
145                 150                 155                 160

Thr Thr Gly Val Tyr Val Lys Met Pro Pro Thr Glu Pro Glu Cys Glu
                165                 170                 175

Lys Gln Phe Gln Pro Tyr Phe Ile Pro Ile Asn
            180                 185
```

What is claimed is:

1. A method for suppressing an immune response comprising contacting B7-positive lymphocytes with a B7-binding molecule and an IL4-binding molecule, wherein an immune response is thereby suppressed.

2. The method of claim 1, wherein the immune response is a B cell response.

3. The method of claim 1, wherein the immune response is a T cell response.

4. A method for inhibiting tissue transplant rejection by a subject, the subject being a recipient of transplanted tissue, which method comprises administering to the subject a B7-binding molecule and an IL4-binding molecule so a primary and secondary immune response is suppressed thereby inhibiting tissue transplant rejection by the subject.

5. A method for inhibiting graft versus host disease in a subject which method comprises administering to the subject a B7-binding molecule and an IL4-binding molecule so a primary and secondary immune response is suppressed thereby inhibiting tissue transplant rejection by the subject.

6. The method of claim 1, 4, or 5, wherein the B7-binding molecule is a CTLA4Ig fusion protein.

7. The method of claim 6, wherein the CTLA4Ig fusion protein is a fusion protein having a first amino acid sequence containing amino acid residues from position 1 to position 125 of the amino acid sequence corresponding to the extracellular domain of CTLA4 and a second amino acid sequence containing amino acid residues corresponding to the hinge, CH2 and CH3 regions of human immunoglobulin Cγ1.

8. The method of claim 1, 4, or 5, wherein the B7-binding molecule is a CD28Ig/CTLA4Ig fusion protein hybrid.

9. The method of claim 8, wherein the CD28Ig/CTLA4Ig fusion protein hybrid is a fusion protein hybrid having a first amino acid sequence consisting of a portion of the extracellular domain of CD28 receptor which portion binds B7 fused to a second amino acid sequence consisting of a portion of the extracellular domain of CTLA4 receptor which portion binds B7 and a third amino acid sequence of the hinge, CH2 and CH3 regions of human immunoglobulin Cγ1.

10. The method of claim 1, 4, or 5, wherein the IL4-binding molecule is a monoclonal antibody which specifically recognizes and binds to IL4.

11. The method of claim 1, 4, or 5, wherein the IL4-binding molecule is a soluble IL4 receptor which recognizes and binds to IL4.

* * * * *

Digitized by Google

EXHIBIT 10

THIS EXHIBIT HAS BEEN REDACTED IN ITS ENTIRETY

EXHIBIT 11

THIS EXHIBIT HAS BEEN REDACTED IN ITS ENTIRETY

EXHIBIT 12

THIS EXHIBIT HAS BEEN REDACTED IN ITS ENTIRETY

EXHIBIT 13

THIS EXHIBIT HAS BEEN REDACTED IN ITS ENTIRETY

EXHIBIT 14

Volume 118 / Number 2 / February 19[illegible]

THE JOURNAL OF IMMUNOLOGY®

Official Journal of The American Association of Immunologists

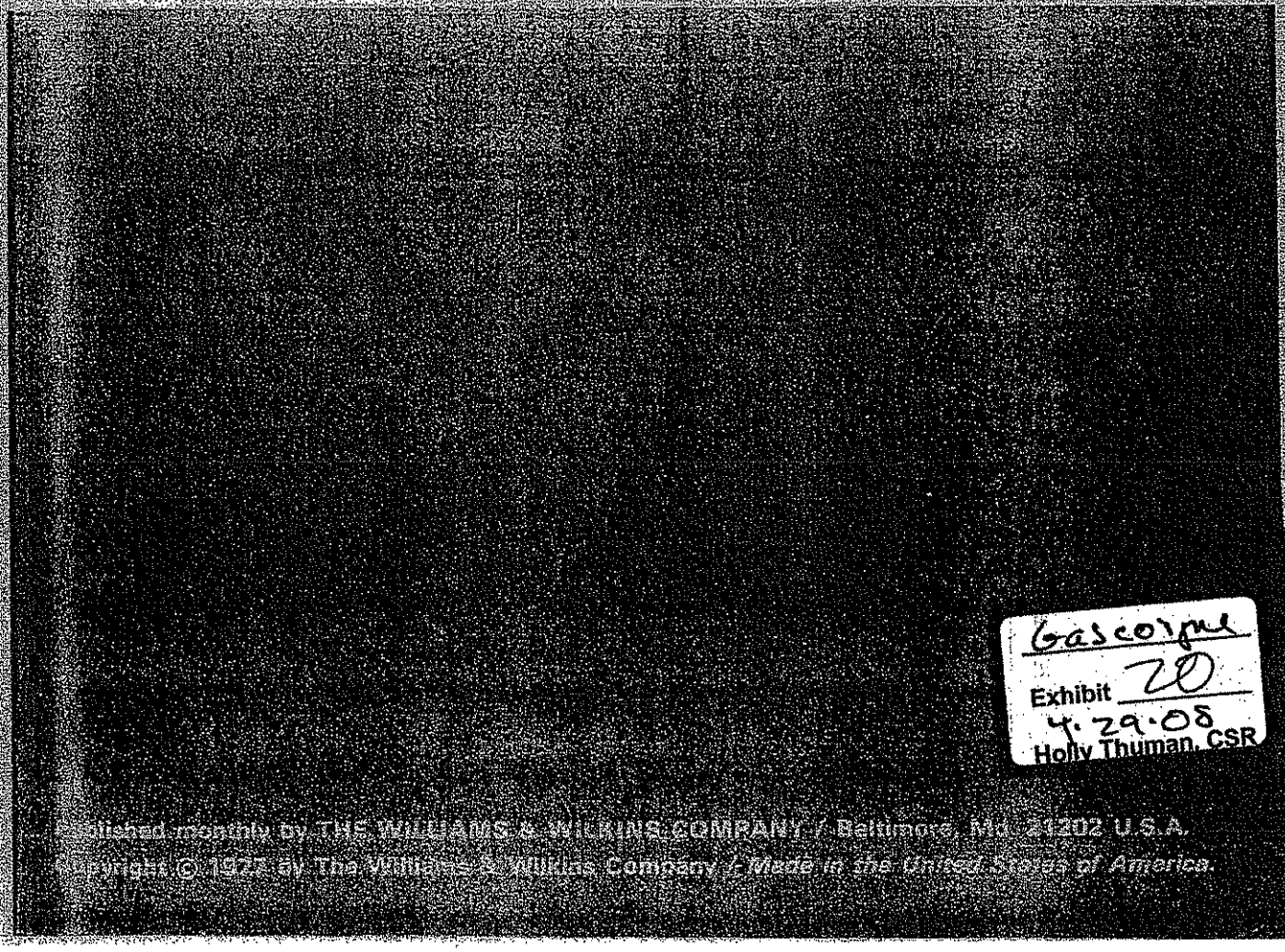

Gascoigne
Exhibit 20
4.29.08
Holly Thuman, CSR

Published monthly by THE WILLIAMS & WILKINS COMPANY / Baltimore, Md. 21202 U.S.A.
Copyright © 1977 by The Williams & Wilkins Company / Made in the United States of America.

The material on this page was copied from the collection of the National Library of Medicine by a third party and may be protected by U.S. Copyright law.

THE JOURNAL OF IMMUNOLOGY
Vol. 118, No. 2, February 1977
Printed in U.S.A.
Copyright © 1977 by The Williams & Wilkins Co.

CHARACTERIZATION OF TWO SPECIES OF Fc FRAGMENTS OBTAINED FROM RAT IgG2a BY PROLONGED PAPAIN DIGESTION[1]

WILLIAM P. AREND,[2,3] MARK A. HERMODSON AND DAVID C. TELLER

From the Veterans Administration Hospital, Seattle, Washington 98108, and the Departments of Medicine and Biochemistry, University of Washington School of Medicine, Seattle, Washington 98195

Prolonged papain digestion of rat IgG2a produced two molecular species of Fc fragments, termed Fc(I) and Fc(II). Studies by gel filtration chromatography and polyacrylamide gel electrophoresis in SDS/urea indicated that the two subunit polypeptide chains in each Fc preparation were associated by non-covalent bonds only. By analytical ultracentrifugation Fc(I) was found to have a m.w. of 47,100 and a sedimentation coefficient of 4.08S. Fc(II) had a m.w. of 39,800 and a sedimentation coefficient of 3.83S. The m.w. for the subunit chains of Fc(I) and Fc(II) were 25,300 and 20,300, respectively, as determined by analytical ultracentrifugation under dissociating conditions. Calculation of the frictional coefficient ratios indicated that both Fc fragments possessed compact globular structures.

The difference in size between these two Fc fragments probably was due to a loss of some carboxy-terminal residues in Fc(II). Both Fc fragments possessed nearly identical amino-terminal amino acid sequences. Papain cleavage occurred primarily between residues 233/234 and 234/235. The carbohydrate compositions of the two species of Fc fragments were similar.

It was concluded that under acid and reducing conditions papain cleavage of rat IgG2a occurred to the carboxy-terminal side of the hinge region. Prolonged papain digestion led to secondary attack in the carboxy-terminal end of the Cγ3 domain at an unidentified site, or sites, producing a stable second species of Fc fragments.

Papain digestion of IgG from most species yields primarily Fab and Fc fragments. Human IgG subclasses vary in their susceptibility to papain digestion with IgG3 being the most sensitive, IgG1 and IgG4 being intermediate, and IgG2 demonstrating resistance to papain cleavage (1). Furthermore, variations in digestion conditions, including the pH, time of exposure to papain, and the presence or absence of reducing agents, give rise to fragments other than Fab or Fc (2–4).

The primary site of papain digestion has been shown to be between residues 225/226 in human IgG1, between residues 230/231 in human IgG2, and between residues 225/226 in rabbit IgG (5). In one study prolonged papain digestion of rabbit IgG led to progressive cleavage of the amino-terminal portion of the Cγ2 domain (6). Studies on mouse immunoglobulins revealed that the relative susceptibility to papain cleavage was in the order IgG2b > IgG2a > IgG1 with the sites of cleavage not established (4).

Recent studies have described four rat IgG subclasses: IgG1, IgG2a, IgG2b, and IgG2c (7). IgG2a is the major subclass, comprising half, or more, of the circulating IgG in rats. Structural studies on rat Fc of defined subclass specificity have not been reported. During the course of studies on IgG catabolism in the rat, the observation was made that prolonged papain digestion of rat IgG2a yielded a mixture of Fc fragments. The studies reported in this paper describe the production and characterization of these Fc fragments. The results support the conclusion that papain cleavage in the rat IgG2a molecule, under acid and reducing conditions, occurs primarily to the C-terminal side of the inter-heavy chain disulfide bonds between residues 233/234 and 234/235. Upon prolonged exposure to papain further digestion probably occurs in the C-terminal portion of the Cγ3 domain. The results of studies on the biologic properties of these two Fc fragments are reported separately (8).

MATERIALS AND METHODS

Preparation of rat IgG2a. Normal rat γ-globulins (Cohn Fraction II, prepared from the sera of Sprague-Dawley or Wistar strain rats) was purchased from Miles Laboratories, Kankakee, Ill. IgG2a was obtained by elution from a DEAE cellulose column (DE52, Whatman, Kent, England) with 10 mM phosphate buffer, pH 7.4. The IgG2a preparations usually gave a single line when tested in double diffusion in agar against anti-rat sera or anti-rat IgG (Miles Laboratories and Schwarz-Mann, Orangeburg, N. Y.). Occasionally trace contamination with IgG2b was present, as determined by agar diffusion studies with antisera specific for rat IgG subclasses (kindly provided by Dr. H. Bazin, Brussels, Belgium).

Papain digestion. Papain digestion of rat IgG was carried out by using modifications of the method described by Porter (9). Rat IgG2a (20 mg/ml in 10 mM sodium acetate, pH 5.5) was preincubated with 10 mM cysteine and 2 mM EDTA for 2 hr at 37°C. Mercuri-papain (Sigma Chemical Co., St. Louis, Mo., or Worthington Biochemical Corporation, Freehold, N. J.) was added to give an enzyme to protein ratio of 1:100 by weight. Incubation was carried out for 16 hr in a shaking water bath. The papain digestion was stopped by making the mixture 15 mM in *N*-ethyl maleimide or 15 mM in iodoacetamide. Subsequent purificaion of Fc by gel filtration chromatography, ion-exchange chromatography, and immunoadsorbtion was performed as described recently (10). Approximate m.w. of the IgG2a Fc fragments were obtained from the elution profiles on a Sephadex G-100 column (Pharmacia Fine

Submitted for publication August 2, 1976.

[1] This work was supported by the Veterans Administration and by Grants AI-10825, GM-15253 and GM-13401 from the United States Public Health Service.

[2] Recipient of a Clinical Investigator award from the Veterans Administration.

[3] Address for correspondence: Veterans Administration Hospital, 4435 Beacon Avenue South, Seattle, Washington 98108.

The material on this page was copied from the collection of the National Library of Medicine by a third party and may be protected by U.S. Copyright law.

Chemicals, Inc., Piscataway, N. J.) equilibrated with 0.2 M sodium borate, 0.16 M NaCl, pH 8.0. This column was calibrated with human γ-globulin for determination of the excluded volume, plus bovine serum albumin (BSA, m.w. 66,000), ovalbumin (OA, m.w. 45,000), and ribonuclease A (Ribo A,[4] m.w. 13,700) as included markers.

Pepsin digestion. This procedure was performed on purified rat IgG2a by using the conditions described by Turner and Bennich (11). IgG2a (30 mg/ml in 0.1 M sodium acetate, pH 4.5) was incubated with pepsin (Sigma Chemical Co. or Worthington Biochemical Corp.) at an enzyme to protein ratio of 1:100 and digestion was carried out in a 37°C shaking water bath for 24 hr. The reaction was stopped by adjusting the pH to 8.0 with borate buffer and NaOH. Fragment pFc' was isolated by elution on a Sephadex G-100 column equilibrated with borate buffer.

Polyacrylamide gel electrophoresis in DTT-SDS urea. Polyacrylamide gel electrophoresis was carried out on the purified rat Fc samples with the conditions described by Fairbanks *et al.* (12). The best characterization of the Fc fragments was obtained with 7.5% polyacrylamide in the presence of 1% sodium dodecyl sulfate (SDS) and 6 M urea after the samples had been pretreated with 40 mM dithiothreitol (DTT), SDS, and urea. Molecular weight markers utilized in each electrophoresis run included BSA, OA, chymotrysinogen A (CHY, m.w. 25,700), myoglobin (MYO, m.w. 17,600), and insulin (INS, m.w. 5750) (all from Schwarz-Mann). Ten micrograms of each IgG2a fragment preparation, or of each m.w. marker, were added to electrophoresis buffer (containing DTT, SDS, and urea) preheated on a boiling water bath. The protein solutions were then boiled for 5 min and heated further for 30 min at 45°C. In some experiments the samples were not boiled before heating at 45°C and subsequent application to the gel. Electrophoresis was carried out for 4 hr, with subsequent fixation and staining with Coomassie Blue performed as described elsewhere (12). The stained gels were scanned and m.w. of the major peaks of the IgG2a fragments were estimated from a calibration plot of the logarithm of m.w. markers against their relative mobility. The relative mobility represented a ratio of the distance migrated by the sample in relation to the migration of pyronin Y dye in each gel. The relative mobilities were corrected for variations in gel length resulting from washing.

Amino acid content and sequences. Amino acid analyses were performed on the purified IgG2a fragments with a Durrum amino acid analyzer (by AAA Laboratories, Seattle, Wash.). The amino-terminal amino acid sequences were determined on a Beckman Model 890C sequencer (Spinco Division of Beckman, Inc., Palo Alto, Calif.) according to the procedure of Hermodson *et al.* (13). Selected residues (Val, Ile and Phe) were quantitated in the first 10 cycles. In each case where sequence was observed, the quantities of the determined PTH-amino acids accounted for more than 60% of the expected amounts based on the quantity of degraded peptide. The stepwise yields of the degradations were 95 to 96% per cycle. Each of three different preparations of Fc(I) or Fc(II) were analyzed through 10 cycles.

Carboxypeptidase digestion. Samples of the Fc and pFc' fragments (30 to 40 nmoles of each peptide chain) were lyophilized and dissolved in 0.2 ml borate buffer containing 50 nmoles norleucine as an internal standard (14). The samples were subjected to digestion at 37°C by a mixture of carboxypeptidase A (Sigma, 5 units, 100 μg) and carboxypeptidase B (Sigma, 3.5 units, 25 μg). The exact amount of each peptide digested was determined by hydrolysis and amino acid analysis of a sample of the peptide with the norleucine internal standard. Samples were drawn at "0 time" (about 30 sec), 30 min, and 3 hr, then were quenched in acetic acid and lyophilized. Amino acid analyses were performed with the standard system used for hydrolysates, and thus Ser, Asn, and Gln were not resolved.

Carbohydrate analyses. The hexose content of the Fc fragments and of pFc' were determined by the phenol-sulfuric acid method (15). Samples of the three specimens were hydrolyzed in 2 N HCl overnight in evacuated tubes at 110°C. The hexosamine content was determined on the dried hydrolysates by the *p*-dimethylaminobenzaldehyde method (16).

Sedimentation equilibrium and sedimentation velocity. Sedimentation studies were performed with a Beckman Model E ultracentrifuge equipped with a ultraviolet absorption scanning system linked to a PDP-12 computer. Sedimentation velocity experiments were of the moving boundary type with the scanning system (17). Sedimentation equilibrium experiments were of the high speed type with methodology and computer programs as described by Teller (17, 18). The Rayleigh interference photographs were processed using an automatic densitometer (19).

The Fc fragments were studied in neutral buffer (0.16 M NaCl, 0.2 M sodium borate, pH 8.0) and under dissociating conditions in 6 M guanidine hydrochloride. For the latter experiments the Fc samples were made 6 M in urea and placed immediately in a boiling water bath. After boiling for 10 min the samples were dialyzed against 6 M urea, and then were further dialyzed for 3 days against 6 M guanidine hydrochloride, 0.1 M 2-mercaptoethanol (2-ME). Both Fc(I) and Fc(II) fragments in borate buffer behaved as self-associating systems of the monomer-dimer type. These associations were very weak and were insignificant under the conditions of the *in vivo* experiments in the accompanying paper (8). The m.w. of the smallest species was calculated by the method of Hoagland and Teller (20) as described by Teller (17). In 6 M guanidine hydrochloride, 0.1 M 2-ME, the preparations were non-ideal. Minimum m.w. were estimated at infinite dilution of protein by described methods (21, 22).

Apparent specific volumes were calculated from the amino acid composition and carbohydrate analyses, as described by Cohn and Edsall (23) and Longsworth (24), respectively. These values were corrected for 6 M guanidine hydrochloride by described methods (25).

Miscellaneous. The concentrations of rat IgG2a, Fc, and pFc' preparations were determined by absorbance at 280 nm with extinction coefficients ($E_{1cm}^{1\%}$) of 14.4 for IgG2a, and 12.2 for Fc fragments and pFc'.

RESULTS

Papain digestion. Papain digestion for 15 min or for 16 hr completely cleaved the IgG2a present since no intact IgG2a was observed on gel filtration immediately after digestion. Analysis of the elution profile of the purified Fc fragments from a 16-hr papain digestion on a calibrated Sephadex G-100 column revealed a broad pattern which represented the summation of two smaller peaks (Fig. 1). Upon pooling of the

[4] Abbreviations used in this paper: Fc(I) and Fc(II), the larger and smaller species of Fc fragments, respectively, obtained after 16 hr of papain digestion of rat IgG2a; DTT, dithiothreitol; PTH, phenylthiohydantoin; Ribo A, ribonuclease A; CHY, chymotrypsinogen A; MYO myoglobin; and INS, insulin.

The material on this page was copied from the collection of the National Library of Medicine by a third party and may be protected by U.S. Copyright law.

Case 1:06-cv-00500-SLR-MPT Document 252-2 Filed 08/25/2008 Page 13 of 33

ascending and descending limbs of the G-100 peak and further gel filtration, purified preparations of Fc were obtained with estimated m.w. of 44,500 and 33,900 (Table I). These two fragments purified from 16-hr papain digests will be referred to subsequently as Fc(I) and Fc(II).

Gel filtration studies under dissociating conditions showed that the subunits in each of the Fc fragment preparations were held together only by non-covalent bonds. In the presence of 1 M acetic acid and 6 M urea, the Fc(I) preparation gave a single peak on Sephadex G-100 of 30,400 (Table I). Fragments subjected to further reduction and alkylation gave identical results. Under acid conditions the Fc(II) was unstable, yielding a mixture of polypeptides with m.w. between 10,000 and 25,000. Gel filtration on a Sephadex G-100 column equilibrated with 6 M urea in borate buffer and 5 mM iodoacetamide revealed the presence of a single subunit with a m.w. of approximately 25,000 in both Fc preparations. The Fc(I) also gave a peak of undissociated material in urea/borate whereas all of the Fc(II) was dissociated to the basic subunit under these conditions (Table I).

Pepsin digestion. In addition to a major peak with a m.w. of 105,000, pepsin digestion produced a small amount of material possessing an approximate m.w. of 24,000. Gel filtration on a calibrated G-100 column in the presence of 1 M acetic acid and 6 M urea yielded a single peak with an approximate m.w. of 14,000. This pepsin product was felt to represent pFc', with the two chains held together by noncovalent bonds.

Polyacrylamide gel electrophoresis. Polyacrylamide gel electrophoresis in the presence of DTT-SDS-urea was performed in an effort to characterize the subunit structure of each of the Fc fragments. Identical results were obtained with Fc(I) and Fc(II). A single peak with an approximate m.w. of 30,000 was observed when boiled samples were applied to the gels (Table II). However, when the samples were not boiled two additional peaks of 19,000 and 13,000 were seen with two-thirds of the material still present as a peak of 30,000. Pepsin fragment pFc' demonstrated a single peak of 14,600 under these electrophoresis conditions with samples subjected to either pretreatment. Identical results were obtained with 10% polyacrylamide gels or when the reducing agent, DTT, was not present.

These results suggested that each of the Fc fragments possessed a single subunit with an estimated m.w. of 30,000 by PAGE.

Sedimentation equilibrium and sedimentation velocity. The Fc fragments were studied by analytical ultracentrifugation in an effort to determine more precisely their size, subunit structure, and conformation. In neutral buffer the smallest m.w. species of Fc(I) and Fc(II) were 47,100 and 39,800, respectively

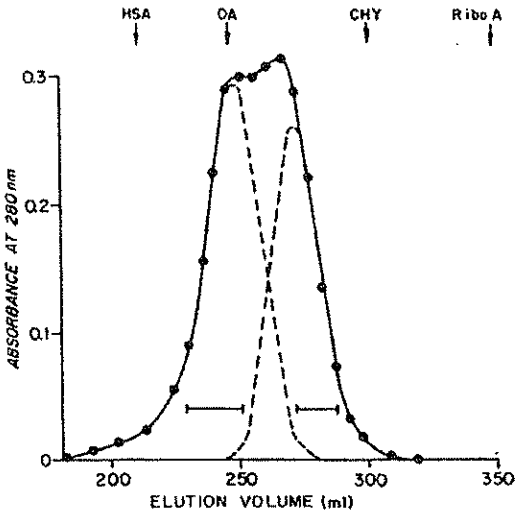

Figure 1. The Sepadex G100 elution profile of IgG2a Fc obtained after 16 hr papain digestion (*solid line*). The G100 column was equilibrated at 4°C with 0.2 M sodium borate, 0.16 M NaCl, pH 8.0; column size 2.50 x 87.7 cm with V_e 145 ml. The broad curve can be resolved into two smaller peaks, indicated by the *dashed lines*. Two pools were made of the ascending and descending limbs, as shown by the *horizontal bars*, and each pool was further characterized by repeat gel filtration on the same calibrated G100 column. The two pools contained Fc fragments with approximate m. w. of 44,500 and 33,900.

TABLE I

Molecular weights of Fc fragments estimated by gel filtration[a]

Gel Filtration Conditions	Molecular Weights[b]	
	Fc(I)	Fc(II)
Borate buffer	44,500 ± 900	33,900 ± 500
1 M acetic acid/6 M urea	30,400 ± 800	[c]
Borate buffer/6 M urea/ 5 mM iodoacetamide	54,700 ± 2,500[d] 24,400 ± 1,200[d]	25,800 ± 1,500

[a] The m.w. were estimated on Sephadex G100 columns, calibrated as outlined in *Materials and Methods* and in the legend for Fig. 1.

[b] The molecular weight data represent the mean ± 1 S.D. from four different gel filtration runs in each case.

[c] Data could not be obtained because of instability under acid conditions.

[d] Approximately equal amounts of undissociated and dissociated material were present.

TABLE II

Molecular weights of major chain subunits estimated by polyacrylamide gel electrophoresis[a]

Protein	Relative Mobility[b]		Molecular Weight[b]	
	Boiled[c]	Not boiled[d]	Boiled[c]	Not boiled[d]
BSA	0.145	0.172		
OA	0.263	0.275		
CHY	0.389	0.410		
MYO	0.478	0.523		
INS		0.762		
Fc(I)	0.347	0.378	30,500	30,000
		0.494		18,500
		0.579		13,000
Fc(II)	0.342	0.382	31,000	29,500
		0.490		19,000
		0.585		12,800
pFc'	0.502	0.548	15,800	14,600

[a] All samples were pretreated with 40 mM DTT, 1% SDS, and 6 M urea and run on 7.5% gels in the presence of 1% SDS and 6 M urea.

[b] The data for relative mobility and m.w. represent the mean of two samples for each test protein analyzed in each gel run. Separate PAGE runs were made for samples either boiled or not boiled.

[c] In this electrophoresis run, all samples were added to the buffer with DTT, SDS, and urea, in a boiling water bath and were heated at 100°C for 5 min. The samples were further heated at 45°C for 30 min before application to the gels.

[d] In this run, the samples were not boiled but were only heated at 45°C for 30 min in the presence of DTT, SDS, and urea.

The material on this page was copied from the collection of the National Library of Medicine by a third party and may be protected by U.S. Copyright law.

Case 1:06-cv-00500-SLR-MPT Document 252-2 Filed 08/25/2008 Page 14 of 33

(Table III). These preparations both exhibited a tendency toward self-association of a single thermodynamic species. Under dissociating conditions (6 M guanidine HCl and 0.1 M 2-ME) the m.w. of the subunit chains in Fc(I) and Fc(II) were 25,300 and 20,300, respectively. Fc(I) was homogeneous as revealed by superposition of m.w. averages. Fc(II) was slightly heterogeneous as revealed by the average m.w.: M_n = 21,600 ± 1000, M_w 22,200 ± 600, M_z = 23,100 ± 300 and M_{z+1} = 23,800 ± 900. Both Fc preparations were boiled before exposure to guanidine HCl (see *Methods*). In contrast, analysis of an Fc(II) sample which was not boiled revealed marked heterogeneity, with the presence of many species of smaller sizes.

The sedimentation coefficients ($s_{20,w}$) of the Fc(I) and Fc(II) fragments were 4.08S and 3.83S, respectively, as determined on quite dilute solutions (Table III). The frictional coefficient rations (f/f_o), calculated from the sedimentation coefficients, were 1.19 for Fc(I) and 1.14 for Fc(II).

These results indicated that the Fc preparations were homogeneous and that each possessed one polypeptide chain subunit with a m.w. of approximately one-half that of the parent molecule. The Fc(II) fragment differed from the Fc(I) in that it was 15 to 20% smaller. Both Fc fragments possessed compact globular structures.

Immunologic studies. Double diffusion in agar showed lines of complete identity between Fc(I) and Fc(II) by using antisera to rat serum or anti-rat IgG (Fig. 2). Immunization of rabbits with each of these preparations produced antisera which also showed lines of complete identity between the two Fc preparations. In contrast, each of these fragments showed partial nonidentity with pFc' with the same antisera (Fig. 2). The spur of Fc(I) over pFc' was always stronger than that of Fc(II) over pFc'. On immunoelectrophoresis Fc(I) and Fc(II) showed identical electrophoretic distributions whereas the pFc' showed more anodal migration.

Amino acid composition. Further chemical analyses were performed in order to clarify the structural differences between the two Fc fragment preparations. The amino acid compositions of Fc(I) and Fc(II) were generally similar when corrected for differences in chain length, with a few exceptions (Table IV). The Fc(I) contained 5.3 Met residues per chain length of 214 amino acids and the Fc(II) showed 5.6 Met residues per chain of 180 amino acids, indicating no loss of Met in the latter preparation. In addition, Fc(II) possessed relatively more Pro and Glx than expected, in comparison with Fc(I), and less Ile, Lys, Ser and Val. These data suggest that the peptide missing from Fc(II) may have been deficient in the former amino acids and enriched in the latter, in comparison with the rest of the Fc(II) fragment. In contrast, pFc' was clearly different from the Fc fragments. The pFc' was relatively rich in Met, Tyr, and Gly, and was relatively poor in Val, Ile, and Phe.

None of the Fc or pFc' preparations contained any CM Cys, indicating an absence of exposed half-cystine residues. PE Cys determinations, performed after complete reduction and alkylation, indicated that both Fc(I) and Fc(II) probably contained four half-cystine residues (Table IV).

Carbohydrate composition. The total hexose and hexosa-

TABLE III

Analysis of Fc fragments by analytical ultracentrifugation

	Fc(I)	Fc(II)
Partial specific volume ($\bar{v}$):[a]		
in borate buffer	0.722	0.722
in 6M guanidine HCl	0.720	0.719
Molecular weight:		
in borate buffer	47,100 ± 500	39,800 ± 600
in 6M guanidine HCl	25,300 ± 230	20,300 ± 300
Sedimentation coefficient ($s_{20,w}$)[b]	4.08 ± 0.08	3.83 ± 0.10

[a] The partial specific volumes were calculated from the amino acid and carbohydrate compositions (see *Materials and Methods*).

[b] The sedimentation coefficients were weight-averaged values obtained in the concentration range of 0.14 to 0.40 mg/ml.

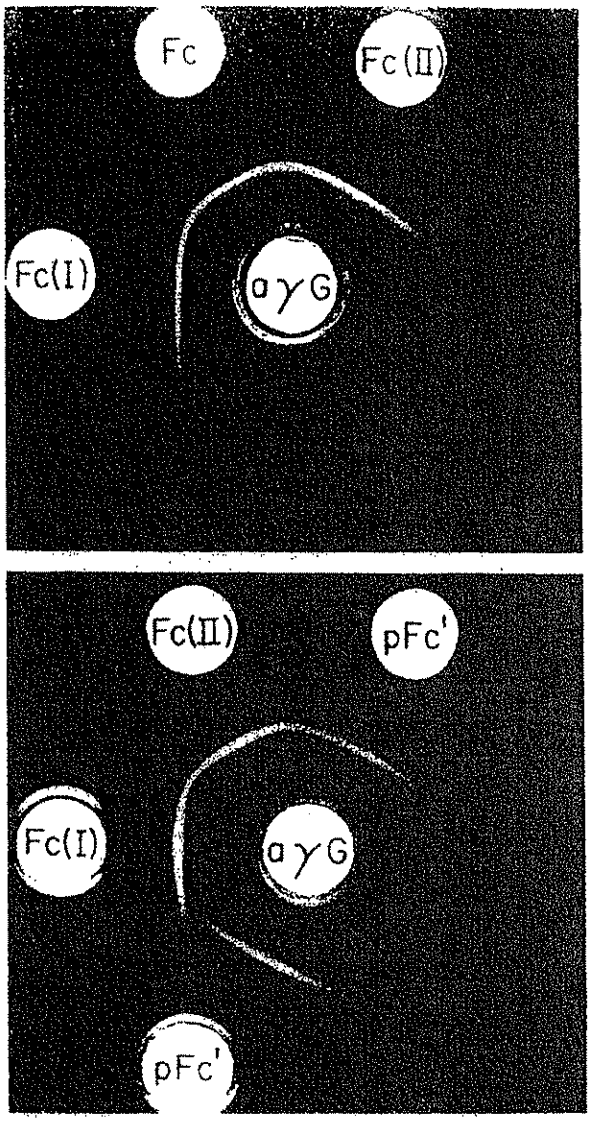

Figure 2. Double diffusion in agar of the immunoglobulin fragments. Fc stands for fragments obtained after 15 min of papain digestion; Fc(I) and Fc(II) represent the two species obtained after 16 hr of papain digestion. The antiserum is rabbit anti-rat IgG. The *upper* immunodiffusion pattern indicates complete identity between Fc and Fc(I) or Fc(II). The *lower* pattern shows complete identity between Fc (I) and Fc(II), with each of these preparations showing a spur over the pFc' line, indicating only partial identity.

The material on this page was copied from the collection of the National Library of Medicine by a third party and may be protected by U.S. Copyright law.

Case 1:06-cv-00500-SLR-MPT Document 252-2 Filed 08/25/2008 Page 15 of 33

mine content was determined for the three species of molecules. Fc(I) and Fc(II) contained similar amounts of carbohydrates, whereas pFc' had less than half the amount of hexose and hexosamine (Table V). The slightly decreased amounts of carbohydrates in Fc(II) in comparison with Fc(I) were not felt to be significant. Analyses of sialic acid content were not performed.

Amino-terminal analyses. Amino acid sequence analyses were performed on three different preparations of both Fc(I) and Fc(II) and indicated that these Fc fragments had very similar amino-terminal sequences: Leu-Gly-Gly-Pro-Ser-Val-Phe-Ile-Phe-Pro (Table VI). This sequence is identical to that of mouse IgG2a Fc between residues 235 and 244 (26), and to Fc from human IgG1 (27), or rabbit IgG (28) between residues 235 and 241. The Fc(I) was slightly heterogenous as 65% of the molecules possessed the above sequence and 35% commenced at Leu 234.

TABLE IV

Amino acid composition of Fc and pFc' fragments[a]

Amino Acid	Fc(I) (47,100 M.W.)	Fc(II) (39,800 M.W.)	pFc (24,000 M.W.)
Asx	20.7	17.8	10.1
Thr	19.4	16.9	10.7
Ser	18.8	15.1	10.1
Glx	27.6	25.0	15.1
Pro	19.8	18.0	11.1
Gly	11.8	10.8	9.0
Ala	5.7	4.3	3.0
Val	19.4	15.4	7.2
Met	5.3	5.6	4.0
Ile	9.1	6.8	3.2
Leu	11.6	9.7	6.3
Tyr	6.5	6.4	4.5
Phe	10.2	8.3	3.7
His	7.9	6.2	4.1
Lys	17.0	13.6	8.3
Arg	5.3	4.6	2.7
CM Cys[b]			
PE Cys[c]	3.5	3.4	2.4

[a] Numbers of each amino acid present assuming a total of 214 residues/chain for Fc(I), 180 residues/chain for Fc(II), and 108 residues/chain for pFc'. The data represent the mean of determinations from three separate protein preparations in each case with the S.D. being half a residue or less.

[b] No CM Cys was present in any preparation.

[c] PE Cys data were obtained after complete reduction and alkylation.

TABLE V

Carbohydrate composition of Fc and pFc' fragments

	Fc(I)	Fc(II)	pFc'
Starting amount (μg)	280	230	140
Hexose present (μg)	13	10	5
% by weight	4.6	4.3	3.6
residues/chain[a]	6.08	4.79	2.38
Hexosamine present (μg)	7.5	4.5	2.0
% by weight	2.7	2.0	1.4
residues/chain[a]	3.50	2.16	0.95

[a] For these calculations the m.w. of subunit chains of Fc(I) and Fc(II) were assumed to be one-half that of the dimeric fragment as determined by analytical ultracentrifugation. The m.w. of a subunit chain of pFc' was assumed to be 12,000.

TABLE VI

Amino-terminal sequences of Fc fragments from different species

Fc fragment[a]	232	235	240
Human IgG1	Pro-Glu-Leu-	Leu-Gly-Gly-Pro-Ser-Val-Phe-Leu-Phe-Pro	
Rabbit IgG	Pro-Glu-Leu-	Leu-Gly-Gly-Pro-Ser-Val-Phe-Leu-Phe-Lys	
Mouse IgG2a	Pro-Asp-Leu-	Leu-Gly-Gly-Pro-Ser-Val-Phe-Ile-Phe-Pro	
Rat IgG2a	– –	Leu-Leu-Gly-Gly-Pro-Ser-Val-Phe-Ile-Phe-Pro	

[a] Data summarized from other studies include the structure of Fc from human IgG1 (27), rabbit IgG (28) and mouse IgG2a (26).

Fragment Fc(II) gave the same general N-terminal sequence as Fc(I). Approximately half of the Fc(II) began at Leu 235 and one-quarter, commenced at Leu 234 with the same sequence through residue 244 as was seen with Fc(I) (Table VI). The remainder of the Fc(II) showed a slight heterogeneity at the earlier residues (235–238) with homogeneity at residues 239–244. Small amounts of Gly and Pro in the first cycle, Glu and Pro in the second cycle, Val in the third cycle and Ser in the fourth cycle, were present in both Fc(II) and Fc obtained after 15 min of papain digestion (data not shown). The sum of the residues in the earlier cycles was approximately equal to that of Ser-Val-Phe-Ile-Phe-Pro seen in the fifth through 10th cycles, indicating that the cleavage site was still between residues 234/235.

Carboxy-terminal analyses. On digestion with a mixture of carboxypeptidases A and B, both Fc preparations failed to release molar quantities of amino acids. At both 0 time and 30 min no residues were observed from Fc(I), whereas at 3 hr small amounts of Leu (0.3 moles/mole peptide digested) and Ser/Asn/Gln (0.3 moles/mole) were released. The Fc(II) appeared to be slightly more susceptible to carboxypeptidase digestion. At 30 min Fc(II) yielded both Leu (0.3 moles/mole) and Ser/Asn/Gln (0.4 moles/mole). The 3-hr digestion of Fc(II) exhibited further digestion with Leu (0.4 moles/mole), Ser/Asn/Gln (0.5 moles/mole), Tyr (0.3 moles/mole), and His (0.3 moles/mole) all released. The same results were obtained with carboxypeptidase digestions of two different Fc(I) or Fc(II) preparations. It should be noted that no significant amounts of Lys or Arg were released, as carboxypeptidase B is specific for these two amino acids. Since considerably less than one mole of any amino acid was released per mole of peptide, even though a relatively large amount of enzyme was employed, it was concluded that the carboxy-termini of both Fc(I) and Fc(II) were not readily susceptible to carboxypeptidase digestion.

In contrast, pFc' was very susceptible to carboxypeptidase digestion with numerous residues released in yields greater than 0.5 moles/mole peptide digested at all time periods examined.

DISCUSSION

The results of these studies indicate that prolonged papain digestion of rat IgG2a produced a mixture of two species of Fc fragments with m.w. of 47,100 and 39,800. It is unlikely that these two Fc fragments resulted because of differential susceptibility of IgG subpopulations to papain digestion. The starting material was column-purified rat IgG2a and both 15 min and 16 hr of exposure to papain yielded complete digestion to Fab and Fc fragments. Both Fc(I) and Fc(II) were composed of two equal polypeptide chains, associated by non-covalent

The material on this page was copied from the collection of the National Library of Medicine by a third party and may be protected by U.S. Copyright law.

Case 1:06-cv-00500-SLR-MPT Document 252-2 Filed 08/25/2008 Page 16 of 33

bonds. The m.w. of the single subunit chains in Fc(I) and Fc(II) were 25,300 and 20,300, respectively. The identity of N-terminal amino acid sequences make it probable that Fc(II) was deficient in a C-terminal peptide in comparison with Fc(I). Studies on some biologic properties of these Fc fragments are reported separately, with the results of biochemical characterization reported herein permitting some correlations to be made between structure and function (8).

The primary sites of papain cleavage of rat IgG2a, under acid and reducing conditions, were to the C-terminal side of the hinge region, between residues 233/234 and 234/235. This site of digestion has been described frequently for pepsin but is not one of the common sites for papain cleavage (5). Prolonged papain digestion of rabbit IgG, particularly under acid conditions, has been reported to result in cleavage to the C-terminal side of the hinge region (6, 29). Conformational changes in the Cγ2 domain of the rat IgG2a molecule during Cohn fractionation or during papain digestion under reducing and acid conditions may have rendered the polypeptide chains susceptible to cleavage at these sites. It is unlikely that other proteolytic enzymes possibly contaminating our rat IgG2a or papain preparations led to the cleavage observed. Plasmin has been found in Cohn fraction II (30) but this enzyme appears to attack the exposed portion of the IgG molecule to the N-terminal side of the hinge region (31). Acid-treated IgG is cleaved by plasmin between the Cγ2 and Cγ3 domains, resulting in Facb fragments (32). Although both pepsin and chymotrypsin may cleave between residues 234 and 235, these proteases usually lead to more extensive degradation of the Cγ2 domain than was observed in our studies.

The results of our studies suggest that the Fc(II) fragment resulted because of secondary digestion by papain at a site(s) in the C-terminal portion of the Cγ3 domain. The amino-terminal sequence analyses indicate that both Fc(I) and Fc(II) commenced at residues 234 and 235, and offer strong evidence against there being any significant difference between these preparations at the N-terminus. From accurate m.w. determinations by analytic ultracentrifugation, chain lengths of 214 residues and 180 residues were estimated for Fc(I) and Fc(II), respectively. Evidence for homogeneity of the subunit chains of both Fc(I) and Fc(II) were obtained by gel filtration in urea/borate, PAGE in SDS/urea, and analytical ultracentrifugation in guanidine-HCl.

The C-terminal portion of the Fc(II) fragment was slightly more susceptible to carboxypeptidase digestion than was that of Fc(I) fragment, although poor yields of amino acids were obtained. These results do not establish whether the C-terminus in Fc(II) was heterogeneous or only somewhat more exposed. The nature of the amino acids released from Fc(II) by carboxypeptidase digestion, and of the amino acid compositions of Fc(I) and Fc(II), does not establish where the site(s) of secondary papain attack might be. The retention of equal amounts of Met residues in Fc(I) and Fc(II) indicate that this amino acid may be located on the N-terminal side of residue 410, similar to mouse IgG2a and different from rabbit IgG or human IgG1 where Met is located at position 428 (26). Assuming a 34 amino acid loss in Fc(II) suggests that secondary papain cleavage occurred in the region of residues 410–420. Papain is known to attack human IgG3 between residues 433/434 to yield fragment Fc′ (11). Evidence for papain digestion of a subpopulation of human IgG molecules in the region around residue 410 has recently been reported (33).

The results of studies in the analytical ultracentrifuge indicated that both Fc fragments possessed compact globular structures. The Fc(II) was more susceptible to dissociation in 6 M urea/borate than was Fc(I). The non-covalent interactions between the chains in Fc fragment occur primarily in the Cγ3 region as Cγ2 domains readily separate when covalent interactions are interrupted (34, 35). The loss of 34 C-terminal residues from Fc(II) in our studies apparently led to a weakening, but not to an elimination, of the non-covalent interactions between the Cγ3 domains.

Anomalous m.w. data were obtained by both gel filtration and by PAGE in these studies. The falsely low values for m.w. of Fc(II) obtained by gel filtration in neutral buffer may have been secondary to conformational alterations of this peptide, or to an interaction with the gel. The falsely high values for m.w. of the subunit chains of both Fc(I) and Fc(II) by PAGE in SDS/urea is consistent with the known tendency for the size of glycoproteins to be overestimated by using this technique. In contrast to the experience of others, we were not able to obtain lower values for m.w. by using more concentrated polyacrylamide gels (36).

Some evidence was obtained to indicate that unless precautions were observed the Fc fragments suffered further proteolytic degradation under denaturing and dissociating conditions, reflecting the experience of others (12). If the samples were not boiled to inactivate any residual proteolytic enzyme activity, degradation products were observed both by PAGE in SDS/urea and by analytical ultracentrifugation in guanidine HCl. Two major proteolytic fragments of a subunit chain of Fc were observed, probably representing isolated chains of Cγ2 and Cγ3 domains. It is likely that under denaturing and dissociating conditions, residual papain in the Fc preparations attacked the molecules in the exposed areas between the domains. No degradation products smaller than 14,000 m.w. were observed by PAGE, suggesting that more complete proteolysis did not occur. There was no evidence to indicate that the Fc(II) fragment was composed of isolated Cγ2 domains, or of two disulfide-linked hinge regions plus one complete and one partial Cγ2 domain as has been observed with human IgG1 (35).

Acknowledgment. The authors wish to thank Douglas Webster for excellent technical assistance and Dr. Mart Mannik for helpful discussions and review of the manuscript.

REFERENCES

1. Virella, G., and R. M. E. Parkhouse. 1971. Papain sensitivity of heavy chain sub-classes in normal human IgG and localization of antigenic determinants for the sub-classes. Immunochemistry 8:243.
2. Michaelsen, T. E., and J. B. Natvig. 1973. Characterization of subclass-related $F(ab)_2$, Fab/c and Fch fragments obtained by short papain digestion of human IgG myeloma proteins. Scand. J. Immunol. 2:299.
3. Leslie, R. G. Q., M. D. Melamed, and S. Cohen. 1971. The products from papain and pepsin hydrolysis of guinea-pig immunoglobulins γ_1G and γ_2G. Biochem. J. 121:829.
4. Gorini, G., G. A. Medgyesi, and G. Doria. 1969. Heterogeneity of mouse myeloma γG globulins as revealed by enzymatic proteolysis. J. Immunol. 103:1132.
5. Nisonoff, A., J. E. Hopper, and S. B. Spring. 1975. The antibody molecule. Academic Press, New York. P. 179.
6. Utsumi, S. 1969. Stepwise cleavage of rabbit immunoglobulin G by papain and isolation of four types of biologically active Fc fragments. Biochem. J. 112:343.
7. Bazin, H., A. Beckers, and P. Querinjean. 1974. Three classes and four (sub)classes of rat immunoglobulins: IgM, IgA, IgE and IgG_1, IgG_{2a}, IgG_{2b}, IgG_{2c}. Eur. J. Immunol. 4:44.

The material on this page was copied from the collection of the National Library of Medicine by a third party and may be protected by U.S. Copyright law.

Case 1:06-cv-00500-SLR-MPT Document 252-2 Filed 08/25/2008 Page 17 of 33

8. Arend, W. P., and D. E. Webster. 1977. Catabolism and biological properties of two species of rat IgG2a Fc fragments. J. Immunol. 118:395.
9. Porter, R. R. 1959. The hydrolysis of rabbit γ-globulin and antibodies with crystalline papain. Biochem. J. 73:119.
10. Arend, W. P., and F. J. Silverblatt. 1975. Serum disappearance and catabolism of homologous immunoglobulin fragments in rats. Clin. Exp. Immunol. 22:502.
11. Turner, M. W. and H. Bennich. 1968. Subfragments from the Fc fragment of human immunoglobulin G. Biochem. J. 107:171.
12. Fairbanks, G., T. L. Steck, and D. F. H. Wallach. 1971. Electrophoretic analysis of the major polypeptide of the human erythrocyte membrane. Biochemistry 10:2606.
13. Hermodson, M. A., L. H. Ericsson, and K. Titani. 1972. Application of sequenator analyses to the study of proteins. Biochemistry 11:4493.
14. Ambler, R. P. 1967. Carboxypeptidases A and B. Methods Enzymol. 11:436.
15. Ashwell, G. 1966. New colorimetric methods of sugar analysis. Methods Enzymol. 8:85.
16. Davidson, E. A. 1966. Analysis of sugars found in mucopolysaccharides. Methods Enzymol. 8:52.
17. Teller, D. C. 1973. Characterization of proteins by sedimentation equilibrium in the analytical ultracentrifuge. Methods Enzymol. 27:346.
18. Yphantis, D. A. 1964. Equilibrium ultracentrifugation of dilute solutions. Biochemistry 3:297.
19. De Rosier, D. J., P. Munk, and D. J. Cox. 1972. Automatic measurement of interference photographs from the ultracentrifuge. Anal. Biochem. 50:139.
20. Hoagland, V. D., Jr., and D. C. Teller. 1969. Influence of substrates on the dissociation of rabbit muscle D-glyceraldehyde 3-phosphate dehydrogenase. Biochemistry 8:594.
21. Harris, C. E., R. D. Kobes, D. C. Teller, and W. J. Rutter. 1969. The molecular characteristics of yeast aldolase. Biochemistry 8:2442.
22. Roark, D. E., and D. A. Yphantis. 1969. Studies of self-associating systems by equilibrium ultracentrifugation. Ann. N. Y. Acad. Sci. 164:245.
23. Cohn, E. J., and J. T. Edsall. 1943. *In* Proteins, Amino Acids and Peptides. Reinhold, New York. P. 370.
24. Longsworth, L. G. 1953. Diffusion measurements, at 25°, of aqueous solutions of amino acids, peptides, and sugars. J. Am. Chem. Soc. 75:5705.
25. Lee, J. C., and S. N. Timasheff. 1974. The calculation of partial specific volumes of proteins in guanidine hydrochloride. Arch. Biochem. Biophys. 165:268.
26. Bourgois, A., M. Fougereau, and J. Rocca-Serra. 1974. Determination of the primary sequence of a mouse IgG2a immunoglobulin: Amino-acid sequence of the Fc fragment. Eur. J. Biochem. 43:423.
27. Edelman, G. M., B. A. Cunningham, W. E. Gall, P. P. Gottlieb, U. Rutishauser, and M. J. Waxdal. 1969. The covalent structure of an entire gamma-G immunoglobulin molecule. Proc. Natl. Acad. Sci. 63:78.
28. Fruchter, R. G., S. A. Jackson, L. G. Mole, and R. R. Porter. 1970. Sequence studies of the Fd section of the heavy chain of rabbit immunoglobulin G. Biochem. J. 116:249.
29. Stewart, G. A., and D. R. Stanworth. 1975. The effect of acid treatment upon the susceptibility of rabbit IgG to proteolytic cleavage with various enzymes. Immunochemistry 12:713.
30. Maillard, J., and C. Favreau. 1975. Specific and nonspecific channels leading to proteolysis in antibody preparations. Br. J. Exp. Pathol. 56:139.
31. Connell, G. E., and R. H. Painter. 1966. Fragmentation of immunoglobulin during storage. Can. J. Biochem. 44:371.
32. Connell, G. E., and R. R. Porter. 1971. A new enzymic fragment (Facb) of rabbit immunoglobulin G. Biochem. J. 124:53P.
33. Ciccimarra, F., F. S. Rosen, and E. Merler. 1975. Localization of the IgG effector site for monocyte receptors. Proc. Natl. Acad. Sci. 72:2081.
34. Charlwood, D. A. and S. Utsumi. 1969. Conformation changes and dissociation of Fc fragments of rabbit immunoglobulin G as a function of pH. Biochem. J. 112:357.
35. Ellerson, J. R., D. Yasmeen, R. H. Painter, and K. J. Dorrington. 1976. Structure and function of immunoglobulin domains. III. Isolation and characterization of a fragment corresponding to the Cγ2 homology region of human immunoglobulin G. J. Immunol. 116:510.
36. Melcher, U., and J. W. Uhr. 1976. Cell surface immunoglobulin. XVI. Polypeptide chain structure of mouse IgM and IgD-like molecule. J. Immunol. 116:409.

The material on this page was copied from the collection of the National Library of Medicine by a third party and may be protected by U.S. Copyright law.

EXHIBIT 15

Article No. jmbi.1999.3128 available online at http://www.idealibrary.com on IDEAL* J. Mol. Biol. (1999) 293, 67–79

JMB

Folding and Association of the Antibody Domain C_H3: Prolyl Isomerization Preceeds Dimerization

Michael J. W. Thies[1], Josef Mayer[1], John G. Augustine[2] Christin A. Frederick[2], Hauke Lilie[3] and Johannes Buchner[1]*

[1]*Institut für Organische Chemie und Biochemie Technische Universität München, Lichtenbergstrasse 4 85747, Garching, Germany*

[2]*Dana Farber Cancer Institute Harvard Medical School 44 Binney Street, Boston MA, 02115, USA*

[3]*Institut für Biotechnologie Universität Halle, Kurt Mothestrasse 3, 06120, Halle Germany*

**Corresponding author*

The simplest naturally occuring model system for studying immunoglobulin folding and assembly is the non-covalent homodimer formed by the C-terminal domains (C_H3) of the heavy chains of IgG. Here, we describe the structure of recombinant C_H3 dimer as determined by X-ray crystallography and an analysis of the folding pathway of this protein.

Under conditions where prolyl isomerization does not contribute to the folding kinetics, formation of the β-sandwich structure is the rate-limiting step. β-Sheet formation of C_H3 is a slow process, even compared to other antibody domains, while the subsequent association of the folded monomers is fast. After long-time denaturation, the majority of the unfolded C_H3 molecules reaches the native state in two serial reactions, involving the re-isomerization of the Pro35-peptide bond to the *cis* configuration. The species with the wrong isomer accumulate as a monomeric intermediate. Importantly, the isomerization to the correct *cis* configuration is the prerequisite for dimerization of the C_H3 domain. In contrast, in the Fab fragment of the same antibody, prolyl isomerization occurs after dimerization demonstrating that within one protein, comprised of highly homologous domains, both the kinetics of β-sandwich formation and the stage at which prolyl isomerization occurs during the folding process can be completely different.

© 1999 Academic Press

Keywords: crystal structure; antibody; protein folding; C_H3 domain; PPIase

Introduction

Folding can be viewed as a hierarchical process starting with local, non-covalent interactions of amino acid residues to form elements of secondary structure, followed by the merging of these elements which finally leads to a unique tertiary structure (Jaenicke, 1987; Baldwin & Rose, 1999). This sequential pathway is especially evident for α-helical proteins where units of secondary structure are defined by interactions of amino acid side-chains close in sequence. In contrast, β-sheet structures originate from interactions of residues far apart in the amino acid sequence. For these proteins, the smallest stable unit of secondary structure seems to be a β-hairpin, i.e. two β-strands connected by a loop (Muñoz *et al.*, 1997; Schönbrunner *et al.*, 1997b; Ramirez-Alvarado *et al.*, 1999). In some proteins, however, the complete tertiary β-sheet structure is required to stabilize the individual β-strands (Coto & Hamaguchi, 1982a; Pham *et al.*, 1998). This implies that the formation of individual regions of secondary structure must be closely coupled to that of native, tertiary structure. Consistent with these varied requirements, the kinetics of formation of β-sheet structures have been shown to cover a wide range, from hours to milliseconds, indicating that, despite the complexity of the reaction, β-sheet formation is not intrinsically slow. Examples of fast-folding β-sheet proteins include interleukin 1β which acquires 90% of its native conformation within 25 ms (Varley *et al.*, 1993) and cold shock proteins the

Abbreviations used: ANS, 8-anilino-1-naphthalen sulfonic acid; C_H3, third constant domain of the antibody heavy chain; Fab, fragment of MAK33, containing V_L, V_H, C_L and C_H1; GdmCl, guanidine hydrochloride; NaDoc, sodium desoxycholate; PPIase, peptidyl-prolyl isomerase of the cyclophilin type; MAK33, monoclonal antibody from mouse of the subtype κ/IgG1; NCS, non-crystallographic symmetry.

E-mail address of the corresponding author: johannes.buchner@ch.tum.de

0022-2836/99/410067–13 $30.00/0

© 1999 Academic Press

folding process of which is diffusion-controlled (Jacob *et. al.*, 1997).

Protein folding has been studied predominantly with small monomeric, one-domain proteins, the unfolding of which is completely reversible (Kim & Baldwin, 1992). In comparison, the quantitative kinetic analysis of the folding reaction of larger and multimeric proteins is often hampered by aggregation as the major irreversible side reaction (Jaenicke, 1987). The mechanism of protein association is far from clear and remains an area of conflicting viewpoints with suggestions ranging from "induced fit" to "lock-and-key" reactions (Shakhnovich, 1999).

Antibodies and their constituent domains which consist of two antiparallel β-sheets linked by a buried disulfide bond (Huber *et al.*, 1976; Deisenhofer, 1981), provide an excellent system to study the folding and assembly of an all β-sheet protein. The folding process of the C_L domain, i.e. the constant part of the immunoglobulin light chain, has been studied extensively by Goto & Hamaguchi (1982a,b). In the intact antibody, this domain associates with the C_H1 domain of the heavy chain. Structure formation of the isolated C_L domain is fast in principle, however slow folding phases occur due to the isomerization of proline-peptide bonds which are in the *cis* configuration in the native state (Goto *et al.*, 1979). This reaction has a high energy barrier and has been identifed as a rate-limiting reaction in the folding of a number of proteins (Garel & Baldwin, 1973; Schmid, 1998). Lateron is a class of enzymes that catalyze this isomerization reaction during protein folding (Fischer *et al.*, 1984; Lang *et al.*, 1987; Schmid, 1998).

To further analyze antibody folding we have embarked on studying the structure formation process of the murine monoclonal antibody MAK33. The antibody is directed against the muscle-specific isoform of human creatine kinase (E.C.2.7.3.2.: CK-MM) (Buckel *et al.*, 1987). Using the Fab fragment of MAK 33 (which consists of the entire light chain and the two N-terminal domains of the heavy chain) we wished to know how folding and association are coupled in this system (Lilie *et al.*, 1995). We found that the two chains of the Fab can associate at different stages of folding depending on the isomerization state of the *cis* proline residues and the disulfide bonds between the chains. Specifically, association could preceed prolyl isomerization. However, a more detailed analysis was not possible due to the complex pairwise interactions of the four different domains. Furthermore, unfolding is not completely reversible, thus hindering spectroscopic analyses.

In order to further address the relationship between folding and association of antibody domains, we decided to use the C_H3 dimer, the most simple natural model system available. While the domain interactions in the Fab fragment involve two different pairs of domains (V_L-V_H and C_L-C_H1, respectively), the C-terminal domains of the heavy chains (C_H3) associate non-covalently to form a homodimer. Previously, it had been shown that the C_H3 dimer can be isolated by limited proteolysis (Isenman *et al.*, 1979). Refolding of the unfolded dimer is completely reversible and involves a step which is limited by the isomerization of a proline-peptide bond (Isenman *et al.*, 1979) which is in the *cis* configuration in the native state

To further investigate β-sheet folding and association in this model system, we cloned the C_H3 fragment of the antibody MAK33 and expressed it recombinantly in *Escherichia coli*. The three-dimensional structure of the recombinant C_H3 dimer was solved by X-ray crystallography. The structure provides an additional means of analyzing the solution data with respect to the protein environment of key residues involved in the folding process of immunoglobulin domains. The kinetic analysis of the folding process allowed us to ask whether intermediates are involved in the folding process and at which stage prolyl isomerization occurs.

Results

The three-dimensional structure of the C_H3 domain of the antibody MAK33

The three-dimensional structure of the C_H3 domain was determined using the molecular replacement method. Crystallographic data and refinement statistics are listed in Table 1. The protein exists in the crystal as a dimer, the overall structure of which is shown in Figure 1(a). Each monomer is crystallographically independent and exhibits the tertiary structure found in the C1 subset of constant domains as defined by Williams & Barclay (1988). The root-mean-square (rms) deviation for the superposition of the two monomers of the dimer, using only all C^α atoms or all atoms of the two monomers, is 0.14 Å and 0.34 Å, respectively (the first three residues are excluded in both cases). The C_H3 monomer consists of two β-sheets composed of strands A, B, E, D and strands G, F, C, C', respectively. The two sheets are connected by a canonical intradomain disulfide linkage between Cys28 of strand B and Cys86 of strand F. As in other immunoglobulin domains, the disulfide bond is buried within the protein molecule and is surrounded by numerous hydrophobic residues, in particular, Val9, Ile30, Val40, Trp42, and Val88, all of which lie within van der Waals contact distance (<4.5 Å) to either of the cysteine residues. The fluorescence of Trp42 is quenched as a consequence of its proximity to this intramolecular disulfide bridge under native conditions. From the structure it is clear that displacement of Trp42 from the immediate environment of the disulfide linkage, resulting in a marked increase in the fluorescence intensity, destabilizes the protein and thus provides a marker for the unfolded state in solution studies.

Table 1. Data collection and refinement statistics

A. Data collection	
Space group	$P21$
Unit-cell dimensions: (a, b, c) (Å)	48.74, 42.78, 50.46
β (deg.)	105.93
Resolution range (Å)	50.0 - 2.2
Unique reflections	10,340
Redundancy	5.58
Completeness (%)	93.4 (83.6)
R_{merge} (%)[a]	10.4 (27.3)
I/s	10.1 (3.2)
B. Refinement	
No. of protein atoms	1622
No. of water molecules	88
Resolution range (Å)	8.0 - 2.2
Unique reflections	9338
Completeness (%)	92.5
R-factor (%)[b]	20.5
Free R-factor (%)[c]	25.7
rmsd from ideal values[d]: bond length (Å)	0.006
rmsd from ideal values[d]: bond angles (deg.)	1.15
Temperature factor: all atoms	32.25
Temperature factor: main-chain atoms	30.84
Temperature factor: side-chain atoms	38.07
Temperature factor: water molecules	43.30

Values in parenthesis correspond to the highest resolution shell (2.20-2.26Å).

[a] $R_{merge} = S|I - \langle I\rangle|S\langle I\rangle$.

[b] R-factor $= S|F_o - F_c|/S|F_o|$.

[c] Free R is as for R-factor but calculated for a test set of 5% comprising reflections not used in the refinement.

[d] Root-mean-squared deviations (rmsd) are given from ideal values.

Another hallmark of immunoglobulin domains is the presence of at least one *cis*-proline residue. As mentioned above, the isomerization of this proline-peptide bond from a *trans* to a *cis* configuration is a rate-limiting step in the folding of Ig domains (Isenman *et al.*, 1979). It has recently been shown that the immediate environment surrounding the proline residue in the antibody domains influences the rate of isomerization catalyzed by prolyl peptidyl *cis/trans* isomerase (Lilie *et al.*, 1995). In C_H3, a *cis*-proline peptide bond is found at residue 35 located in the loop connecting strands B and C (Figure 1(a)). This residue is located in a small pocket on the surface of the protein, and within a 3.2 Å radius there are two bulky hydrophobic side-chain residues, Phe34 and His90. Also, the side-chain of Gln91 lies over the main-chain of the proline residue, forming an additional barrier to isomerization.

Based on the sequence alignment of more than 75 different immunoglobulin domains only one of them, gc3 from mouse, does not have a proline residue (it has a serine residue instead) at the corresponding C_H3 *cis*-proline position (Wels *et al.*, 1984). A survey of six immunoglobulin structures indicates that, like in the C_H3 structure, this proline residue is always found in the *cis* configuration in the intact heavy chain. The *cis*-proline in all cases stacks on the proceeding hydrophobic residue, which is usually a Phe or Tyr.

The dimeric interface (Figure 1(b), (c) and (d)) between the two monomers is composed of conserved residues found within the A, B, E, D β-sheet. Salt bridges at the ends of the dimeric interface are formed between the acidic residues of loop DE of each monomer and basic residues of loop AB of the opposing monomer (Figure 1(d)). Highly conserved hydrophobic residues found on strand F of each monomer stack in the middle of the interface. These include the three bulky hydrophobic residues Phe66, Tyr68 and Lys70.

The stability of recombinant C_H3

The stability of the recombinant C_H3 domain was analyzed by guanidine hydrochloride (GdmCl)-induced unfolding/refolding transitions. The shift of the equilibrium between native and denatured states was monitored both by fluorescence and CD spectroscopy. Because the C_H3 domain is a homo-dimer under native conditions, the denaturation process of C_H3 comprises both dissociation and unfolding reactions.

We studied the denaturation process at different C_H3 concentrations. Upon unfolding, the fluorescence emission wavelength of C_H3 was red-shifted (343 nm → 353 nm) and the fluorescence intensity increased threefold. As shown in Figure 2, at a C_H3 dimer concentration of 0.3 μM or higher, no significant change in signal occured at GdmCl concentrations lower than 0.4 M GdmCl. The complete loss of tertiary structure was reached at GdmCl concentrations higher than 1.4 M GdmCl. Between 0.4 and 1.3 M GdmCl, the protein undergoes a cooperative conformational transition with the respective midpoints depending on the protein concentration. A 20-fold increase in protein concentration (6.1 μM C_H3 dimer) caused a shift of the transition midpoint from 0.75 M to 1.0 M GdmCl. In addition to tertiary structure, we monitored the loss of secondary structure during unfolding by CD measurements. The transition from the native to the unfolded protein was again cooperative, with a midpoint at 1.0 M GdmCl at 4.1 μM dimeric C_H3 (Figure 2). This agrees well with the results from the fluorescence measurements performed at the same protein concentration. The identical results obtained from the transitions measured by fluorescence and CD are an indication of a two-state equilibrium unfolding transition. An isoemissive point observed for the fluorescence spectra of the native and the denatured protein confirms this two-state behavior (data not shown). Since it is very unlikely that more than two species exhibit the same fluorescence intensity at this wavelength, the denaturation equilibrium of C_H3 can be described by a two state transition, according to equation (1):

$$N_2 \overset{K}{\rightleftharpoons} 2U \qquad (1)$$

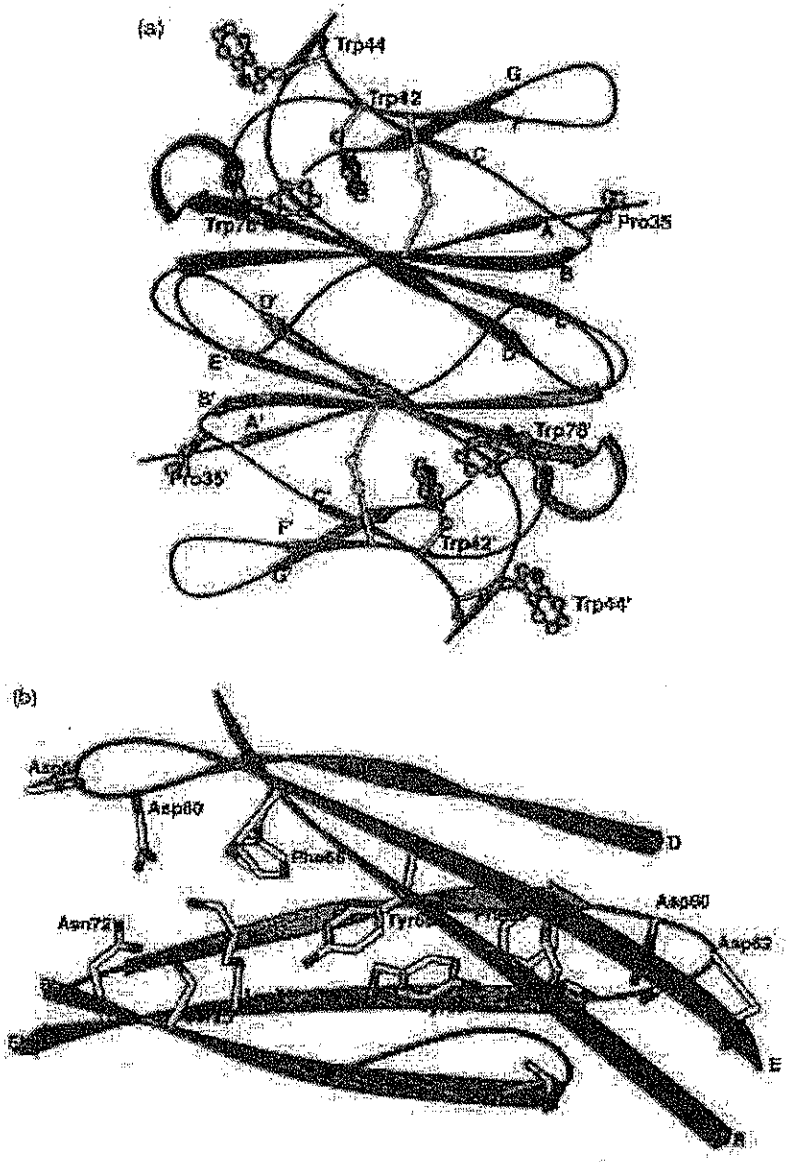

Figure 1 (*legend opposite*)

with N_2 representing the native, dimeric C_H3, and U the unfolded monomer.

Taken together, the results show that the unfolding of C_H3 is completely reversible. It was not possible to detect any intermediates at equilibrium conditions due to the highly cooperative nature of the transitions. Calculating the stability for C_H3 by linear extrapolation according to Neet & Tim (1994) from the data shown in Figure 2 resulted in a value for $\Delta G_{U \rightarrow N}$ of $-66.5(\pm 1.5)$ kJ mol^{-1}.

Folding of C_H3 is not concentration-dependent

To investigate the folding process of C_H3, the protein was first completely denatured in 6 M GdmCl at room temperature for two hours. Then, folding and reassociation were initiated by a 240-fold dilution of the denaturant at 4 °C. The acquisition of the native conformation, as monitored by fluorescence and CD, is slow and can be described adequately only by three exponential phases

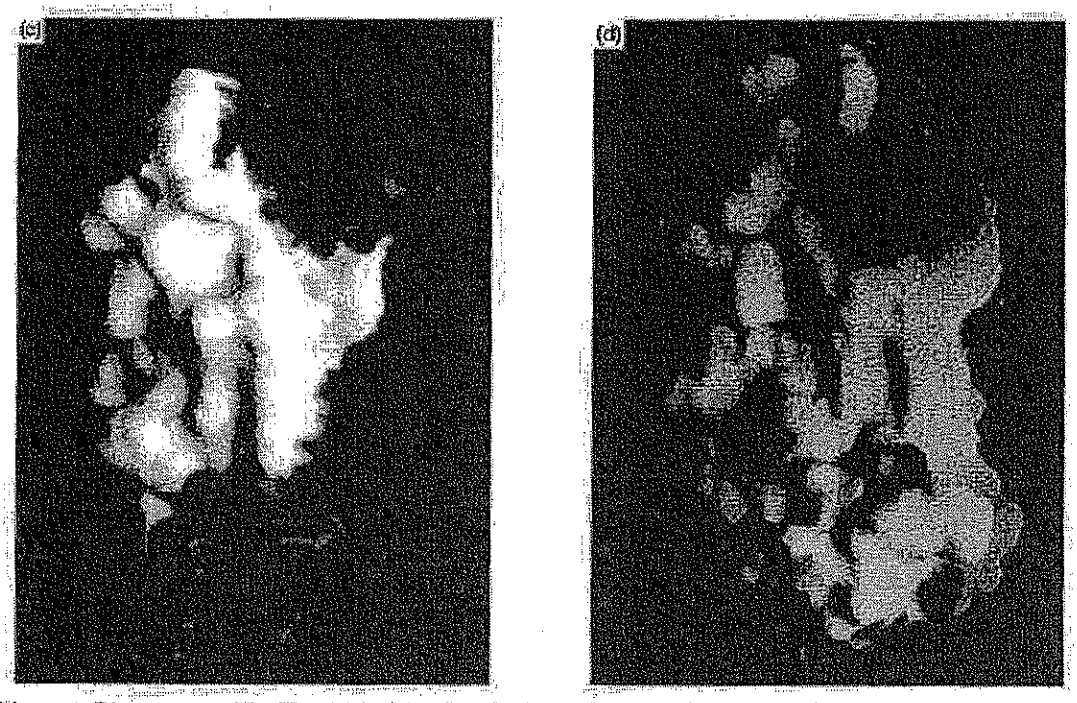

Figure 1. Diagram and GRASP model of the C_H3 domain. (a) Overall dimeric model of C_H3. The tryptophan and *cis*-proline residues are in ball-and-stick representation. The disulfide bridge connecting the sheets of each monomer is highlighted in yellow. This Figure was generated in SETOR (Evans, 1993). (b) Interface of the C_H3 dimer. The residues interacting within the dimeric interface are indicated in stick representation. This Figure was generated in SETOR (Evans, 1993). (c) A representation of a C_H3 monomer with the dimerization interface in white. (d) A surface representation of the dimeric interface of a C_H3 monomer showing positive (in blue), negative (in red) and neutral (in white) charged surfaces. This model was made using GRASP (Nicholls & Honig, 1991).

(Figure 3(a) and (b)). The first exponential phase had an apparent rate constant of $k_1 = 1.1 \times 10^{-2}\ s^{-1}$ and accounted for 14% of the fluorescence signal. The rates of the other folding phases were $k_2 = 5.2 \times 10^{-4}\ s^{-1}$ and $k_3 = 1.6 \times 10^{-4}\ s^{-1}$ with an amplitude of reaction of 86%. The folding steps characterized by k_2 and k_3 are consecutive and the reaction with the rate of k_1 occurs in parallel (see below).

In Figure 3, the signal of the refolding kinetics is compared to the signal of the native and the denatured protein. These data show that 82% of the total change in signal could be detected by fluorescence and 80% by CD. Since the manual mixing experiments have a dead time of about five seconds, these results imply that the lacking signal represents changes in secondary or tertiary structure which occur during this time span. To further analyze the initial folding reactions, stopped-flow fluorescence experiments with a dead time of 2 ms were performed. Here, 10% of the change in signal occured in the dead time of the measurement suggesting that there may be some rapid structural changes upon initiation of refolding. Whether some C_H3 molecules reach the native state in a fast folding reaction or whether a common intermediate is formed is not resolved by these experiments.

Since C_H3 is a dimer even at a concentration as low as 10^{-10} M (Isenman *et al.*, 1979), the protein concentration could have an effect on the folding kinetics if association of C_H3 is rate limiting. The analysis of refolding kinetics performed at different C_H3 concentrations showed that none of the three phases were influenced, suggesting that either dimerization is not rate limiting during refolding, or that this process did not cause any change in signal. Since we know from the crystal structure that there is no tryptophane residue in the dimer interface, a direct influence of association on the fluorescence properties of C_H3 was not expected (Figure 1(a) and (b)).

Taken together, the folding kinetics of C_H3 can be described by three rate constants (k_1, k_2 and k_3). Additionally, part of the change in signal (10% in stopped-flow measurements) could be either attributed to rapid reactions on one folding pathway or to the general formation of a fast folding species of C_H3.

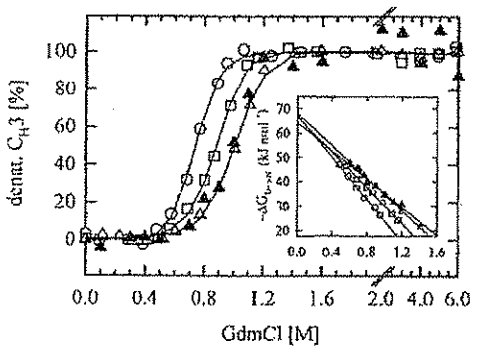

Figure 2. GdmCl-dependent unfolding and refolding transitions of C_H3. Samples were incubated for six days at 20 °C in 0.1 M Tris-HCl (pH 8.0) and varying GdmCl concentrations. For the fluorescence measurements the excitation wavelength was set to 280 nm. Spectra were recorded from 290 to 400 nm and analyzed at 355 nm. The C_H3 dimer concentration was 0.2 μM (○), 1.6 μM (□) and 4.1 μM (△), respectively. For the CD experiment, the ellipticity was recorded at 213 nm (▲) at a protein concentration of 4.1 μM. All measurements were carried out at 20 °C.

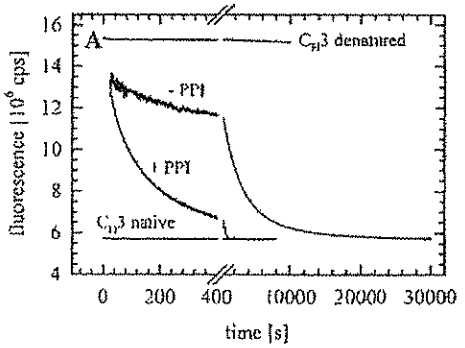

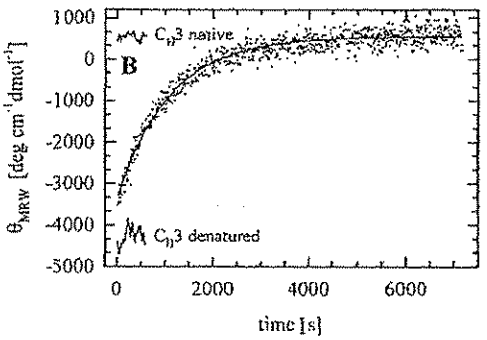

Figure 3. Refolding kinetics of C_H3.(a) The regain of native fluorescence were monitored at a C_H3 dimer concentration of 0.3 μM by tryptophane fluorescence in 0.1 M Tris-HCl, 25 mM GdmCl (pH 8.0), at 4 °C. The excitation wavelength was set to 295 nm. Emission was detected at 355 nm. C_H3 was denatured for two hours in 6 M GdmCl at room temperature. Acceleration of the folding reaction was achieved by addition of fivefold molar excess of PPIase. (b) CD kinetics were performed in the same buffer at the same temperature. Ellipticity was recorded at 213 nm. The concentration of dimeric C_H3 was 8.2 μM.

Prolyl isomerization is a rate-limiting step in C_H3 folding

The isomerization of the Xaa-Pro peptide bond is a rate-limiting step in C_H3 folding (Isenman *et al.*, 1979). To analyze which phase of the folding reaction is affected by prolyl isomerization, we decided to use a peptidyl-prolyl isomerase (PPIase) of the cyclophilin type ($k_{cat}/K_m = 6.9 \times 10^6$ M^{-1} s^{-1}) to catalyze this step (Lilie *et al.*, 1993). In its native structure, C_H3 contains one *cis* proline residue (Pro35) which is part of an exposed loop (Figure 1(a)). Therefore, this residue should be accessible to the folding catalyst. To determine the contribution of proline *cis-trans* isomerization during folding of C_H3, refolding experiments were performed in the presence of a fivefold molar excess of PPIase. As shown in Figure 3(a), addition of PPIase strongly accelerated the folding process. A further increase of the PPIase concentration had no additional effect on the refolding kinetics. Analyzing the rate constants of the folding kinetics showed that one of the slow reactions was accelerated markedly in the presence of PPIase. This result was confirmed by double-jump experiments (data not shown). In these experiments, C_H3 was unfolded for only a few seconds. This is sufficient to completely dissolve secondary and tertiary structure, but the isomeric state of the Pro-peptide bond remains unchanged (Schmid, 1986). Furthermore, the slow phase depended on prolyl isomerization as well as the GdmCl concentration (data not shown), suggesting that the isomerization is linked to a change in the conformation of the protein. The other two phases are not influenced by prolyl isomerization. Since the two slow reactions are very similar in their rate constants, it was not possible to assign the prolyl isomerization to one of these reactions based on this experiment only. Therefore, a more detailed analysis, directly measuring the population of a proline-determined folding intermediate, was performed.

Refolding of denatured C_H3 is decelerated by an intermediate

The major folding pathway of C_H3 involves at least one kinetically trapped folding intermediate. To investigate the appearance of this intermediate, we carried out triple-jump experiments. In these experiments, the C_H3 domain was first completely unfolded. Then the protein was allowed to refold

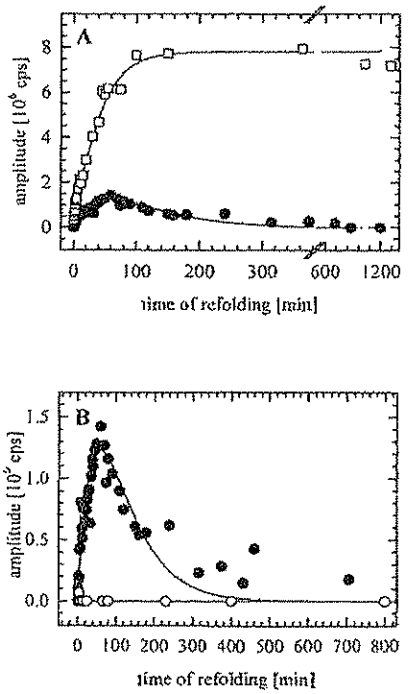

Figure 4. Population of a C_H3 folding intermediate. For the triple-jump experiments, refolding was carried out in 0.1 M Tris-HCl, 25 mM GdmCl (pH 8.0), at 4 °C. The dimer concentration of C_H3 was 0.3 μM. At different points of time, the unfolding reaction was initiated by adding GdmCl to a final concentration of 2.5 M. The final protein concentration was 0.2 μM. Fluorescence kinetics were monitored at 355 nm. The excitation wavelength was 295 nm. (a) Amplitude distribution of the formation of native C_H3 (□) and of the population of the folding intermediate (●). (b) Population of the intermediate in the presence (○) and absence (●) of a fivefold molar excess of PPIase.

and, after different times (0 - 1440 minutes), GdmCl was added to initiate unfolding. This procedure allows us to measure the amount of native C_H3 and the folding intermediate by their stability as determined by GdmCl-induced unfolding (Schmid, 1986). Whereas unfolding of native C_H3 can be described by a mono-exponential fit, unfolding of refolded C_H3 in triple-jump experiments yielded denaturation kinetics which consist of two phases (data not shown). The rate constant for the slow phase ($k_u^s = 2.5 \times 10^{-4}$ s^{-1}) corresponds to the unfolding of native C_H3, whereas the fast one ($k_u^f = 3.4 \times 10^{-3}$ s^{-1}) represents the denaturation of a folding intermediate. Figure 4(a) shows the amplitude distribution for the formation of native C_H3 and the population of the intermediate during refolding. Importantly, there is no lag phase in the formation of native protein (represented by open squares) as would be expected for a serial mechanism. Instead, at the beginning of the folding process native C_H3 is formed more rapidly than the intermediate, clearly indicating a parallel folding pathway. Compared with the rate constants obtained from the renaturation kinetics (k_1, k_2, k_3), the formation of the native C_H3 domain as determined from the amplitude distribution can be described adequately by the same mechanism with the same rate constants $k_1^t = 1.0 \times 10^{-2}$ s^{-1}, $k_2^t = 1.2 \times 10^{-3}$ s^{-1} and $k_3^t = 5.1 \times 10^{-4}$ s^{-1} (the exponent t indicates that these values were obtained from triple-jump experiments). Furthermore, this experiment confirmed that some C_H3 molecules reach the native state in a fast reaction (Figure 4(a); compare also Figure 3(a) and (b)). The second curve in Figure 4(a) (described by the filled circles) represents the population of the intermediate during folding. The intermediate appeared with the rate constant 4.9×10^{-4} s^{-1} (k_a) and subsequently disappeared with the rate constant 5.6×10^{-4} s^{-1} (k_d). These results imply that the slow rate constants (k_2, k_3) obtained from the refolding experiments are due to the formation and disappearance of this folding intermediate, because they are very similar to the values of k_a and k_d, respectively.

To test whether prolyl isomerization is involved in the formation of the intermediate, we performed triple-jump experiments in the presence of PPIase. In Figure 4(b), the amplitude distributions of the intermediate in the presence and absence of PPIase are compared. In the presence of PPIase, only a small amount of intermediate could be detected in the early beginning of the refolding process. Moreover, the time course of formation and disappearance is altered markedly. The maximum accumulation of the intermediate is shifted to about two minutes compared to 60 minutes in the absence of PPIase. This implies that mainly the reaction which is responsible for the disappearance of the intermediate must be accelerated by PPIase causing the low accumulation of the intermediate.

Based on these data, simulations were performed supposing that the folding process can be described by a sequence of reactions which starts from the denatured state, comprises the formation of the intermediate (with the respective rate constant k_a) and the subsequent regain of the native state. A mechanism consisting of two serial folding reactions (U → I → N) failed to describe the kinetics of C_H3 formation and intermediate population adequately. However, a fit considering an additional parallel pathway gave excellent agreement with the experimentally determined rate constants (see Materials & Methods). Additionally, extrapolation of the amplitude of the native C_H3 to 0 minute refolding resulted in a small fraction of an additional folding species (about 5%). This might indicate a fast-folding species which reached the native state within the dead time of the experiment.

Notably, these results show that the majority of C_H3 molecule folds *via* an intermediate to the native state (equation (2a)). This intermediate is

separated from the native state by a prolyl isomerization-coupled folding reaction. Aside from this proline-determined folding pathway, two fast-folding reactions lead directly to the native state, one occuring in the dead time of the reaction (as determined by stopped flow experiments, called k_x), and the other with the rate constant k_1 ($1.1 \times 10^{-3} s^{-1}$), respectively (equation (2b)):

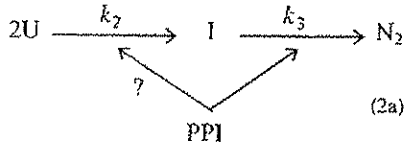

(2a)

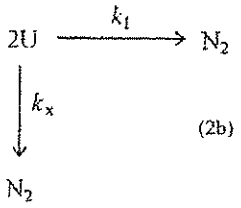

(2b)

where I stands for the folding intermediate.

Prolyl isomerization occurs before association of C_H3

Lastly, we were interested in defining at which stage of the folding process association to form the dimer takes place. As described above, a concentration-dependent folding reaction could not be observed by fluorescence spectroscopy. This result may be explained either by the assumption that dimerization is not rate limiting in the overall renaturation kinetics, or that association is the last step of folding and does not change the environment of the aromatic side-chains. To discriminate between the two possibilities, we decided to analyze the time course of association by chemical crosslinking and subsequent SDS-PAGE. The time course of dimerization was quantified by densitometry of the monomer and dimer bands (Figure 5(a)). The crosslinking experiments yielded a rate constant of $k = 2.5 \times 10^{-4} s^{-1}$ for the formation of the dimer and disappearance of the monomer, respectively. As in the case of spectroscopic measurements, the rate of dimerization did not depend on the protein concentration.

From the fluorescence measurements, we knew already that PPIase influences the two slow phases k_2 and k_3 of the folding reaction (see also equation (2a)). Now, we examined whether PPIase had any effect on dimerization by crosslinking. In Figure 5(b), the time courses of the formation of C_H3 dimers in the presence and in the absence of PPIase are compared. Addition of PPIase accelerated the dimerization of C_H3. We were not able to fit this curve because of the low number of resolvable data points. However, a reasonable estimate of the rate would be that the formation of the dimer is at least 20-fold faster than in the absence of PPIase.

Thus, the experimentally determined apparent rate constants for the association reaction clearly indicate that prolyl isomerization is necessary and rate limiting for the association reaction of C_H3. Additionally, this experiment showed that the reaction with the rate constant k_3 represents the *trans* → *cis* prolyl isomerization.

The results can be summarized as follows:

$$2U_t \xrightarrow{k_2} 2I_t \xrightarrow{k_3} 2I_c \xrightarrow{k_{assoc.}} N_2 \qquad (3a)$$

where U_t stands for the unfolded C_H3 domain with Pro35 in the *trans* position, I_t is the folding intermediate with *trans* Pro35, I_c with *cis* Pro35. $k_{assoc.}$ represents the fast association step which could not be resolved kinetically.

Additionally, a fast-folding reaction leads to the native state, presumably starting from a denatured state with all proline residues in their native configuration:

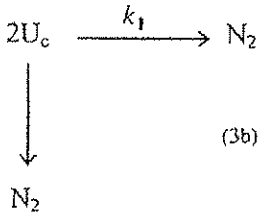

(3b)

with U_c as the fast-folding species.

Discussion

In the present study we have analyzed the folding process of the C_H3 domain of the monoclonal antibody MAK33. This small protein represents an interesting model for β-sheet folding and association. Since native C_H3 is a dimer, the protein concentration affects the apparent stability as determined by equilibrium unfolding transitions. A similar result was obtained previously for the human C_H3 domain (Sumi & Hamaguchi, 1982). Because of the high degree of cooperativity of the unfolding transition, it is not possible to detect intermediates in the transition region by fluorescence and CD measurements (Privalov & Khechinashvili, 1974). Therefore, the denaturation equilibrium of C_H3 can be described by a two-state transition. The calculated intrinsic stability of $-66.5(\pm 1.5)$ kJ mol^{-1} for C_H3 is in the range of -42 to -113 kJ mol^{-1} typically found for dimeric proteins (Neet & Tim, 1994). In contrast, the stability of the human C_H3 domain was previously deter-

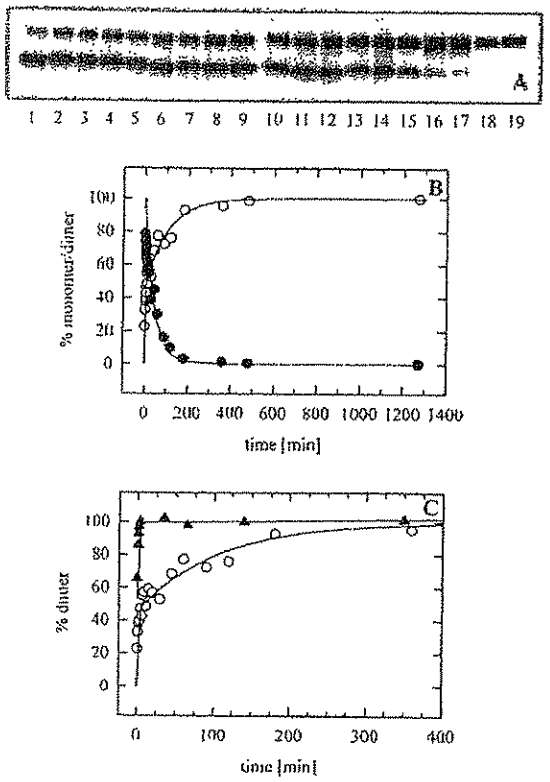

Figure 5. Dimerization of C_H3 during refolding. Crosslinking experiments were carried out in 50 mM Hepes (pH 8.0), at 4 °C. The C_H3 dimer concentration was 0.3 μM. During refolding, samples of 5 μg protein were taken, crosslinked with glutaraldehyde and precipitated. (a) Coomassie-stained SDS gel. (b) Time course for the formation of the C_H3 dimer (○) and for the disappearance of the monomer (●). (c) Influence of PPIase on the time course of association of C_H3. Dimer formation without PPIase (○) is compared to the association in the presence of PPIase (▲).

mined to be only −23 kJ mol^{-1} which is comparable to the stabilities of the C_L (Sumi & Hamaguchi, 1982) and the V_L domain (Rowe & Tanford, 1973). This value was obtained from a calculation using the binding model for denaturants according to Tanford (1970) and Pace & Vanderburg (1979). This model was developed for monomeric proteins. Therefore the calculation may have yielded an underestimated ΔG^0 value for human C_H3. Calculating ΔG^0 for C_H3 from MAK33 in the same way as for human C_H3 resulted in a lower stability of −30 kJ mol^{-1}. Thus, the suggestion that antibody domains exhibit similar thermodynamic stabilities (Sumi & Hamaguchi, 1982), may be true only for monomeric domains. Since the C_H3 dimer clearly deviates from this behavior, association seems to contribute significantly to the stabilization by additional non-covalent intermolecular interactions (Figure 1(b)). In agreement with this suggestion, amino acid side-chains forming a patch at the center of the dimerization interface of C_H3 have been shown to be the energetic key residues in domain dissociation and unfolding (Dall'Acqua *et al.*, 1998). These well-defined interactions between the two monomers may be responsible for the slow denaturation of the domain compared to other proteins of the same size (Sumi & Hamaguchi, 1982; Isenman *et al.*, 1979).

The β-sheet folding is an entropically ambitious event. Amino acid residues, which are far apart in the polypeptide chain, must interact correctly in the three-dimensional space to form stabilizing interactions (Clark *et al.*, 1997). Dependent on the length of the polypeptide chain between the corresponding residues, several trials may be necessary to achieve a stable "native" interaction. Therefore, the overall folding process of complex β-sheets, such as the β-barrel of C_H3, is much slower than α-helix formation. Nevertheless, in addition to the spectroscopically accessible folding phases, a fast "burst phase" reaction which could not be resolved even by stopped-flow techniques is also part of the folding pathway of C_H3. In contrast to the literature, in which burst phase values of about 30% of the entire amplitude (Matthews, 1993) were reported, we could only detect a small burst phase (10%) for the folding of C_H3. This burst phase during C_H3 folding was not caused by a hydrophobic collapse, since no ANS binding could be observed. Interestingly, the small β-sheet proteins tendamistat and Csp showed no loss in signal due to a hydrophobic collapse (Schönbrunner *et al.*, 1997a; Jacob *et al.*, 1997). These results indicate that rapid chain collapse is not an essential step in protein folding. In the case of C_H3, it might be that the loss of signal represents a fast-folding species reaching the native state in the dead time of the measurement. Also, a contribution to this change in signal could be the dilution of the denaturant and therefore the altered solvent environment (Qi *et al.*, 1998). We suggest that a minority of fast-folding molecules reach the native state during the dead time of the measurement on an additional, parallel folding pathway in agreement with the finding that about 5% of the C_H3 molecules become native in the dead time of the triple-jump experiment.

Analyzing the accessible kinetics of β-sheet protein folding revealed that small β-sheet proteins, in which folding is not influenced by prolyl isomerization and association reactions, reaches the native state in an apparent one-step reaction within milliseconds (Schönbrunner *et al.*, 1997a; Jacob *et al.*, 1997). In contrast, folding of immunoglobulin domains seems to be a more time-consuming process than folding of simple β-sheet proteins. The refolding kinetics of the monomeric C_L domain take a few seconds after short-time denaturation where the *cis/trans* prolyl isomerization does not contribute to the folding kinetics (Goto & Hamaguchi, 1982a). In contrast, folding of short-time denatured C_H3 is completed within about 200

seconds at room temperature. Thus, even in the absence of prolyl isomerization, folding of C_H3 is much slower than that of the C_L domain. Since dimerization is not rate limiting under these conditions, the results imply that the kinetics of β-barrel formation is significantly different in the two highly homologous antibody domains.

After long-time denaturation, where proline re-isomerization contributes to the refolding kinetics, C_L folds much slower to the native state than after short-time denaturation. The refolding kinetics consisted of two phases and was completed after 150 seconds at 25 °C (Goto & Hamaguchi, 1982a). In contrast, folding of the C_H3 after long-time denaturation takes 60 minutes at 20 °C and five hours at 4 °C, respectively. Focussing on this slow pathway (determined by the rate constants k_2 and k_3), we found that the majority of the C_H3 molecules fold *via* an intermediate to the native state. This majority originates from the equilibrium between C_H3 molecules with Pro35 in *trans* and molecules with Pro35 in the native *cis* configuration in the denatured state. We found that upon long-time denaturation, about 95 % of the molecules contain a *trans* Pro35-peptide bond. The reason for the population of the folding intermediate and the rate-limiting step of the entire folding reaction is the isomerization of this Pro35-peptide bond from the *trans* to the *cis* configuration (represented by the rate constant k_3). Altering the velocity of this reaction by changing the temperature or by addition of PPIase confirmed that this reaction is responsible for the appearance and disappearance of the intermediate. The subsequent dimerization is a fast reaction, both in short-time denatured C_H3, where Pro35 remains in the native configuration or when prolyl isomerization is catalyzed by PPIase. The activation energy of prolyl isomerization reactions of about 80 kJ mol^{-1} (Schmid, 1998) is a high barrier in protein folding which many proteins must overcome to reach the native state. Especially in antibodies, which contain many *cis* proline residues in the native structure (Huber *et al.*, 1976; Deisenhofer, 1981), the isomerization process is often rate limiting in folding (Goto & Hamaguchi, 1982a; Lang *et al.*, 1987; Lilie *et al.*, 1993, 1995; Freund *et al.*, 1996; Jaeger & Plückthun, 1997) and the reason for the accumulation of folding intermediates.

Prolyl isomerization can be accompanied by changes of the secondary and tertiary structure of the protein. This becomes evident when the rate of isomerization is influenced by the presence of a denaturant. In antibody domains this is not always the case. For the C_L domain, the isomerization reaction was not influenced by GdmCl (Goto & Hamaguchi, 1982a). In agreement with this finding, we had previously shown that in MAK33 Fab, re-isomerization of the *cis*-proline-peptide bond is not a perequisite for association of the monomers during the folding process (Lilie *et al.*, 1995). Association occurred regardless of the isomeric state. Interestingly, the isomerization reaction could be efficiently catalyzed by PPIase even in the dimeric folding intermediate (Lilie *et al.*, 1993). In contrast, C_H3 can only dimerize when the Pro35-peptide bond is in the *cis* configuration. Since this isomerization reaction is GdmCl-dependent, it is reasonable to assume that structural changes are involved which are necessary to form the association-competent domain interface. The crystal structure suggests that Pro35 is engaged in a hydrogen bond with His90 and may thus contribute to the stabilization of the β-sheet. In the absence of this interaction (i.e. in the *trans* configuration of the Pro35-peptide bond), His90 could move around and disrupt the packing.

Taken together, our results imply that for highly homologous antibody domains, both the kinetics of β-sheet formation and the relationship between prolyl isomerization and association are completely different. The molecular basis for these differences remains to be elucidated.

Materials and Methods

Reagents

PPIase (Cyclophilin A from human T-cells) was a kind gift from Dr Kurt Lang (Roche Diagnostics). Polymyxin B sulfate was from Sigma.

Protein expression and purification

The *E. coli* strain JM83 containing the plasmid pSM20 was used for the expression and periplasmic secretion of C_H3. The cells were grown in SB medium at 26 °C. A 1 mM sample of IPTG was added to start the expression and 2 mM GSSG to create an oxidizing environment required for disulfide bond formation. After 24 hours, the cells were harvested and the pellet was resuspended in 50 mM NaCl, 20 mM Mops (pH 7.5) followed by an additional centrifugation step. The periplasmic protein contents were extracted by treating the cells with 10 mM Mops, 5 mM EDTA (pH 7.0) and 1 mg/ml polymyxin-B sulfate (Storm *et al.*, 1977). The solution was shifted to pH 5.0 and loaded onto a SP Sepharose column (Amersham Pharmacia). Bound protein was eluted with a linear salt gradient (0 to 0.5 M NaCl) in 50 mM sodium phosphate, 50 mM Tris-HCl (pH 5.0). After the pH was shifted to 8.0 and the solution was dialyzed against 0.1 M Tris-HCl (pH 8.0), the protein was loaded on a Superdex 75 pg gel filtration column (Amersham Pharmacia). The purity of the eluted protein was confirmed by silver-stained SDS-Page.

Crystallization and data collection

Crystals were grown from sitting drops containing equal volumes of 10 mg/ml C_H3 (0.4 mM dimer concentration) and reservoir solution containing 0.1 M Tris-HCl (pH 8.5) and 2.0 M ammonium sulfate at 18 °C. Large (0.15 mm × 0.04 mm × 0.08 mm), single crystals grew within one week. Diffraction data were collected at room temperature from CuKa radiation generated by a Rigaku RTP500 RC rotating-anode generator using a Mar imaging plate. The crystals belong to space group $P2_1$ with cell dimensions $a = 48.74$ Å, $b = 42.78$ Å, $c = 50.46$ Å and $B = 105.93°$. The crystallographic asymmetric unit

contains two monomers and approximately 41 % solvent with a Matthews Coefficient of 2.1 Å^3/Da and a cell volume of 100,982 Å^3 (Collaborative Computational Project, 1994). Reflection files were indexed using the program DENZO (Otwinowski & Minor, 1997) and subsequently scaled by the program SCALEPACK(2). A summary of data collection statistics is shown in Table 1.

Structure determination and model refinement

The structure of the C_H3 domain was solved by the molecular replacement method using a monomeric subunit of the human Fc2 immunoglobulin gamma-1 chain (Deisenhofer, 1981), the amino acid sequence is 61 % identical with that of C_H3, as a search model in the AMoRe program (Navaza, 1994). The rotation function calculation yielded one prominent peak with a correlation coefficient of 9.6 as opposed to 7.2 for the next highest peak. The first-body translation search found two solution vectors with correlation coefficients of 29.8 and 27.3 as opposed to the next highest solution with a correlation coefficient of 19.2. The rotation functions found within the two highest translation peak solutions correspond with the first and fifth rotation peaks, respectively. A second-body translation search confirmed these two solutions from the first-body translation. The human Fc2 input model was then transformed using the two rotation and translation vectors to yield the "C_H3 molecule" model. After an initial rigid body refinement a $2F_o - F_c$ map was calculated yielding a strong electron density and the molecular packing was checked showing no conflicts between symmetry-related molecules. Side-chains of the solution were then mutated and rebuilt into the initial C_H3 molecule model with the program O (Jones *et al.*, 1991). In the subsequent position and *B*-factor refinements utilizing XPLOR (Brünger, 1992), non-crystallographic symmetry (NCS) restraints and solvent flattening were applied. After three rounds of refinement, the NCS restraints were removed and water molecules were finally added to the model using the wARP program (Perrakis *et al.*, 1997). The first three residues of each monomer gave no traceable electron density, so they were not included in the final refinement and model. Of the non-glycine residues, 93.2 % are in the most favored regions, while no residues lie in the energetically disallowed regions of the Ramachandran plot. Overall refinement statistics are given in Table 1.

Guanidine hydrochloride denaturation measurements

Guanidine hydrochloride (GdmCl) denaturation transitions were measured at different protein concentrations in the case of the fluorescence experiments, and at a C_H3 dimer concentration of 4.1 µM in the circular dichroism (CD) experiments. All experiments were carried out in 0.1 M Tris-HCl (pH 8.0), at 20 °C and different GdmCl concentrations. The samples were incubated for six days at room temperature to achieve equilibrium. The fluorescence excitation wavelength was set to 280 nm. The emission spectra were recorded from 290 to 400 nm and analyzed with regard to the shift of the fluorescence maximum and the change in the intensity at 355 nm. The ellipticity was detected at 213 nm. The exact GdmCl concentration of the samples was calculated from the respective refraction indices (Schmid, 1989). The free energies of the unfolding transitions were fitted as described by Neet & Tm (1994), Tanford (1970) and Pace & Vandenburg (1979).

Spectroscopic techniques

Circular dichroism (CD) spectra and kinetics were recorded in a Jasco J 715 spectropolarimeter with a PTC 343 peltier unit. The experiments were carried out in quartz cuvettes of 0.1 and 0.5 cm pathlength. Far-UV CD spectra were recorded from 190 to 250 nm in 50 mM KH_2PO_4 (pH 8), at 20 °C. All spectra were buffer-corrected. Kinetics were measured at 213 nm in 0.1 M Tris-HCl (pH 8), at 4 °C.

The fluorescence of C_H3 was determined using a Spex FluoroMax-2 fluorimeter and a 1 cm stirred and thermostated cell. The excitation wavelength was set to 280 or 295 nm. Spectra were recorded from 290 to 400 nm. For kinetics, the fluorescence emission was detected at a wavelength of 355 nm. The spectral bandwidths were 2 nm for excitation and 7 nm for emission, respectively.

Stopped-flow measurements

Stopped-flow experiments were performed in a SX-18MV stopped-flow spectrofluorimeter (Applied Photophysics) with a thermostated cell. The conditions were the same as described for the fluorescence measurements.

Triple-jump experiments

This type of experiment is based on the different stability of folding intermediates and the native state of a protein against denaturation. First, C_H3 was completely unfolded in 6 M GdmCl, 0.1 M Tris-HCl (pH 8) for two hours at 20 °C. Then, folding was initiated by diluting the denaturant ([GdmCl] = 25 mM, [C_H3 dimer] = 0.3 µM). After different times (0 - 1440 minutes) unfolding was initiated by increasing the GdmCl concentration to 2.5 M ([C_H3] = 0.2 µM). Folding intermediates which were formed during the time range of refolding, unfold with different kinetics due to their intrinsic stability. Since unfolding of C_H3 is characterized by one rate constant, folding intermediates can be detected by the occurence of additional folding phases and rate constants, respectively. The folding and unfolding reactions were followed by the change in fluorescence (see above) at 4 °C.

Chemical crosslinking and densitometry

Crosslinking was carried out as described by Jaenicke & Rudolph (1989). During renaturation, crosslinking experiments were performed in 50 mM Hepes (pH 8.0); 80 mM glutaraldehyde was added at different time points and, after two minutes at 37 °C, the reaction was stopped with 80 mM $NaBH_4$ in 0.1 M NaOH. The protein was precipitated with sodium desoxycholate (NaDoc) and trichloric acid (TCA) (Bensadoun & Weinstein, 1976), resolubilized in Laemmli-buffer and separated on SDS-PAGE. Additionally, refolding and crosslinking experiments were carried out in the presence of PPIase.

The amount of monomers and dimers of C_H3 present in the crosslinked samples was quantified by densitometry of Coomassie-stained gels with a Sharp JX-330 scanner. The digitized protein bands were analyzed

using the Image Master 1D Prime software (Amersham Pharmacia Biotech).

Kinetic simulations and curve fits

Renaturation kinetics and triple jump results were simulated and fitted by least-squares calculations with the following equation system using the Sigma Plot software (Jandel Scientific):

$$d[U]/dt = -k_1[U]$$
$$d[U]/dt = -k_2[U]$$
$$d[I]/dt = -k_2[U] - k_3[I]$$
$$d[N]/dt = -k_3[I]$$

with the unfolded C_H3 $[U]_0 = 100$, the intermediate $[I]_0 = 0$, the native protein $[N]_0 = 0$ and $0 < k_1 < 1$, $0 < k_2 < 1$ and $0 < k_3 < 1$ at the start of the reaction. The underlying model was:

$$U \xrightarrow{k_1} N \quad \text{and} \quad U \xrightarrow{k_2} I \xrightarrow{k_3} N$$

Unfolding kinetics were fitted according to the following model:

$$d[N]/dt = -k_u[N]$$

with $0 < k_u < 1$.

Fitting the renaturation kinetics of the triple-jump experiments were achieved by using a fit including two parallel unfolding reactions:

$$d[N]/dt = -k_u^n[N] \quad \text{(for the reaction N} \longrightarrow \text{U)}$$

$$d[N]/dt = -k_u^{in}[I] \quad \text{(for the reaction I} \longrightarrow \text{U)}$$

where I represents an intermediate ($0 < k_u < 1$, $0 < k_u^{in} < 1$).

Protein Data Bank accession number

The coordinates of the C_H3 dimer have been deposited in the Brookhaven Protein Data Bank with the accession code 1CQK.

Acknowledgments

We thank Holger Grallert for stimulating discussions and Helmut Lenz for support throughout the years. Work was supported by the Deutsche Forschungsgemeinschaft, the European Union and the Fonds der chemischen Industrie.

References

Baldwin, R. L. & Rose, G. D. (1999). Is protein folding hierarchic? *Trends Biochem. Sci.* 24, 26-33.

Bensadoun, A. & Weinstein, W. (1976). Assay of proteins in the presence of interfering materials. *Anal. Biochem.* 70, 241-250.

Brünger, A. T. (1992). *XPLOR Version 3.1: A System for X-ray Crystallography and NMR*, Yale University Press, New Haven, CT.

Buckel, P., Huebner-Parajsz, C., Mattes, R., Lenz, H., Haug, H. & Beauramp, K. (1987). Cloning and nucleotide sequence of heavy and light-chain cDNAs from a creatin-kinase-specific monoclonal antibody. *Gene*, 51, 13-19.

Clark, P. L., Liu, Z.-P., Rizo, J. & Gierasch, L. M. (1997). Cavity formation before stable hydrogen bonding in the folding of a beta-clam protein. *Nature Struct. Biol.* 4, 883-886.

Collaborative Computational Project Number 4 (1994). The CCP4 suite: programs for protein crystallography. *Acta Crystallog. sect. D.* 50, 760-763.

Dall'Acqua, W., Simon, A. L., Mulkerrin, M. G. & Carter, P. (1998). Contribution of domain interface residues to the stability of antibody C_H3 domain homodimers. *Biochemistry*, 37, 9266-9273.

Deisenhofer, J. (1981). Crystallographic refinement and atomic models of a human Fc fragment and it's complex with fragment B of protein A from *Staphylococcus aureus* at 2.9 and 2.8 Å resolution. *Biochemistry*, 20, 2361-2370.

Evans, S. V. (1993). SETOR: hardware lighted three-dimensional solid model representations of macromolecules. *J. Mol. Graph.* 11, 134-138.

Fischer, G., Bang, H. & Mech, C. (1984). Determination of enzymatic catalysis for the cis-trans-isomerization of peptide binding in proline-containing peptides. *Biomed. Biochim. Acta* 43, 1101-1111.

Freund, C., Honegger, A., Hunziker, P., Holak, T. A. & Plückthun, A. (1996). Folding nuclei of the scFv fragment of an antibody. *Biochemistry*, 35, 8457-8464.

Garel, J. R. & Baldwin, R. L. (1973). Both the fast and slow folding reactions of ribonuclease A yield native enzyme. *Proc. Natl Acad. Sci. USA*, 70, 3347-3351.

Goto, Y. & Hamaguchi, K. (1982a). Unfolding and refolding of the constant fragment of the immunoglobulin light chain. *J. Mol. Biol.* 156, 891-910.

Goto, Y. & Hamaguchi, K. (1982b). Unfolding and refolding of the constant fragment of the immunoglobulin light chain. Kinetic role of the intrachain disulfide bond. *J. Mol. Biol.* 156, 911-926.

Goto, Y., Azuma, T. & Hamaguchi, K. (1979). Refolding of the immunoglobuline light chain. *J. Biochem.* 85, 1427-1438.

Huber, R., Deisenhofer, J., Colman, P. M., Matsushima, M. & Palm, W. (1976). Crystallographic structure studies of an IgG molecule and an Fc fragment. *Nature*, 264, 415-420.

Isenman, D. E., Lancet, D. & Pecht, I. (1979). Folding pathways of immunoglobulin domains. The folding kinetics of the $C_\gamma3$ domain of human IgG1. *Biochemistry*, 18, 3327-3336.

Jarob, M., Schindler, T., Balbach, J. & Schmid, F. X. (1997). Diffusion control in an elementary protein folding reaction. *Proc. Natl Acad. Sci. USA*, 94, 5622-5627.

Jaeger, M. & Plückthun, A. (1997). The rate-limiting steps for the folding of an antibody scFv fragment. *FEBS Letters*, 418, 106-110.

Jaenicke, R. (1987). Folding and association of proteins. *Prog. Biophys. Mol. Biol.* 49, 117-237.

Jaenicke, R. & Rudolph, R. (1989). Folding proteins. In *Protein Structure: A Practical Approach* (Creighton, T. E., ed.), pp. 191-223, IRL Press, Oxford, New York, Tokyo.

Jones, T. A., Zou, J. Y., Cowan, S. W. & Kjeldgaard, M. (1991). Improved methods for building protein models in electron density maps and the location of

errors in these models. *Acta Crystallog. sect. A*, 47, 110-119.
Kim, P. S. & Baldwin, R. L. (1992). Specific intermediates in the folding reactions of small proteins and the mechanism of protein folding. *Annu. Rev. Biochem.* 51, 247-265.
Lang, K., Schmid, F. X. & Fischer, G. (1987). Catalysis of protein folding by prolyl isomerase. *Nature* 329, 268-270.
Lilie, H., Lang, K., Rudolph, R. & Buchner, J. (1993). Prolyl isomerases catalyze antibody folding in vitro. *Protein Sci.* 2, 1490-1495.
Lilie, H., Rudolph, R. & Buchner, J. (1995). Association of antibody chains at different stages of folding: prolyl isomerization occurs after the formation of quaternary structure. *J. Mol. Biol.* 248, 190-201.
Matthews, C. R. (1993). Pathways of protein folding. *Annu. Rev. Biochem.* 62, 653-683.
Muñoz, V., Thompson, P. A., Hofrichter, J. & Eaton, W. A. (1997). Folding dynamics and mechanism of β-hairpin formation. *Nature*, 390, 196-199.
Navaza, J. (1994). AMoRe: an automated package for molecular replacement. *Acta. Crystallog. sect. A*, 50, 157-163.
Neet, K. E. & Tim, D. E. (1994). Conformational stability of dimeric proteins: quantitative studies by equilibrium denaturation. *Protein Sci.* 3, 2167-2174.
Nicholls, A. & Honig, B. (1991). A rapid finite difference algorithm utilizing successive over-relaxation to solve the Poisson-Boltzmann equation. *J. Comp. Chem.* 12, 435-445.
Otwinowski, Z. & Minor, W. (1997). Processing of X-ray diffraction data collected in oscillation mode. *Methods Enzymol.* 276, 307-326.
Pace, C. N. & Vanderburg, K. E. (1979). Determining globular protein stability: guanidine hydrochloride denaturation of myoglobin. *Biochemistry*, 18, 288-292.
Perrakis, A., Sixma, T. K., Wilson, K. S. & Lamzin, V. S. (1997). wARP: improvement and extension of crystallographic phases by weighted averaging of multiple refined dummy atomic models. *Acta Crystallog. sect. D*, 53, 448-455.
Pham, T.-N., Koide, A. & Koide, S. (1998). A stable single-layer β-sheet without a hydrophobic core. *Nature Struct. Biol.* 5, 115-119.
Privalov, P. L. & Khechinashvili, N. N. (1974). A thermodynamic approach to the problem of stabilization of globular protein structure: a calorimetric study. *J. Mol. Biol.* 86, 665-684.
Qi, P. X., Sosnick, T. R. & Englander, S. W. (1998). The burst phase in ribonuclease A folding and solvent dependence of the unfolded state. *Nature Struct. Biol.* 5, 882-884.
Ramirez-Alvarado, M., Kortemme, T., Blanco, F. J. & Serrano, L. (1999). β-hairpin and β-sheet formation in designed linear peptides. *Bioorg. Med. Chem.* 7, 93-103.
Rowe, E. S. & Tanford, C. (1973). Equilibrium and kinetics of the denaturation of a homogeneous human immunoglobulin light chain. *Biochemistry*, 12, 4822-4827.
Schmid, F. X. (1986). Fast-folding and slow-folding forms of unfolded proteins. *Methods Enzymol.* 131, 70-82.
Schmid, F. X. (1989). Spectral methods of characterizing protein conformation and conformational changes. In *Protein Structure: A Practical Approach* (Creighton, T. E., ed.), IRL Press, Oxford, New York, Tokyo.
Schmid, F. X. (1998). Catalysis of protein folding by prolyl isomerases. In *Molecular Chaperones in the Life Cycle of Proteins* (Fink, A. L. & Goto, Y., eds), pp. 361-389, Marcel Dekker Inc. New York.
Schönbrunner, N., Koller, K.-P. & Kiefhaber, T. (1997a). Folding of the disulfide-bonded β-sheet protein Tendamistat: rapid two-state folding without hydrophobic collapse. *J. Mol. Biol.* 268, 526-538.
Schönbrunner, N., Pappenberger, G., Scharf, M., Engels, J. & Kiefhaber, T. (1997b). Effect of preformed correct tertiary interactions on rapid two-state Tendamistat folding: evidence for hairpins as initiation sites for β-sheet formation. *Biochemistry*, 36, 9057-9065.
Shakhnovich, E. I. (1999). Folding by association. *Nature Struct. Biol.* 6, 99-102.
Storm, D. R., Rosenthal, K. S. & Swanson, P. E. (1977). Polymyxin and related peptide antibiotics. *Annu. Rev. Biochem.* 46, 723-763.
Sumi, A. & Hamaguchi, K. (1982). Denaturation by guanidine hydrochloride of the Fc(t) and pFc' fragments of human immunoglobulin G^1. *J. Biochem.* 92, 823-833.
Tanford, C. (1970). Protein denaturation. C. Theoretical models for the mechanism of denaturation. *Advan. Protein Chem.* 24, 1-95.
Varley, P., Gronenborn, A. M., Christensen, H., Wingfield, P. T., Pain, R. H. & Clore, G. M. (1993). Kinetics of folding of the all-beta sheet protein interleukin-1 beta. *Science*, 260, 1110-1113.
Wels, J. A., Word, C. J., Rimm, D., Der-Balan, G. P., Martinez, H. M., Tucker, P. W. & Blattner, F. R. (1984). Structural analysis of the murine IgG3 constant region gene. *EMBO J.* 3, 2041-2046.
Williams, A. F. & Barclay, A. N. (1988). The immunoglobulin superfamily-domains for surface recognition. *Annu. Rev. Immunol.* 6, 381-405.

Edited by A. R. Fersht

(Received 6 July 1999; received in revised form 11 August 1999; accepted 20 August 1999)

EXHIBIT 16

THIS EXHIBIT HAS BEEN REDACTED IN ITS ENTIRETY